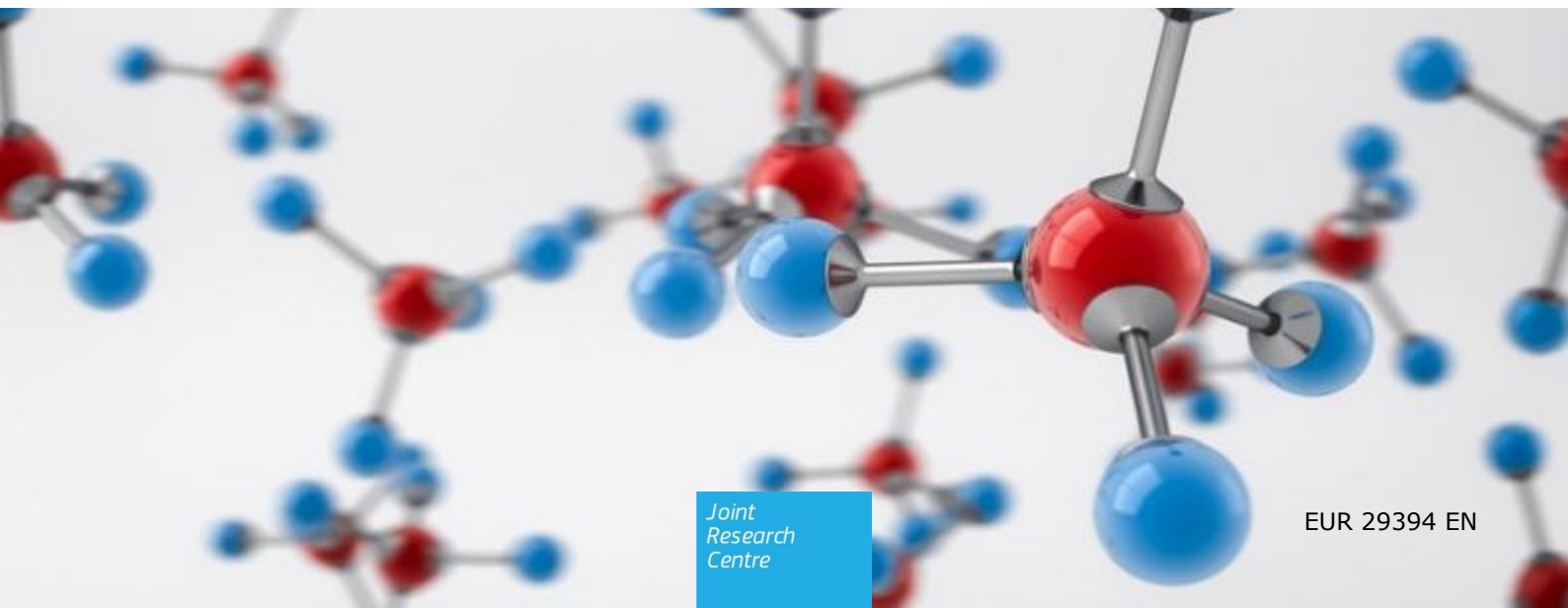


## JRC SCIENCE FOR POLICY REPORT

# Global trends of methane emissions and their impacts on ozone concentrations

Van Dingenen, R., Crippa, M.,  
Maenhout, G., Guizzardi, D.,  
Dentener, F.

2018



This publication is a Science for Policy report by the Joint Research Centre (JRC), the European Commission's science and knowledge service. It aims to provide evidence-based scientific support to the European policymaking process. The scientific output expressed does not imply a policy position of the European Commission. Neither the European Commission nor any person acting on behalf of the Commission is responsible for the use that might be made of this publication.

#### Contact information

Name: R. Van Dingenen  
Address: European Commission, Joint Research Centre, via E. Fermi 2749, I-21027 Ispra, ITALY  
Email: rita.van-dingenen@ec.europa.eu

#### JRC Science Hub

<https://ec.europa.eu/jrc>

JRC113210

EUR 29394 EN

PDF	ISBN 978-92-79-96550-0	ISSN 1831-9424	doi:10.2760/820175
Print	ISBN 978-92-79-96551-7	ISSN 1018-5593	doi:10.2760/73788

Luxembourg: Publications Office of the European Commission, 2018

© European Union, 2018

The reuse policy of the European Commission is implemented by Commission Decision 2011/833/EU of 12 December 2011 on the reuse of Commission documents (OJ L 330, 14.12.2011, p. 39). Reuse is authorised, provided the source of the document is acknowledged and its original meaning or message is not distorted. The European Commission shall not be liable for any consequence stemming from the reuse. For any use or reproduction of photos or other material that is not owned by the EU, permission must be sought directly from the copyright holders.

All content © European Union 2017, except: cover, 2017. Source: <https://www.dreamstime.com/stock-images-methane-molecules-image25465304> and where indicated in the text.

How to cite this report: Van Dingenen, R., Crippa, M., Maenhout, G., Guizzardi, D., Dentener, F., *Global trends of methane emissions and their impacts on ozone concentrations*, EUR 29394 EN, Publications Office of the European Union, Luxembourg, 2018, ISBN 978-92-79-96550-0, doi:10.2760/820175, JRC113210

# Contents

Abstract .....	1
Foreword .....	2
Acknowledgements .....	3
Executive summary .....	4
1 Introduction .....	8
2 The global methane budget, trends, and changing background ozone .....	9
2.1. The global methane (CH <sub>4</sub> ) budget .....	9
2.2. Observationally derived CH <sub>4</sub> trends .....	9
2.3. Ozone (O <sub>3</sub> ) trends in Europe and the world .....	11
2.3.1 O <sub>3</sub> observations .....	11
2.3.2 Model attribution of O <sub>3</sub> trends to CH <sub>4</sub> emissions .....	13
3 Trends of anthropogenic CH <sub>4</sub> emissions .....	16
3.1. Past CH <sub>4</sub> emissions .....	17
3.1.1 Europe, USA and other OECD countries .....	17
3.1.2 Russia, China and India and other countries in transition .....	19
3.2. Sectoral break-down of the anthropogenic CH <sub>4</sub> emissions .....	20
3.2.1 Emissions from agricultural soils, livestock and other agricultural sources ..	20
3.2.2 Fugitive emissions from fossil fuel production, transport by pipelines and other energy industries .....	21
3.2.3 Solid waste and waste water emissions .....	23
3.2.4 Other remaining sources.....	23
3.3. Future CH <sub>4</sub> emissions .....	25
3.3.1 Mitigation potentials .....	25
3.3.2 Emission scenarios .....	30
4 Air quality impacts of CH <sub>4</sub> emissions .....	39
4.1. Current O <sub>3</sub> exposure patterns .....	39
4.2. Future trends in background O <sub>3</sub> from CH <sub>4</sub> emissions.....	40
4.3. Future health impacts from CH <sub>4</sub> -induced O <sub>3</sub> .....	42
4.4. Future crop impacts from CH <sub>4</sub> -induced O <sub>3</sub> .....	45
4.5. Role of CH <sub>4</sub> in closing the GHG emissions gap.....	47
4.6. Summary of impacts .....	48
5 Conclusions and way forward .....	49
5.1. Current understanding of observed changes of CH <sub>4</sub> and O <sub>3</sub> concentrations .....	49
5.2. Current knowledge on the geographical distribution of CH <sub>4</sub> emissions and on the contributing sources.....	50
5.3. Policy-relevant CH <sub>4</sub> emission scenarios until 2050 and contributions to O <sub>3</sub> concentrations in Europe and other parts of the world .....	51

5.4. Benefits for human health, crops and climate of CH <sub>4</sub> emission reductions in the EU alone, and through collaboration with other parties.....	51
5.5. Promising economic sectors to effectively achieve CH <sub>4</sub> emission reductions.....	52
5.6. The way forward.....	53
References .....	55
List of abbreviations and definitions .....	66
List of figures .....	68
List of tables .....	71
ANNEXES .....	72
Annex 1. The EDGAR v4.3.2 CH <sub>4</sub> emissions .....	72
A.1.1.1 EDGAR-IPCC sector aggregation.....	72
A.1.1.2 Agricultural soils and livestock .....	73
A.1.1.3 Fugitive emissions from fossil fuel production and transmission.....	73
Annex 2. Future emission scenario families .....	78
Annex 3. World regions aggregation .....	85
Annex 4. Modelling O <sub>3</sub> responses from CH <sub>4</sub> emissions.....	87
Annex 5. O <sub>3</sub> impact on health and crop yields .....	93

## **Abstract**

Methane is a greenhouse gas and air pollutant producing health damaging tropospheric ozone. By 2050 in Europe 6,000 to 11,000 ozone-related premature deaths can be avoided per year (worldwide 70,000 to 130,000) when implementing ambitious methane reduction strategies worldwide. This works informs Europe's forthcoming methane strategy.

## Foreword

Methane is the 2<sup>nd</sup> most important anthropogenic greenhouse gas after carbon dioxide. Since the pre-industrial era, methane concentrations have more than doubled, and at present sources related to human activities are about 50% larger than natural ones. After a period of stagnation, methane concentrations are increasing again since the last decade, and by 2020, may reach levels that match the most pessimistic projections used in the IPCC AR5 report. There are contrasting scientific hypotheses on the reasons for this uptick in methane, with a number of studies pointing to increasing emissions from agriculture, fossil fuel production and distribution, and in developing countries, solid waste in landfills and wastewater management.

It is often forgotten by policymakers that methane is also an important precursor of ozone in the troposphere. Ozone itself is a greenhouse gas and short-lived climate forcer, but it is also an atmospheric pollutant responsible for harmful impacts on human health and damage to crops and vegetation and for which air quality standards have been established. In various parts of the world environmental policies aim to reduce ground level ozone, but there is a risk that increasing methane emissions will counteract those regional efforts. Because methane stays about 10 years in the atmosphere, chemical mechanisms that lead to widespread ozone formation involve methane sources from everywhere in the world and mitigation efforts must become a global goal. Therefore, the UNECE Convention on Long Range Transport of Air Pollution and the European Commission commissioned studies to assess the role of methane in ozone air pollution and provide relevant and efficient options for control strategies.

This report shows how methane emission reductions can play a key-role in reducing ground level ozone in Europe and in the world. By 2050, between 70,000 to 130,000 annual premature deaths can be avoided globally, and 6,000 to 11,000 in the European Union alone, when the world consistently reduces CH<sub>4</sub> emissions to reach climate, air pollution and other sustainability objectives (compared to doing nothing). Europe's contribution to global methane emissions is too small to make the difference — a global collaborative approach to reduce methane emissions is essential not only for climate but also for air pollution. We know that there are low hanging fruits in several sectors where emission reductions may be cheap or even be profitable. This report presents methane emission reduction opportunities in the energy, waste and wastewater, and agricultural sectors, and provides additional reasons to reduce these emissions from a health and food-security perspective. It also highlights the risks for human health and environment that may come with inaction. Finally, it gives us all good reasons for expanding international cooperation to achieve better air quality for everyone in the world, reducing impacts of global climate change at the same time!

**Laurence Rouil**, Head of the environmental modelling and decision making department of INERIS, and chair of the EMEP Steering Body to the Convention Long Range Transport of Air Pollution.

## **Acknowledgements**

The authors are grateful for the fruitful discussions with the European Commission's Directorate-General for Environment (DG ENV), in particular A. Zuber, S. Brockett, and V. André. This report was supported by the European Commission's Administrative Arrangement AMITO II (JRC 34007-2015 NFP ENV N°070201/2015/720629/AA/ENV.C3), and greatly benefitted from the collaborative work performed in the UNECE CLRTAP Task Force on Hemispheric Transport of Air Pollution. We highly appreciate the European Commission's Joint Research Centre's (JRC) internal reviews by J. Wilson, A. Leip, and P. Bergamaschi, and the external reviews by A. Innamorati and B. Van Doorslaer (Directorate-General for Agriculture - DG AGRI), G. Klaassen (Directorate-General for Climate Action - DG CLIMA), B. Devlin and M. Zsigri (Directorate-General for Energy - DG ENER), L. Rouil (INERIS) and L. Höglund-Isaksson (IIASA).

## **Authors**

Van Dingenen, R., Crippa, M., Maenhout, G., Guizzardi, D., Dentener, F.

## Executive summary

### Policy context

A significant proportion of the urban and rural population of Europe is exposed to concentrations of **ozone** (O<sub>3</sub>) that are near or above the target values set by the Ambient Air Quality directive (2008) and the guidance levels provided by the World Health Organisation (EEA, 2017; CLRTAP: Maas and Grennfelt, 2016; WHO, 2006). Air pollution abatement measures under the European Union (EU) National Emission Ceiling Directives (NECD) and internationally, the Convention on Long-range Transboundary Air Pollution (CLRTAP) and its protocols, have achieved significant success, but long-term risks due to O<sub>3</sub> and other pollutants continue to exist. Air pollutants can travel over long distances and over national boundaries, causing negative impacts on human health, agriculture and ecosystems. The main legislative instrument in the EU to achieve the 2030 objectives of the Clean Air Programme is Directive 2016/2284/EU on the reduction of national emissions of certain atmospheric pollutants, which entered into force on 31 December 2016. Following the agreement of the European Parliament and the Council of the European Union, one of the precursors of O<sub>3</sub> air pollution, methane, was not included in the NECD. However, the Commission stated<sup>1</sup> its intention to review methane emissions in the context of assessing options to further reduce ozone concentrations in the EU, and to promote methane reductions internationally.

**Methane** (CH<sub>4</sub>) is an important greenhouse gas (GHG), with a 100-year warming potential 28 times larger than CO<sub>2</sub> (IPCC AR5: Myhre et al., 2013). Climate policies are thus an important means to reduce CH<sub>4</sub> emissions, as it is included in the basket of GHG emissions under the Kyoto protocol and the recently concluded Paris Agreement. Internationally, in the late 2000s the UNFCCC promoted the Clean Development Mechanisms and Joint Implementation plans to reduce CH<sub>4</sub> emissions from venting and flaring in natural gas production and promote the recovery of CH<sub>4</sub> from coal mines and control emissions from waste disposals.

To fulfil the targets of the Kyoto Protocol, the EU introduced in 2009 the Climate & Energy package<sup>2</sup> (406/2009/EC) with an overall GHG emission reduction objective of 20% by 2020 compared to 1990. The 2030 climate and energy framework strengthened these objectives to reach an overall GHG reduction of 40%, and 30% in the non-ETS sector by 2030 compared to 2005 and outlined nationally determined contributions for GHG reduction under the 2015 Paris Agreement.

Worldwide, CH<sub>4</sub> emissions increased by 17% between 1990-2012, compared to a 53% increase in CO<sub>2</sub>. While EU28 CH<sub>4</sub> emissions and the contributions of CH<sub>4</sub> to the overall EU GHG emissions declined substantially in the 1990s, in the last 15 years the rate of decline has been much less. In 2016 CH<sub>4</sub> contributes ca. 11% to the total EU28 GHG emissions (EEA, 2018). Large CH<sub>4</sub> emission reductions between 1990-2012 have occurred in managed landfills sector (-38%), due to the implementation of the directive on the Landfill of Waste (1999/31/EC). In this period, due to phasing out of coal production in Europe, fugitive emissions from coal mining declined by 77%, while those from natural gas operations increased by 16%, subject to high uncertainty. Agricultural

---

<sup>1</sup> DIRECTIVE (EU) 2016/2284; CELEX\_32016L2284\_EN\_TXT.pdf. Declaration by the Commission on the Review of Methane Emissions: "The Commission considers that there is a strong air quality case for keeping the development of methane emissions in the Member States under review in order to reduce ozone concentrations in the EU and to promote methane reductions internationally.

The Commission confirms that on the basis of the reported national emissions, it intends to further assess the impact of methane emissions on achieving the objectives set out in Art. 1 paragraph 2 of the NEC Directive and will consider measures for reducing those emissions, and where appropriate, submit a legislative proposal to that purpose. In its assessment, the Commission will take into account a number of ongoing studies in this field, due to be finalised in 2017, as well as further international developments in this area."

<sup>2</sup> Climate & Energy package: 406/2009/EC; The 2030 climate and energy framework: COM(2014) 15 final; COM(2016)759. <https://unfccc.int/process-and-meetings/the-paris-agreement/the-paris-agreement>

emissions declined much less (-22%), and contributed by 53% to the overall EU28 CH<sub>4</sub> emissions in 2015 (EEA, 2018). Future EU CH<sub>4</sub> emissions will strongly depend on further reductions in this sector. In contrast, worldwide CH<sub>4</sub> emissions increased by 27% between 1990-2012, and the European fraction of global CH<sub>4</sub> emissions declined from 12 to 6%.

This report summarises studies on CH<sub>4</sub> and its impact on O<sub>3</sub> performed at the JRC and external organisations and reviews international developments concerning CH<sub>4</sub>.

### ***Key conclusions***

CH<sub>4</sub> is an important greenhouse gas and also a precursor of the air pollutant O<sub>3</sub>. O<sub>3</sub> stays long enough in the atmosphere to be transported over large regions across the Northern Hemisphere, while CH<sub>4</sub> is globally mixed.

About 60% of the current global methane is emitted by sources like agriculture, landfills and wastewater, and the production and pipeline transport of fossil fuels, while ca. 40% is from natural sources. Globally, CH<sub>4</sub> emissions and concentrations are still increasing, raising concerns for air quality and climate change.

This study, building on evidence from observations and modelling, suggests that CH<sub>4</sub> emission reductions can play a key-role in further reducing O<sub>3</sub> in Europe and in the world. Since Europe's contribution to global CH<sub>4</sub> emissions is currently only about 6%, global cooperation to reduce CH<sub>4</sub> in countries and regions in- and outside of the EU, will also be essential to reduce related O<sub>3</sub> effects in Europe and the world.

### ***Main findings***

After a period of stagnation in the 1990s, during the last decade CH<sub>4</sub> air concentrations are again increasing, and may reach levels projected by the pessimistic climate scenarios for 2020, presented by the IPCC AR5 report.

Unabated, global anthropogenic CH<sub>4</sub> emissions could increase by 35 to 100% (from ca. 330 Tg CH<sub>4</sub> yr<sup>-1</sup> in 2010 to 450-650 Tg CH<sub>4</sub> yr<sup>-1</sup>) by 2050 for a range of pessimistic scenarios. By contrast, optimistic sustainability scenarios, such as those that target the 2° Paris Agreement goals, projected CH<sub>4</sub> emission reductions of up to 50%, to 180-220 Tg CH<sub>4</sub> yr<sup>-1</sup> CH<sub>4</sub> by 2050.

The maximum CH<sub>4</sub>-O<sub>3</sub> mitigation potential would be given by a situation without anthropogenic CH<sub>4</sub> emissions: global ozone damage to crops would be reduced by 26%, and O<sub>3</sub> related mortality by 20%. For Europe we estimate a potential damage reduction by 40% and 34% for crops and health respectively.

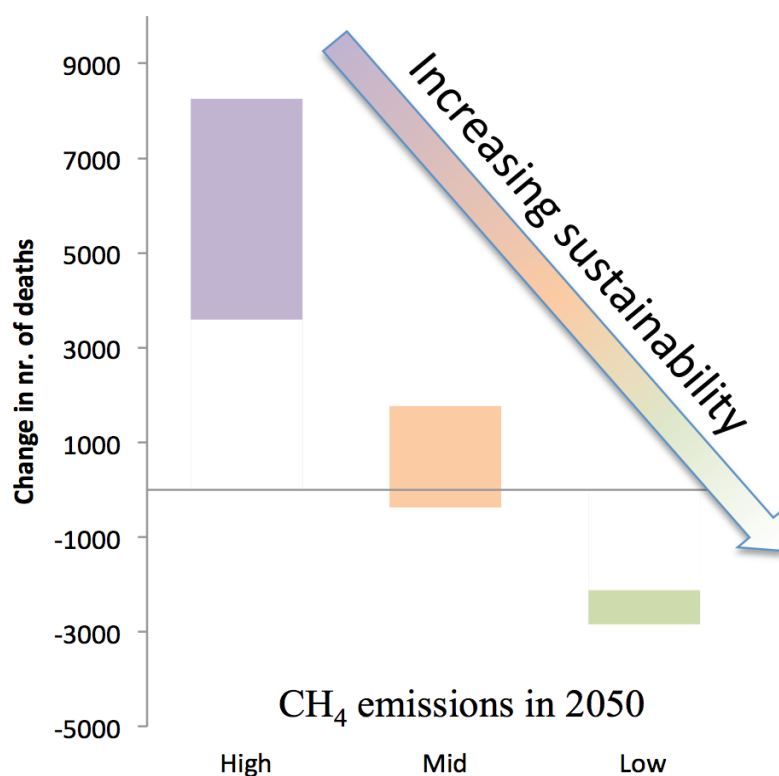
By 2050, for a range of pessimistic scenarios in which CH<sub>4</sub> emissions remain unabated, health-impact weighted O<sub>3</sub> could rise by 2-4.5 ppb globally, causing 40,000 (+12%) to 90,000 (+26%) more O<sub>3</sub> premature deaths compared to present.

Under optimistic sustainability scenarios (e.g. ambitious climate mitigation), O<sub>3</sub> may decrease by 2 ppb (compared to 2010), saving worldwide 30,000 (-9%) to 40,000 (-12%) lives. Such scenarios assume structural changes in the energy, waste and agricultural sectors, together with the implementation of all currently available emission abatement technologies.

Intermediate CH<sub>4</sub> emission reduction scenarios, for instance those compatible with the emission reduction commitments included in the nationally determined contributions of the signatories of the Paris Agreement, would bring down CH<sub>4</sub> emissions substantially compared to the pessimistic scenarios, with the exposure of the global and European population to ozone remaining at 2010 levels.

**Figure ES1.** Change in European O<sub>3</sub>-related premature mortalities linked to CH<sub>4</sub> emissions in 2050, relative to 2010. The 3 colours represent different scenario family characteristics (see section 3.3). High: non-ambitious high emission scenarios; Mid: Moderate ambition; Low: high ambition low-emission scenarios. Population was kept constant at projected 2050 levels to allow comparability.

### Change in premature deaths in the EU28 from 2010 to 2050 for various CH<sub>4</sub> emission scenarios



Source: JRC, this study

The mitigation opportunity, comparing optimistic and pessimistic CH<sub>4</sub> emission scenarios, indicates a benefit for health exposure relevant O<sub>3</sub> concentrations between 5 to 8 ppb in Europe and 4 to 6 ppb globally by 2050. We estimate that the corresponding health gains amount to 80,000 to 130,000 annual premature deaths avoided globally and 6,000 to 11,000 in Europe (EU28- see Fig. ES1). The EU28 is currently responsible for about 6% of the global anthropogenic CH<sub>4</sub> emissions. Reducing Europe's current CH<sub>4</sub> emissions by 10% or 50% would save 50 to 250 premature deaths per year in Europe, and 540 to 2700 worldwide. Since the benefits of CH<sub>4</sub> of emission reductions are globally distributed, global mitigation strategies are most effective in reaching substantial health benefits within and outside individual world regions.

Benefits for food security, using widely accepted O<sub>3</sub> crop damage methodologies, are estimated to amount a 1% increase in global crop production of 4 major crops, and 1.5% in Europe.

CH<sub>4</sub> and O<sub>3</sub> are both important greenhouse gases. By 2030, ambitious CH<sub>4</sub> emission reductions could close 15 to 33% of the emission gap identified by UNEP (2017) between the total commitments in the national determined contributions of the signatories to the Paris Agreement and the emissions needed to reach an end-of-the century 2 °C target.

### ***Related and future JRC work***

JRC provides support to the Convention on Long-Range Transboundary Air Pollution and its Task Force on Hemispheric Transport of Air Pollution under the EMEP programme. JRC further keeps collaborating with and contributing to a host of international organizations (e.g. CLRTAP, AMAP, CCAC, IPCC, OECD, UN Environment, WHO, WMO), to assess the benefits of reducing air pollutants and GHG emissions.

### ***Quick guide***

The report presents an overview of current knowledge on atmospheric methane and ozone concentration trends, anthropogenic emissions and emissions scenarios, with a focus on Europe. CH<sub>4</sub> emissions' influence on ozone concentrations and related impacts on health and crops are derived using the in-house FAsT Scenario Screening Tool (FASST).

# 1 Introduction

Methane (CH<sub>4</sub>) is a greenhouse gas as well as a precursor pollutant to tropospheric ozone (O<sub>3</sub>).

As a greenhouse gas it is included in the basket of emissions under the Kyoto protocol and likewise in the Paris Agreement (2016). Per kg emitted and on a hundred-year time scale, CH<sub>4</sub> is about 28 times as potent for global warming as CO<sub>2</sub> (IPCC AR5 WG1: Myhre et al., 2013; see also section 2). In the atmosphere, CH<sub>4</sub> has a turnover time of about 10 years, allowing it to be relatively homogeneously distributed around the globe.

CH<sub>4</sub> is the dominant anthropogenic volatile organic compound (VOC) contributing to O<sub>3</sub> formation in the global troposphere (Fiore et al., 2002). In the lowest part of the atmosphere, in regions where NO<sub>x</sub> concentrations are sufficiently high, reactions of OH radicals with CH<sub>4</sub> and other substances leads to the production of O<sub>3</sub>. O<sub>3</sub> is a strong oxidant and air pollutant damaging human health (Brunekreef and Holgate, 2002; Jerrett et al., 2009; Malley et al., 2017; Turner et al., 2016), ecosystems and agricultural crops (Fowler et al., 2009; Maas and Grennfelt, 2016; Mills et al., 2011; Pleijel et al., 2018), whilst also affecting climate (Myhre et al., 2017; Stevenson et al., 2013, 2006).

In contrast to the short-lived precursors for tropospheric O<sub>3</sub> (NO<sub>x</sub>, carbon monoxide, and non-methane VOCs), methane is fairly well-mixed in the atmosphere, and primarily affects global *background*<sup>3</sup> concentrations of O<sub>3</sub> (Dentener et al., 2005; Forster et al., 2007).

Management of methane emissions, through their impact on background surface O<sub>3</sub> concentrations, can therefore have a significant impact on air quality, human health and crop productivity.

Its role as a surface O<sub>3</sub> precursor has been the topic of a host of studies, including the HTAP (Dentener et al., 2010) report and Wild et al. (2012). The recently concluded special issue of the scientific journal Atmospheric Chemistry and Physics<sup>4</sup> addresses various relevant aspects of hemispheric transport. These studies pointed to the increasingly important role of CH<sub>4</sub> in determining future O<sub>3</sub> concentrations.

In this report we discuss the potential role for CH<sub>4</sub> emission reductions to further reduce O<sub>3</sub> in Europe. Given the hemispheric nature of O<sub>3</sub>, CH<sub>4</sub> reduction in EU28 should be considered in the context of a broader hemispheric approach to cost-effective reduction of background concentrations.

Policy-relevant questions are:

- What is our current understanding of observed changes of CH<sub>4</sub> concentrations and background O<sub>3</sub>, and modelling capacity to understand these changes?
- What is the current knowledge on the geographical distribution of CH<sub>4</sub> emissions and on the contributing sources?
- What are policy-relevant CH<sub>4</sub> emission scenarios until 2050 and how are they expected to contribute to O<sub>3</sub> concentrations in Europe and other parts of the world?
- What are benefits to human health, crops and vegetation of CH<sub>4</sub> emission reductions in the EU alone, and through collaboration with other parties?
- Which are the most promising economic sectors to effectively achieve CH<sub>4</sub> emission reductions?

---

<sup>3</sup> Ozone concentrations in the absence of anthropogenic emissions, as determined by models. For instance global background ozone would be estimated assuming no global anthropogenic emissions. European background means the situation without European anthropogenic emissions.

<sup>4</sup> [https://www.atmos-chem-phys.net/special\\_issue390.html](https://www.atmos-chem-phys.net/special_issue390.html)

## 2 The global methane budget, trends, and changing background ozone

### 2.1 The global methane (CH<sub>4</sub>) budget

Atmospheric methane (CH<sub>4</sub>) is the second largest contributor to the greenhouse effect and globally contributed about 17% to the direct anthropogenic radiative forcing of all long-lived greenhouse gases in 2016<sup>5</sup> (Butler and Montzka et al., 2017). Currently, the UNFCCC GHG reporting system uses the GWP-100 value of 25, derived from the IPCC AR4 report (Forster et al., 2007). Using the more recent IPCC AR5 (Myhre et al., 2013) GWP-100 value of 28 would further increase the relative importance of CH<sub>4</sub> as a greenhouse gas.

Due to the intermediate atmospheric residence time of about 10 years, action to reduce CH<sub>4</sub> emissions is considered to be an important tool to mitigate global warming in the near-term (Shindell et al., 2012, 2017). Furthermore, reductions in global CH<sub>4</sub> would have significant co-benefits for air quality, the topic of this report.

The global atmospheric CH<sub>4</sub> budget (Saunois et al., 2016a) is determined by many terrestrial and aquatic surface sources. These sources are largely balanced by a number of sinks<sup>6</sup> and a small imbalance related to atmospheric increases. The combined information (Saunois et al., 2016a) from emission inventories, atmospheric concentrations and trends, isotopic composition<sup>7</sup> and inverse modelling<sup>8</sup> suggested average anthropogenic emissions of 352 [340-360] Tg CH<sub>4</sub> yr<sup>-1</sup> for the period 2003-2012 determined from inventories and 328 [259-370] Tg CH<sub>4</sub> yr<sup>-1</sup> from models. Due to methodological differences larger ranges are associated with global natural emissions of methane: 384 [257-524] Tg CH<sub>4</sub> yr<sup>-1</sup> from bottom-up estimates, and 231 [194-296] Tg CH<sub>4</sub> yr<sup>-1</sup> from models. The sum of model-determined natural and anthropogenic sources 558 [540-568] Tg CH<sub>4</sub> yr<sup>-1</sup>, is less uncertain, as it is constrained by our knowledge about the atmospheric contents, sinks and the atmospheric growth rates. Anthropogenic sources contribute by around 60% [50-65%] to global CH<sub>4</sub> emissions (Bergamaschi et al., 2018). Regionally, inverse models, that combine information derived from observations, emissions, and atmospheric transport, can determine the total emissions, but the separate contributions of natural and anthropogenic emissions relies on information from emission inventories and natural emission process models. Therefore, uncertainties of regional natural versus anthropogenic emission estimates are higher than for the global emission budget.

### 2.2 Observationally derived CH<sub>4</sub> trends

Global CH<sub>4</sub> concentrations have increased, with varying rates, from 722 ppb in pre-industrial period to 1850 ppb by the end of 2017, corresponding to an average rate of increase of 4.3 ppb yr<sup>-1</sup>. Direct measurements of atmospheric CH<sub>4</sub> showed a large increase during the 1980s of almost 12 ppb yr<sup>-1</sup>, a slower increase during the 1990s of about 6 ppb yr<sup>-1</sup> and a stabilisation between 1999 and 2006. Since 2007, CH<sub>4</sub> concentrations have risen again significantly with a growth rate of about 6 ppb yr<sup>-1</sup> in 2007-2013 (Dlugokencky et al., 2009) and accelerating to 10 ppb yr<sup>-1</sup> during 2014-2018

<sup>5</sup> Radiative forcing is the change in the net, downward minus upward, radiative flux (expressed in W m<sup>-2</sup>) at the *tropopause* or top of *atmosphere* due to a change in an external driver of *climate change*, i.e. CH<sub>4</sub>. The change typically compares the present with the pre-industrial past, or the future with the present.

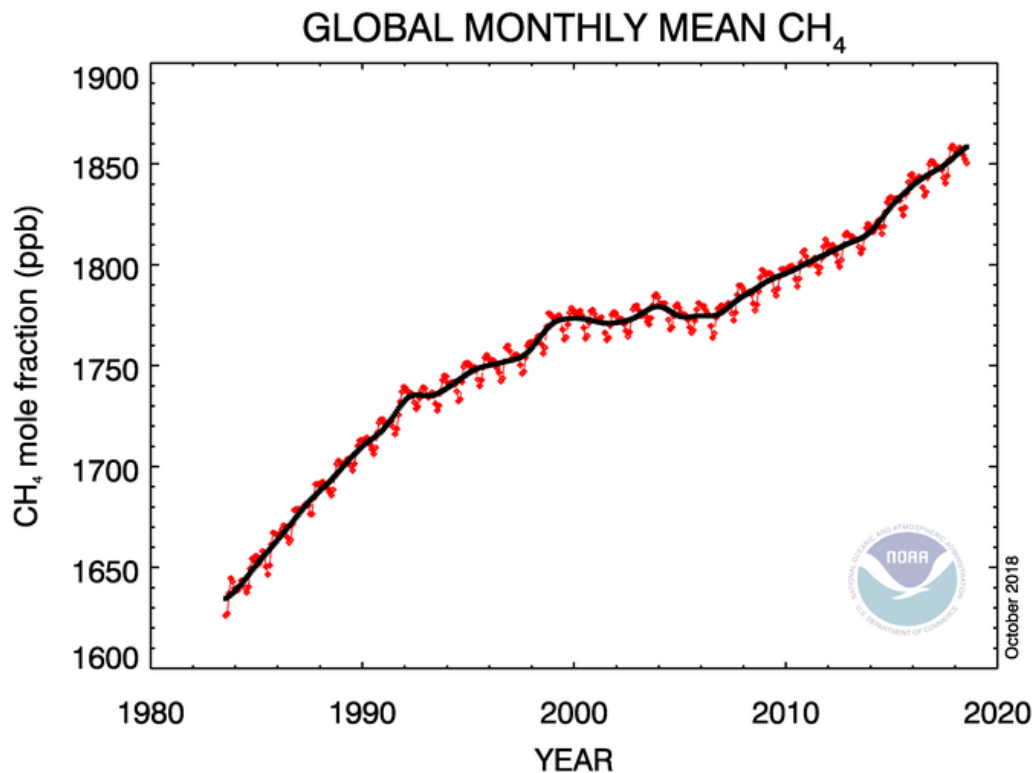
<sup>6</sup> 84 % of the CH<sub>4</sub> sink is due to oxidation by OH radicals in the troposphere, tropospheric oxidation by chlorine radicals accounts for 4%; export and oxidation in the stratosphere 8 %; and oxidation in soils 4 % (Saunois et al, 2016a)

<sup>7</sup> Isotopic composition or signature refers to the ratio of non-radiogenic stable, and stable/unstable radiogenic isotopes in a specific source gas. In this study the analysis is primarily based on the stable isotope <sup>13</sup>C.

<sup>8</sup> Inverse modeling relates a set of observations to the causal factors that produced them. In this case observations of CH<sub>4</sub> are combined with an atmospheric chemical transport model and a-priori estimates of emissions, to produce more accurate emission estimates. For an extensive discussion on the state-of-the-art of inverse modeling see the JRC Science for Policy report by Bergamaschi et al, 2018

as shown in fig. 2.1. The concentration in 2017 is closer<sup>9</sup> to the value of 1925 ppb projected for 2020 by the pessimistic IPCC RCP8.5 climate scenario (associated with an end of the century warming between 3.2 to 5.4 °C) than the optimistic RCP2.6 “2°C” scenario (Saunio et al., 2016b, see section 3.3). The drivers of these fluctuating growth rates and especially for the renewed increasing concentration trend are still not fully understood.

**Figure 2.1.** Atmospheric methane measured as “dry air mole fraction” in ppb. The red dots are globally averaged monthly mean values, whereas the black line shows the long-term trend through a 12-month running mean (removing the average seasonal cycle).



Source: E. Dlugokencky, NOAA/ESRL ([www.esrl.noaa.gov/gmd/ccgg/trends\\_CH4/](http://www.esrl.noaa.gov/gmd/ccgg/trends_CH4/)). Downloaded October 2018.

Changing CH<sub>4</sub> growth rates can be caused both by changing sources (emissions) and sinks (most importantly the OH radical) or a combination of them. Montzka et al. (2011) considered that variability in the OH-radical sink was not likely to explain the observed trend variations until 2008, but a recent inverse modelling study (Rigby et al., 2017) suggest that emissions rose while OH levels decreased. Another study by Turner et al. (2017) suggest a simultaneous decrease of CH<sub>4</sub> emissions and an even larger decrease of the OH-radical to explain observed CH<sub>4</sub> trends, which is not consistent with information from emission inventories. Prather and Holmes (2017) argue that due to large uncertainties of these studies, the observational constraints can also be reconciled with other model solutions, including assuming constant OH-levels.

There are multiple lines of observation-based evidence that suggest an important role for increasing anthropogenic emissions from fossil fuels, as well as agriculture, waste, or

<sup>9</sup> Assuming a continuation of the CH<sub>4</sub> trend by 10 ppb yr<sup>-1</sup>, the concentration at the end of 2020 would reach 1850+30=1880 ppb. The IPCC AR5 projection for the RCP8.5 scenario was 1925 ppb, while the optimistic RCP2.6 scenario projected 1731 ppb for 2020 (see IPCC AR5 WG1: Prather et al., 2013).

natural emissions from tropical wetland to explain the recent methane trend. Studies using isotope signatures (Schwietzke et al., 2016) and ethane to propane ratios (Dalsøren, et al., 2018) suggest that fossil fuel related emissions, e.g. from coal, oil and gas production and distribution may contribute substantially to recent increases in methane concentrations. However, the ethane-to-methane ratios vary greatly among different oil and gas sources, rendering these estimates uncertain. The high uncertainties in estimates for fossil-fuel related CH<sub>4</sub> emissions are illustrated for the US, where Alvarez et al. (2018) use aircraft measurements to estimate a contribution of 13±2 Tg CH<sub>4</sub> yr<sup>-1</sup> emissions from US oil and natural gas supply, 60% higher than estimated by the US EPA inventory.

In contrast, Nisbeth et al. (2016), Schaefer et al. (2016) and Saunio et al. (2017) suggest an increase of biogenic emissions (tropical wetlands, and agriculture). Recently, Worden et al. (2017) proposed that reduced biomass burning emissions could reconcile some of the conflicting conclusions with regard to microbial sources (agriculture, wetlands) and fossil source (oil and gas production). In this context, bottom-up emission inventories are highly uncertain, in particular for fugitive emissions from fossil fuels. Top-down inverse modelling emission estimates can be used to improve inventories, but they are highly dependent on observations, from facility to regional scale (Bergamaschi et al., 2018). In this context, it is imperative that the current observational capacity for CH<sub>4</sub> concentrations is maintained (Houweling et al., 2012). More exact knowledge on the drivers of the recent CH<sub>4</sub> trends will be essential for informing both climate and air pollution policies.

## **2.3 Ozone (O<sub>3</sub>) trends in Europe and the world**

CH<sub>4</sub> and O<sub>3</sub> are connected through large-scale atmospheric chemistry and transport processes. In Section 2.3.1 we present the observational evidence for worldwide and European O<sub>3</sub> trends. Increasing CH<sub>4</sub> concentrations may partly contribute to these increasing trends or, in regions where O<sub>3</sub> declines due to local-to-regional air pollutant emission reductions, counteract these efforts. Models (section 2.3.2) are used to attribute trends in O<sub>3</sub> to specific sources. Concepts often used in this context are background O<sub>3</sub> - a hypothetical O<sub>3</sub> concentration calculated by models, where the absence of anthropogenic sources is assumed. Baseline O<sub>3</sub> refers to observed O<sub>3</sub> concentrations not directly influenced by recently emitted or produced pollution, but including further away influences. Once a long-lived substance is emitted in the atmosphere, it takes about one month to be mixed across the Northern Hemisphere, and about 1 year between the Northern and Southern Hemisphere. Therefore, ozone with a turn-over time of about 22 days, is subject to intercontinental transport, and CH<sub>4</sub> (10 years) is globally mixed.

### **2.3.1 O<sub>3</sub> observations**

From the 1870s to 1950s only very few quantitative measurements exist. Comparison of O<sub>3</sub> observations at the end of the 20th century with earlier data indicates that over the last century surface O<sub>3</sub> in Europe increased by more than a factor of 2 (IPCC AR5; Hartmann et al., 2013). Only nineteen predominantly rural surface global datasets have long-term records that stretch back to the 1970s. 11 out of 13 Northern Hemispheric observation sites had statistically significant positive trends of 1 to 5 ppb per decade, equivalent to a more than doubling of the O<sub>3</sub> concentration since the 1950s (IPCC AR5 WG1:Myhre et al., 2013). Between 1960 and 2000, O<sub>3</sub> increases amounted to 14 ppb, 10 ppb between 1970-2000 and 5 ppb for 1990-2000. The CLRTAP Assessment Report (Maas and Grennfelt, 2016) showed an overall declining trend of peak O<sub>3</sub><sup>10</sup> values over 55 mainly rural stations in Europe over the period 1990-2013 (Fig 2.2). However, annual average O<sub>3</sub> concentrations showed no statistically significant trend over this period.

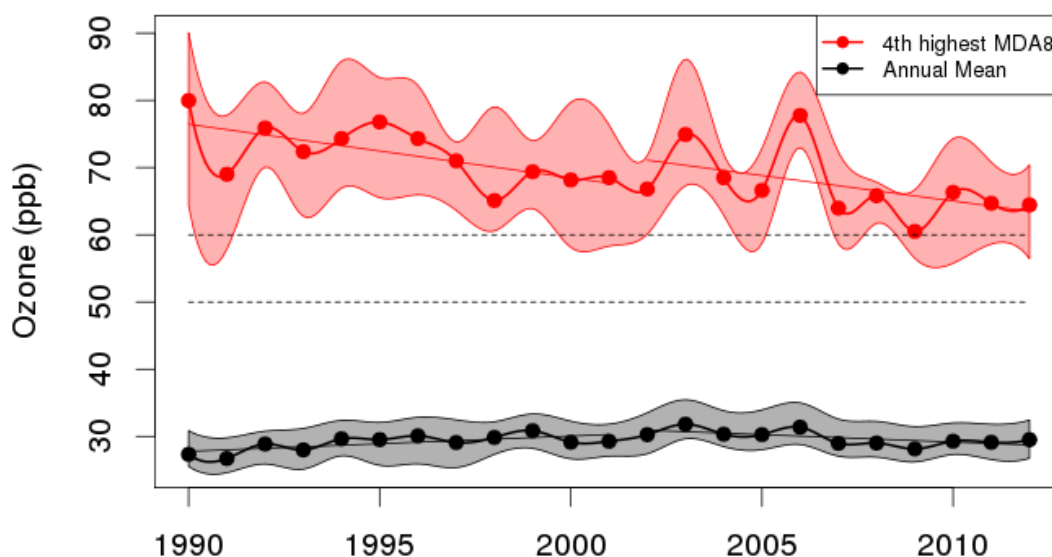
---

<sup>10</sup> Peak ozone is estimated by MDA8- the 4th highest daily maximum of 8 hour running mean O<sub>3</sub> concentrations.

Overall the picture emerges that in Europe and Northern America, declining surface  $O_3$  trends in summer are largely compensated by increasing trends in winter (Gaudel et al., 2018).

The TOAR -Tropospheric Ozone Assessment Report- (Chang et al., 2017; Gaudel et al., 2018) presents the currently most comprehensive worldwide  $O_3$  trend analysis, covering the period 2000-2014. Summertime (April-September) daytime surface  $O_3$  (Fig. 2.3) shows strong reductions in large parts of central Europe, Eastern USA and California, while  $O_3$  strongly increases in Asian regions, downwind of the Asian continent. The  $O_3$  reductions over the Eastern USA are relevant for the inflow over Europe of  $O_3$  in baseline airmasses.  $O_3$  observations since 1977 at Mace Head, a remote station at the western coast of Ireland, have been used to report on increasing  $O_3$  in clean ("baseline") air masses arriving from the Atlantic ocean and not influenced by near-by sources (Simmonds et al., 2004) and have been interpreted as a growing contribution from intercontinental transport. More recently, baseline  $O_3$  remained roughly constant during the 2000s and may have started to decline since 2010 (Derwent et al., 2018).

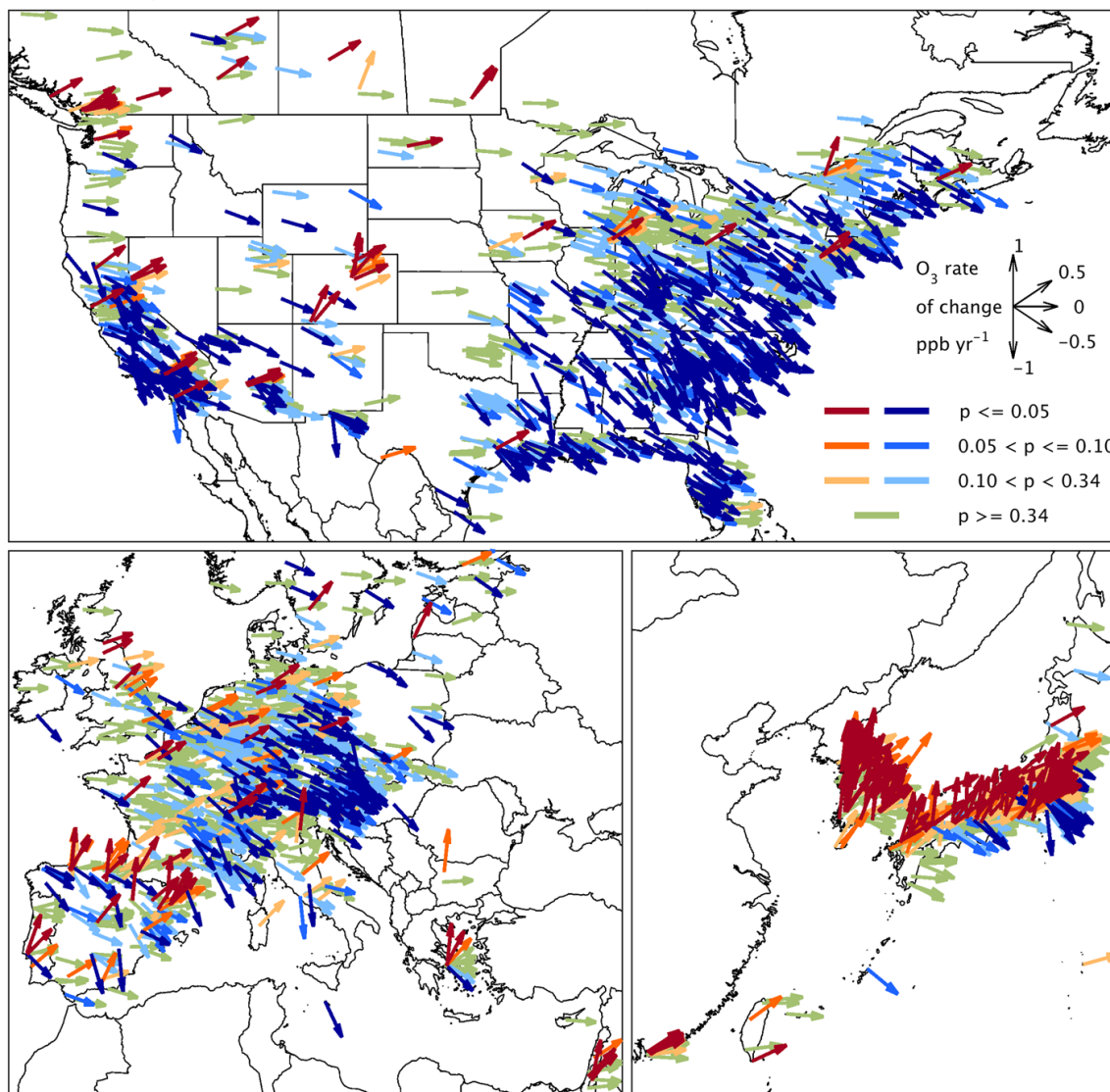
**Figure 2.2.** Evolution of  $O_3$  peak concentrations (4th highest daily maxima 8-hour mean  $O_3$ ; MDA8) and annual mean concentrations at the 54 EMEP European background monitoring stations with satisfactory data coverage. Thick lines indicate the network median and shaded areas the 25th and 75th percentiles. Trend lines are indicative for the periods 1990–2002 and 2002–2012.



Source: CLRTAP Assessment Report (Maas and Grennfelt, 2016)

Satellite-based tropospheric column  $O_3$  retrievals typically detract stratospheric  $O_3$  from total  $O_3$  columns. Different differential methods have been used, and are associated with relatively large errors, but in general indicate a greater tropospheric  $O_3$  column amount in the Northern Hemisphere than in the Southern Hemisphere (Ziemke et al., 2011). Satellite tropospheric column  $O_3$  trend analyses are few, with significant positive trends (2 to 9% per decade) found across broad regions of the tropical South Atlantic, India, southern China, southeast Asia, Indonesia and the tropical regions downwind of China (Beig and Singh, 2007). Trend analysis with a newer generation of satellite data (e.g. OMI and IASI products) reveal broadly similar spatial features, but do not agree on trends (Gaudel et al., 2018), a discrepancy that needs to be resolved to provide robust satellite-based information on tropospheric column  $O_3$  trends with large spatial coverage.

**Figure 2.3.** Trends (2000–2014) of summertime (April–September) daytime average  $O_3$  at available ozone monitoring stations in Europe, North America and Asia (in other world regions very few long-term ozone measurements are available). Vector colours indicate the statistical likelihood (p-values) on the linear trend for each site: blues indicate negative trends, oranges indicate positive trends and green indicates weak or no trend; more likely trends (lower p-values) have greater colour saturation.



Source: Tropospheric Ozone Assessment, Chang et al. (2017); Schultz et al., (2017), DOI:<https://doi.org/10.1525/elementa.243.f1>

### 2.3.2 Model attribution of $O_3$ trends to $CH_4$ emissions

*To what extent can models be used to understand ozone trends and the contribution of  $CH_4$  to these trends?*

Global atmospheric chemistry transport models (ACTMs) are used to simulate past, current and future ozone concentrations. These models ingest spatially resolved emission information, and typically include coarse spatial resolutions of  $1^\circ \times 1^\circ$  to  $3^\circ \times 3^\circ$  longitude-latitude, parameterised descriptions of meteorology and atmospheric transport, oxidation chemistry, and removal processes by wet and dry deposition. Of particular importance for the ozone budget and concentration variability, is the stratosphere-troposphere exchange of ozone, which is subject to large variability and highly uncertain.

Historical 19th century O<sub>3</sub> observations cannot be fully reproduced, with most global models higher than the observations by 5-10 ppb. According to IPCC, this discrepancy is a major factor contributing to uncertainties for calculation of tropospheric ozone radiative forcing (Myhre et al., 2013). Large uncertainties related to the spatial representativeness and accuracy of the past observations, but also a limited understanding of pre-industrial natural emissions, inter-annual variability of stratosphere-troposphere exchange of ozone, and other factors may contribute to these differences between models and observation-based trends.

Using the best available information on air pollutant and CH<sub>4</sub> emission trends, the changes in annual O<sub>3</sub> calculated by a set of HTAP1 global models (Wild et al., 2012), can only explain 30-50% of the observed surface ozone trends from the 1960s to the 2000s (compare to Cooper et al., 2014). However, differences in trends tend to get less in the more recent decades. Indeed regional and global models and observations (supported by an expanded network and better spatial coverage) all indicate relatively constant annual ozone concentrations since the 2000s (fig. 23 of Maas and Grennfelt, 2016; Colette et al., 2017).

*To what extent can the O<sub>3</sub> trends be attributed to CH<sub>4</sub> emissions?*

O<sub>3</sub> is produced by the interaction of sunlight with emissions of nitrogen oxides (NO<sub>x</sub>), carbon monoxide (CO), volatile organic compounds (VOC) and CH<sub>4</sub>. In addition, a substantial part (15-20%) of tropospheric ozone is transported from the stratosphere. Our knowledge of the degradation chemistry of CH<sub>4</sub> and resulting ozone production is based on many decennia of laboratory, field studies and modelling knowledge of a rather uncomplicated chemistry of which the mechanisms are well understood. Nevertheless, the interactions with NO<sub>x</sub> and VOC degradation chemistry, and the resulting radical levels, render an uncertainty of ca. 50% on CH<sub>4</sub> induced O<sub>3</sub> changes over 40 years as calculated by multiple models (Wild et al., 2012). The atmospheric chemistry of ozone is a strongly buffered system: increases in ozone production from rising NO<sub>x</sub>, VOC, or CH<sub>4</sub> emissions, are counteracted by enhanced ozone destruction and shortened ozone lifetimes. The amount of buffering varies among models, and is subject to uncertainty. Model studies indicated that ca. 55% of the ozone budget increases since the pre-industrial era can be attributed to NO<sub>x</sub>, ca. 25% to CH<sub>4</sub>, and 19% to CO and VOCs (Wang et al., 1998) and regionally responses may respond non-linearly according to local conditions. Attribution of ozone changes to sources is useful to understand the past changes and assess the potential to reduce concentrations and impacts. The most frequently used technique to assess the potential of emission reductions to control tropospheric O<sub>3</sub> is to use moderate perturbations (10%-20%) of precursor emissions across different emission sectors.

Using this technique, HTAP1 multi-model analysis (Fiore et al., 2009) showed an annual mean O<sub>3</sub> reduction of 1.1–1.3 ppb averaged over the regions North America, Europe, South Asia and East Asia, for a 20% decrease in global CH<sub>4</sub> concentrations. These O<sub>3</sub> reductions can be compared to regionally and seasonally highly variable surface O<sub>3</sub> observations- ranging from monthly average of 20-35 ppb in winter, and 40-55 ppb in summer (Fiore et al., 2009). Based on these results, and consistent with earlier estimates, they also estimated that currently all anthropogenic CH<sub>4</sub> emissions have contributed 5.5 – 6.5 ppb or 20% to the overall ozone concentration increase<sup>11</sup> since the pre-industrial era. Wild et al. (2012) attributed ca. 1.8 [full model range 1-3; ca. 50% uncertainty] ppb O<sub>3</sub> increase in Europe to global CH<sub>4</sub> emissions trends from 1960-2000. This is about 35% of the overall *modelled* annual O<sub>3</sub> trend in this period and less than 15% of the long-term annual trends *observed* at several surface sites (see above) and

---

<sup>11</sup> Early observations are difficult to interpret and provide not enough coverage to provide a tropospheric average. Northern mid-latitude surface ozone increases from pre-industrial to the 2000s computed by models are about 20 ppb.

about 20-40% of the O<sub>3</sub> trends derived from long-term night-time<sup>12</sup> mountain top observations (Gaudel et al., 2018), representative for changes in the free-troposphere. Therefore, although observations do not provide strong constraints on the contribution of CH<sub>4</sub> to O<sub>3</sub> trends, they also do not contradict the model-estimated contributions from CH<sub>4</sub> to O<sub>3</sub> trends.

In conclusion, currently it is still difficult to establish whether model performance limits our capacity to predict future ozone trends (e.g. Derwent et al., 2018; Parrish et al., 2017). The mismatch of global models to understand ozone trends over the last 4-5 decades may be partly due to spatial representativeness and quality issues with ozone observations, but may also point to limitations of models. In this context, maintaining and expanding the current observational network of rural and remote O<sub>3</sub> concentrations with long time series will be imperative to understand long-term O<sub>3</sub> trends. Although we have relatively good knowledge on the specific contributions of methane to ozone, improving the understanding of the overall ozone budget (ozone production from anthropogenic emissions, natural emissions, stratospheric inflow and deposition processes), will also provide a more convincing case for the role of methane in determining ozone trends.

In the following we assume that our basic knowledge of CH<sub>4</sub> chemistry and trends is sufficient to enable us to assess methane's impact on O<sub>3</sub>.

*What is the policy relevance of the O<sub>3</sub> responses to CH<sub>4</sub> emissions changes?*

Fiore et al. (2002) used a model to estimate that reducing global CH<sub>4</sub> emissions by 50% nearly halved the incidence of high ozone events in the US and is therefore highly relevant for attainment of air quality standards. By combining modelled ozone concentrations with health-impact relationships that also consider exposure of population below the ozone air quality standards (in Europe Maximum daily 8-hour mean ozone of 120 microgram/m<sup>3</sup> or ca. 60 ppb), West et al. (2006) demonstrated that globally about 30,000 less premature deaths per year would result from a 20% reduction in anthropogenic CH<sub>4</sub> emissions. In Chapter 4 of this report, we use the most recent epidemiological evidence to provide updated information. Ozone concentrations around 30-40 ppb and higher are associated with crop yield losses and methane emissions reduction has been identified as a viable method of reducing such losses (West and Fiore, 2005). In Chapter 4 we update these calculations using recent scenarios and ozone metrics.

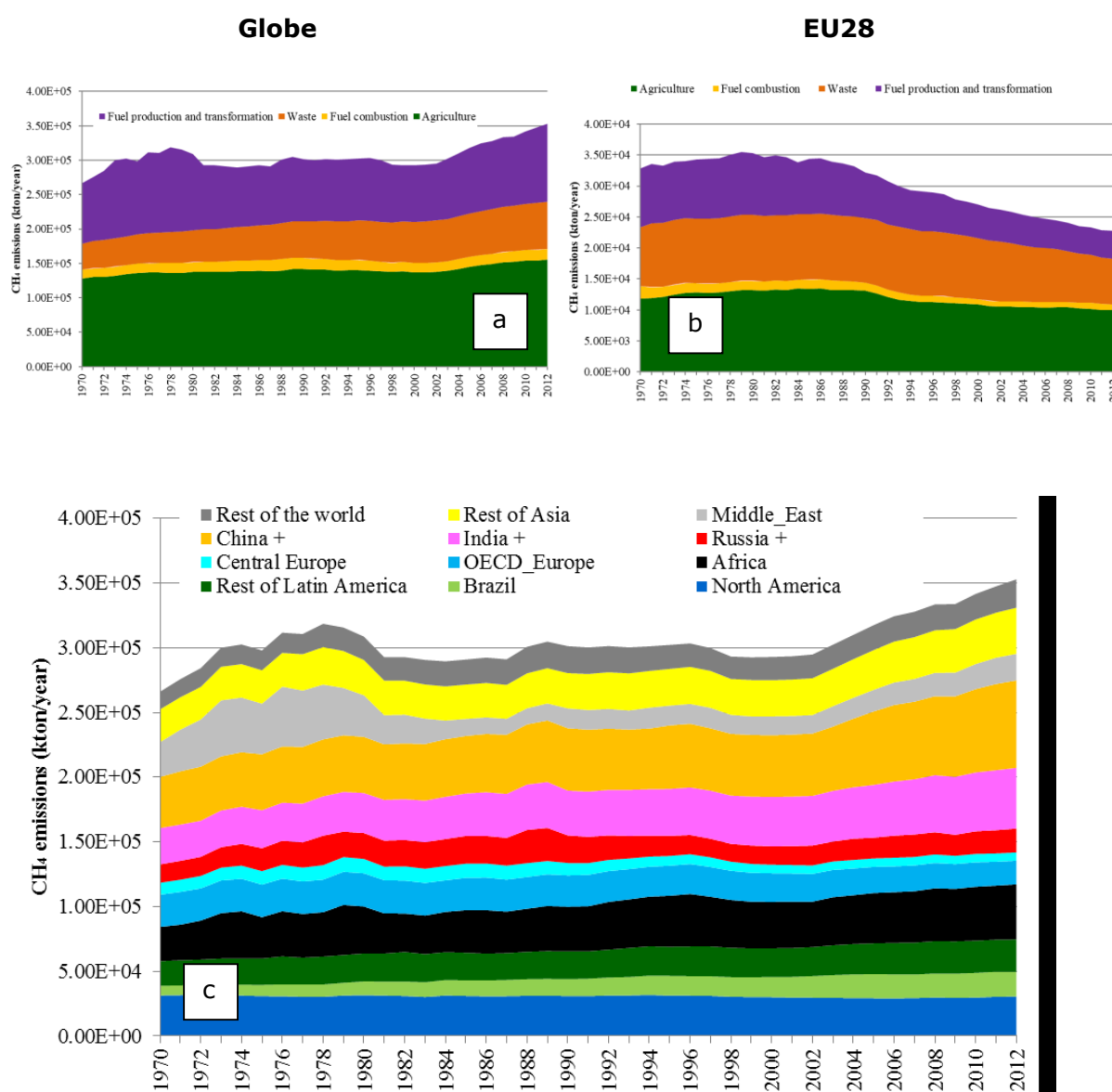
---

<sup>12</sup> Nighttime trends at mountain tops are determined by downward flows from the free troposphere, and are therefore more representative for large scale O<sub>3</sub> changes. CH<sub>4</sub> is expected to exert its influence mostly on these large scales. Of the 8 sites analysed in Gaudel et al. (2018), 6 sites have timeseries starting in the 70s-90s. Of these 6 sites, 5 display positive trends, and 1 negative. Trends differ over seasons.

### 3 Trends of anthropogenic CH<sub>4</sub> emissions

In section 3.1 we use the European Commission's EDGAR global air pollution and greenhouse gas emission database to show the changes of regional and global anthropogenic CH<sub>4</sub> emissions over the last 4 decades, and the growing contribution from new economies to global methane emissions. In section 3.2 we discuss a variety of emission scenarios derived from the CLRTAP air pollution community, RCPs that were used in the IPCC AR5 assessment, as well as 3 marker scenarios (SSPs) that support the IPCC AR6 assessment and scenarios from the European Commissions' Global Energy and Climate Outlook GECO 2017 study (Kitous et al., 2017).

**Figure 3.1.** Methane emissions (kton CH<sub>4</sub> yr<sup>-1</sup>) for (a) the globe, (b) European Union, (c) by world region (region definition Annex 3).



Source: EDGAR4.3.2

### 3.1 Past CH<sub>4</sub> emissions

For our analysis we use EDGARv4.3.2<sup>13</sup> CH<sub>4</sub> emission time series covering the years 1970-2012 and providing consistent emission estimates for all countries worldwide. In previous studies we have demonstrated a good correspondence with CH<sub>4</sub> emissions reported in the UNFCCC national communications (Janssens-Maenhout et al., 2015; Janssens-Maenhout et al., 2017a). Details on the emission methodologies in EDGAR are provided in Annex 1, which also presents a comparison with other widely used emission databases and inventories (GAINS, TNO-MACC and the EU28 GHG inventory). In the following discussion we also contrast EDGAR estimates with those from GAINS and the EU GHG inventory to demonstrate some of the difference in emission databases, and the related uncertainties.

Anthropogenic CH<sub>4</sub> (Fig. 3.1) is mainly released from the agricultural sector (section 3.2.1: enteric fermentation, manure management, waste burning and rice paddies); from the energy sector (section 3.2.2: venting of CH<sub>4</sub> during oil and gas production, and diffusive processes such as coal mine leakage, and gas distribution losses), and landfills and wastewater (section 3.2.3). According to EDGAR, global anthropogenic CH<sub>4</sub> emissions increased by 17% between 1990-2012, compared to a 53% increase in CO<sub>2</sub> emissions. They increased by 16% from 266 to 309 Tg CH<sub>4</sub> yr<sup>-1</sup> between 1970-1980, decreased by 2% from 308 to 301 Tg yr<sup>-1</sup> over the period 1980-1990, decreased by 3% from 301 to 293 Tg CH<sub>4</sub> yr<sup>-1</sup> between 1990-2000, and increased by 20% from 293 to 353 Tg CH<sub>4</sub> yr<sup>-1</sup> between 2000-2012. The latter numbers are well within the emission range of the global synthesis in section 2 provided by Saunio et al., (2016a). Figure 3.2 represents the regional and sectoral distribution of global CH<sub>4</sub> emissions in 2012. Global emissions shares for agriculture, fossil fuel production & transmission and solid waste & wastewater treatment are 44%, 19% and 32%, with large regional differences, as will be discussed below. In comparison GAINS gives larger shares for energy production, and somewhat lower for waste and agriculture (Annex Table A1.2)

#### 3.1.1 Europe, USA and other OECD countries

The 2012 EU28 CH<sub>4</sub> emission shares in EDGAR for agriculture, fossil fuel production & transmission and solid waste & wastewater treatment are, similar to the global emission shares, 44%, 20% and 32%, respectively. For comparison, in 2012 these shares in the EU-GHG inventory (EEA, 2018) were 49%, 19% and 27% respectively, with small differences due to the use of international statistics on activities, and the use of default emission factors in EDGAR.

In EDGARv4.3.2, EU15 CH<sub>4</sub> (the old EU Member States) emissions decreased by on average 0.8% yr<sup>-1</sup> between 1970-2012. An important part of the EU28 CH<sub>4</sub> emission decrease seen is due to the estimated reduction in landfill emissions, by 38% over the period 1990-2012, consistent with the reported EU28 emissions (-36% for 1990-2012). This is in part a direct effect of the more stringent operation of landfills and separation of waste due to the implementation of the EU's landfill directive since the 1990s.

In addition, especially Germany and the UK considerably reduced their coal mining activities (EPTR, 2012), leading to an estimated 96% reduction in their fugitive emissions by 2012 compared to 1990. In the EU28 from 1970-2012, altogether reductions in the fugitive emissions from solid fuels (87% or 7.2 Tg CH<sub>4</sub> yr<sup>-1</sup>) are responsible for the large overall decline by 54% in the energy sector CH<sub>4</sub> emissions, partly compensated by increases in other energy sources (e.g. fugitive emissions from oil and gas +157% or 2.1 Tg CH<sub>4</sub> yr<sup>-1</sup>). For comparison, EEA (2018) reports a decline in the same period of 51% in CH<sub>4</sub> emissions for the energy sector. Reductions in agriculture

<sup>13</sup>([http://edgar.jrc.ec.europa.eu/overview.php?v=432\\_GHG&SECURE=123](http://edgar.jrc.ec.europa.eu/overview.php?v=432_GHG&SECURE=123); [https://data.europa.eu/doi/10.2904/JRC\\_DATASET\\_EDGAR](https://data.europa.eu/doi/10.2904/JRC_DATASET_EDGAR)). Full documentation of this database is presented by Janssens-Maenhout et al. (2017) and summarised in Annex 1. 2012 is the latest year available in EDGAR4.3.2

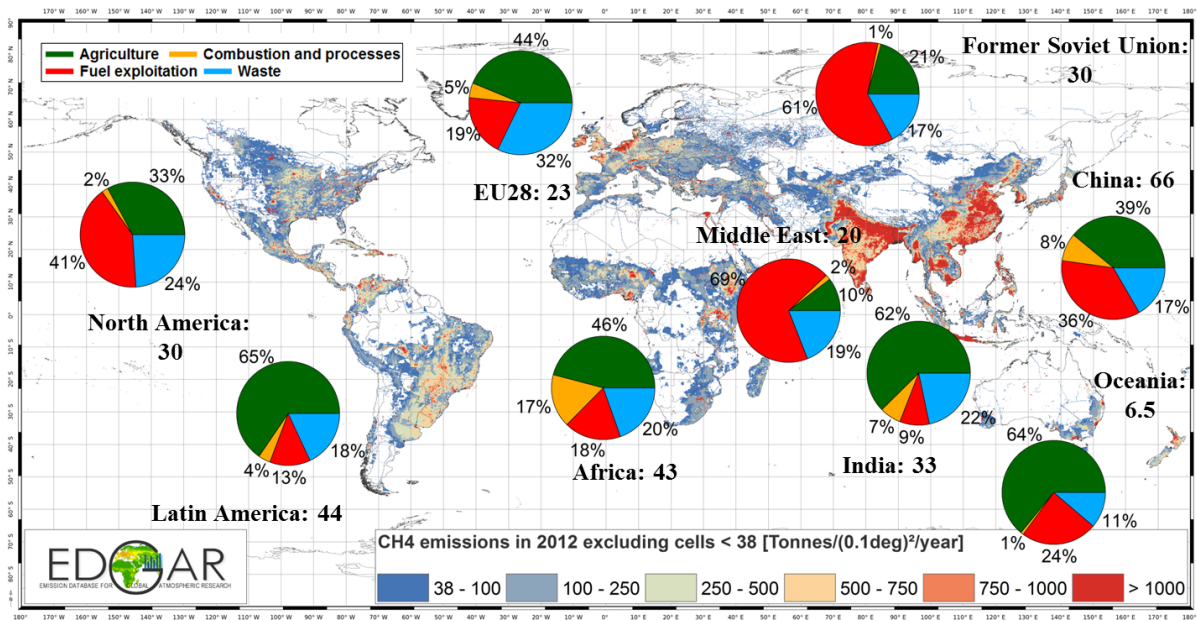
emissions in EDGAR amount to 15% from 1970-2012 and 24% comparing 1990-2012, consistent with the EEA (2018) reported decline of 23% CH<sub>4</sub> emissions in the latter period.

For the group of new (EU13) Member States CH<sub>4</sub> emissions decreased by 0.9% yr<sup>-1</sup> (EDGAR) over the time period 1970-2012, with the strongest emission reduction at the time of the Soviet Union breakup and cease of inefficient and highly polluting activities. Together, the EU28 shows the largest CH<sub>4</sub> emission reductions of all regions in the world in emissions of 0.8% yr<sup>-1</sup> over the period 1970-2012.

In contrast, in the USA, the CH<sub>4</sub> emissions decreased by just 0.2% yr<sup>-1</sup>, from 1970-2012. As in Europe, landfill emissions also substantially declined in the USA, but emissions from fossil fuel production didn't. Despite declining coal mining activities in the USA, increasing emissions from shale oil and gas exploration, in particular since 2007, have more than compensated for the reduction in coal sector emissions.

Unlike the USA and EU15, CH<sub>4</sub> emissions in the remaining OECD countries increased by 0.2% yr<sup>-1</sup> over the period 1970-2012. The three dominant sectors for the 24 industrialised countries of the OECD<sup>14</sup> were in 1990 enteric fermentation (41%), fossil fuel production (28%) and landfills (21%).

**Figure 3.2.** Global CH<sub>4</sub> emissions in 2012 as reported by the EDGARv4.3.2 database with sector specific shares and regional total emissions (Mton=Tg) for major world regions. Gridcells with emissions smaller than 38 tons yr<sup>-1</sup> are not displayed. Definition of EDGAR sectors is given in Annex 1.



Source: EDGARv4.3.2

Table 3.1 gives the EDGAR and GAINS CH<sub>4</sub> regional emissions and their shares for 2012. While the global emissions are similar between the two databases, there are larger differences in regional contributions. According to both databases, China and surrounding regions are in 2012 the dominant and growing emitter of anthropogenic CH<sub>4</sub>. South Asia, Central and South America, Africa, South East Asia, the former Soviet Union, and North America have relatively similar contributions, fluctuating between 9% and 13%. The corresponding GAINS estimates (interpolated to 2012) differ notably for China (48 Tg

<sup>14</sup>OECD countries in 1990: Australia, Austria, Belgium, Canada, Denmark, Finland, France, Germany, Greece, Iceland, Ireland, Italy, Japan, Luxembourg, Netherlands, New Zealand, Norway, Portugal, Spain, Sweden, Switzerland, Turkey, United Kingdom, United States.

CH<sub>4</sub> yr<sup>-1</sup>) due to lower Chinese coal mining emissions in GAINS than in EDGAR), and higher emissions in the middle East and Russia due to higher emissions from oil production in GAINS than in EDGAR (following Höglund-Isaksson, 2017). Comparing EU28 all sector CH<sub>4</sub> emissions in 2012, EDGAR calculates 23 Tg CH<sub>4</sub> yr<sup>-1</sup>, GAINS 17 Tg CH<sub>4</sub> yr<sup>-1</sup>, while the EU GHG inventory (EEA, 2018) reports 19 Tg CH<sub>4</sub> yr<sup>-1</sup>. These differences reflect uncertainties, even for the relatively well-known EU inventory.

**Table 3.1.** CH<sub>4</sub> emissions (Tg CH<sub>4</sub> yr<sup>-1</sup>) and shares<sup>15</sup> (%) by region for EDGAR4.3.2 and GAINS in 2012.

	EDGAR	EDGAR	GAINS
East Asia (China, Korea, Mongolia)	70	19.7%	15.6%
South-Asia (India, Pakistan, Sri Lanka)	47	13.3%	9.8%
Central and South America, Caribbean	44	12.5%	12.1%
Africa	43	12.1%	12.0%
South-East Asia (Indonesia, Philippines, Vietnam)	41	11.7%	11.3%
North America	30	8.6%	11.5%
Reforming economies (former Soviet Union)	30	8.5%	12.5%
Europe (Western and Eastern)	25	7.0%	6.4%
EU28	23	6.5%	5.4%
Middle East	20	5.8%	8.1%
Oceania+Japan	6	2.4%	2.5%

Source: EDGARv4.3.2 and GAINS (Höglund-Isaksson, 2017).

### 3.1.2 Russia, China and India and other countries in transition

Russia's CH<sub>4</sub> emissions are dominated by fossil fuel production and distribution (61%), followed by waste (21%) and agriculture (17%). However, the GAINS model gives a larger share for fossil fuel (79%) and lower for agriculture (7%), the former possibly related to an underestimate in emissions from gas and oil production, and reflecting the large uncertainties associated with natural gas and oil production and distribution.

Due to 3.7-fold increase of the natural gas production activity and two-fold increase in oil production, Russian CH<sub>4</sub> emissions showed a strong increase from 1970-1989, followed by a decrease during 1989-1998 but picking up again from 1998 onwards. Expansion of the pipeline network led to increases in fugitive emissions from the gas transmission pipelines (about 20% of the total gas emissions) and from gas distribution network (about 30%). Since the 1990s, natural gas production has increased, but there has also been investment in better pipeline infrastructure. Russian CH<sub>4</sub> emission trends were further influenced by reduction in enteric fermentation emissions due to a halving of the cattle stock between 1990 and 2000 and a 1.5-fold CH<sub>4</sub> emission increase from landfills between 2000 and 2012.

China is the largest and growing emitter of CH<sub>4</sub> in the world. China's emission profile is dominated by agriculture (39%), fossil fuel production (36%) and waste (17%). The single most important agricultural sector is rice cultivation, with 22% or 14 Tg CH<sub>4</sub> yr<sup>-1</sup> of China's total CH<sub>4</sub> emissions. This is almost four times the CH<sub>4</sub> emissions of rice cultivation

<sup>15</sup> China alone contributes by 66 Tg CH<sub>4</sub> yr<sup>-1</sup> to East Asian emissions. Brazil (19 Tg CH<sub>4</sub> yr<sup>-1</sup>) is the dominant contributor to the Central and South America emissions. Russia contributes by 17 Tg CH<sub>4</sub> yr<sup>-1</sup> to the former Soviet Union emissions. India contributes by 33 Tg CH<sub>4</sub> yr<sup>-1</sup> to South Asian emissions. GAINS data are interpolated between 2010 and 2015. Note that regional aggregations between EDGAR and GAINS may not completely match. Global emissions are 352 Tg CH<sub>4</sub> yr<sup>-1</sup> in EDGAR, and 322 Tg CH<sub>4</sub> yr<sup>-1</sup> in GAINS.

in India (4 Tg CH<sub>4</sub> yr<sup>-1</sup> or 11% in 2012), despite 40% more land being used for rice fields in India than in China. This regional difference is explained by different management practices and production systems. India typically has one harvest per year from ca. one-third rain-fed fields and two-thirds irrigated fields, whereas Chinese rice production is more intensive with two harvests per year from irrigated rice fields and overall 30% higher production. In addition continuously irrigated rice fields emit almost twice as much CH<sub>4</sub> as rain-fed fields.

The moderate increase in total CH<sub>4</sub> emissions in China from 1970 to 2012 is predominantly due to a 6-fold increase in emissions from coal production, partially compensated by a reduction in emissions from rice cultivation of 37% due to the introduction of higher yielding and lower emitting rice varieties.

India, as is the case for China, is a CH<sub>4</sub> emitter of growing world importance. India's emissions are dominated by agriculture (62%), followed by waste (22%) and fossil fuel production (9%). The agricultural CH<sub>4</sub> emissions in India are dominated by enteric fermentation (46% of the 2012 Indian total), and rice cultivation (12%). A moderate increase in total CH<sub>4</sub> emissions by India from 1970 to 2012 is predominantly due to the 80% increase in emissions from enteric fermentation, partially compensated by a reduction in emissions from rice cultivation of 26% similar to that in China. Overall, the CH<sub>4</sub> emission trend from rice cultivation in Asia is relatively constant apart from Thailand.

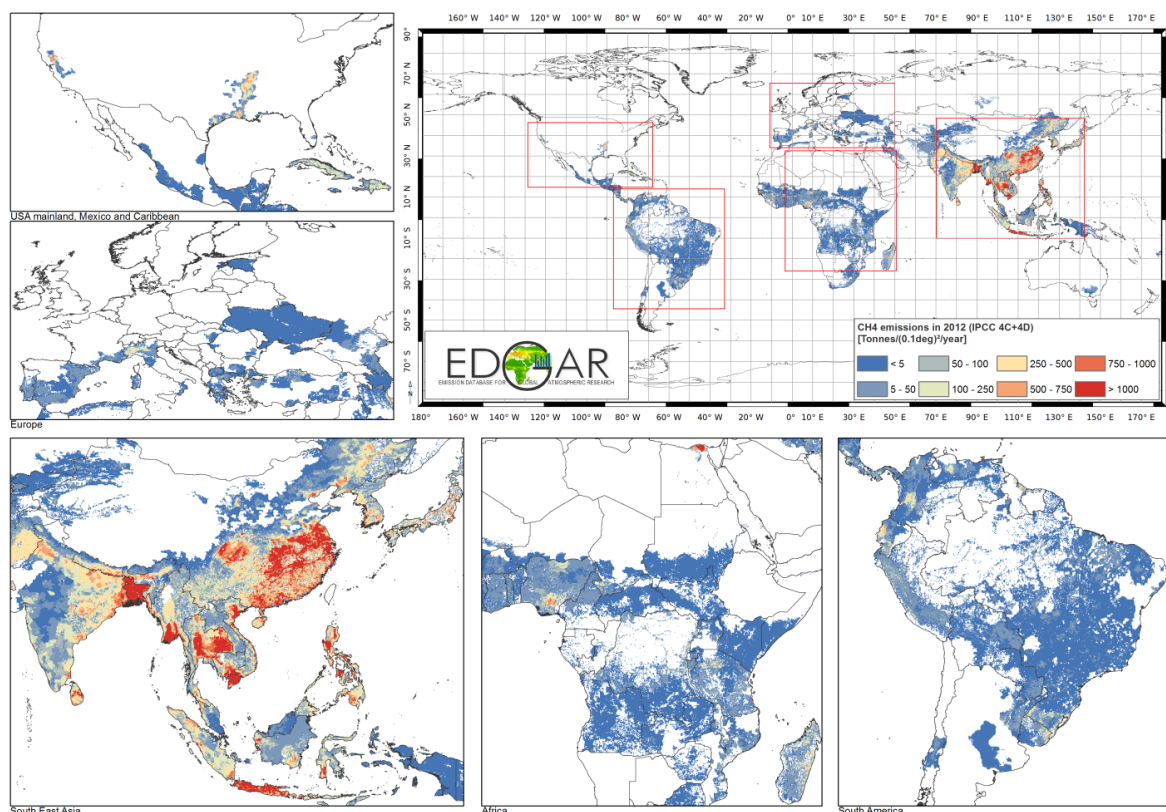
Other developing countries show the highest shares of enteric fermentation and fossil fuel production, but rice cultivation and domestic wastewater together give much higher emissions than solid waste disposal. Emissions from enteric fermentation from African (15.5 Tg CH<sub>4</sub> yr<sup>-1</sup>) and Latin-American (20.9 Tg CH<sub>4</sub> yr<sup>-1</sup>) countries contribute each by ca. 25% and 15% to the global enteric fermentation emissions of 104 Tg CH<sub>4</sub> yr<sup>-1</sup>. Remarkably, enteric fermentation emissions in Brazil almost tripled from 1970-2012. In contrast to Latin America, fossil fuel production in Africa is also a significant contributor to the total CH<sub>4</sub> emissions. Interestingly, both continents show significant CH<sub>4</sub> emissions from charcoal production in the transformation industry sector, 16% and 15% of their total gas and oil production emissions of CH<sub>4</sub> in Africa and Central and South America, respectively and with large emission reduction potential.

## **3.2 Sectoral break-down of the anthropogenic CH<sub>4</sub> emissions**

### **3.2.1 Emissions from agricultural soils, livestock and other agricultural sources**

Global CH<sub>4</sub> emissions from the agricultural sector as a whole were 155 Tg CH<sub>4</sub> yr<sup>-1</sup> (or 44% of the global anthropogenic total) in 2012, with contributions from agricultural soils (primarily rice production) amounting to 38 Tg CH<sub>4</sub> yr<sup>-1</sup> or 11% of the global total, and livestock to 104 Tg CH<sub>4</sub> yr<sup>-1</sup> or 30%. Agricultural waste burning is a minor source with 0.5%, and, manure management represents 3.4% or 12 Tg CH<sub>4</sub> yr<sup>-1</sup> of the global total. Figures 3.3 and 3.4 represent the global distribution of CH<sub>4</sub> emissions from the agricultural soils (mainly rice) and enteric fermentation sectors, respectively, with major contributions from agricultural soils in India, China and Asia, and important contributions from enteric fermentation in Europe, USA and Latin America. Global rice emissions declined by 22% from 1970-2012, accompanied by an increase in production of a factor 2.3 (FAOSTAT, 2014).

**Figure 3.3.** CH<sub>4</sub> emissions from agricultural soils (mainly rice production) in 2012



Source: EDGAR v4.3.2

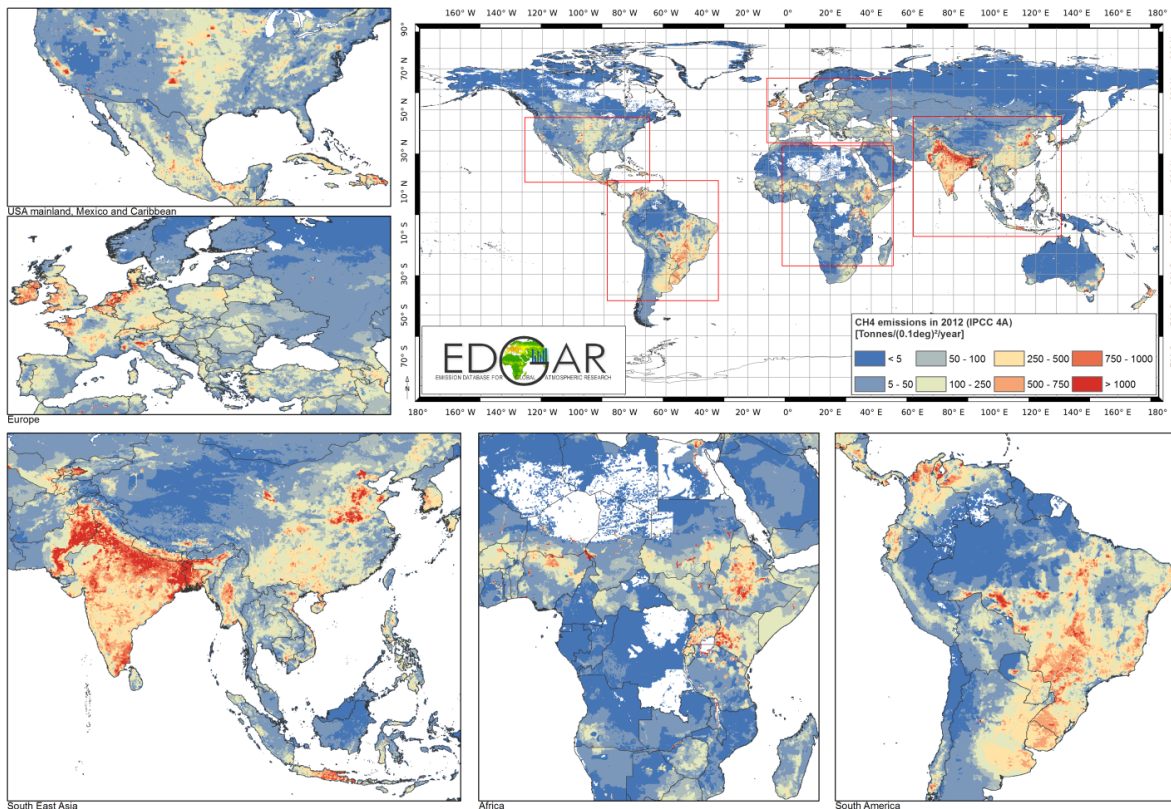
Livestock is a dominant source of GHG emissions. In the EU28, the EU GHG inventory (EEA, 2018) reports that enteric fermentation is responsible for about 81% of the agricultural CH<sub>4</sub> emissions, manure for 17%, while contributions from rice cultivation are about 1%. These ratios are rather constant between 1990-2016. Life cycle analysis using the CAPRI model (Leip et al., 2015) estimates that including the GHG (i.e. CH<sub>4</sub>, N<sub>2</sub>O, CO<sub>2</sub>) emissions related to agriculture in energy, industry or land-use, would more than double the agricultural emissions, with livestock responsible for 81% of the overall GHG emissions.

According to the Medium-term outlook for the EU and agricultural commodity markets (EU Agricultural Outlook, 2017), by 2030 agricultural CH<sub>4</sub> emissions are expected to decline moderately by 6% compared to 2008 while overall GHG emissions (including N<sub>2</sub>O) decrease less (1.5%).

### 3.2.2 Fugitive emissions from fossil fuel production, transport by pipelines and other energy industries

Global fugitive methane emissions from fossil fuel production and transmission were 107 Tg CH<sub>4</sub> yr<sup>-1</sup> in 2012, representing 32% of the estimated global total anthropogenic CH<sub>4</sub> emissions. An increase in CH<sub>4</sub> emissions from charcoal production in the transformation industry (1B1b) (representing 1.3% of global CH<sub>4</sub> emissions) is seen in particular in African countries and China, with a global increase of 2.6 times over the period 1970-2012 from this sector. The need for reducing emissions from charcoal production to mitigate climate change and improve local livelihoods is addressed in a recent FAO (2017) report. Other energy-related emissions (Annex A.1) add marginally to this number.

**Figure 3.4** CH<sub>4</sub> emissions from enteric fermentation in 2012



Source: EDGAR v4.3.2

The green frames in Fig. 3.5 shows the regions of intense coal mining and the blue circles venting from gas & oil production dominating the fossil fuel production emissions. Venting and flaring is an important source of CH<sub>4</sub> in specific regions, contributing globally to 6.5% of total CH<sub>4</sub> in 2012, but up to 25.1% in Middle East, 18.4% in Russia and 10.7% in USA. Such high fuel exploitation regions are important candidates to develop effective emission reduction policies. Fugitive emissions of CH<sub>4</sub> from oil and gas production, transmission and distribution are another rapidly changing and challenging source to quantify. In North America over the period 2005-2012 a shift from coal mining in the North-East (-21%) to gas & oil production in North-Dakota, Montana and Texas in particular (+65%) took place. The USA has become the world's largest producer of both shale gas and tight oil, which together make up almost half of total US gas and oil production (IEA, 2017). By 2017 the US has already become a net exporter of gas, and may also become a net exporter of oil in the next decade (IEA, 2017). In Europe a much larger 87% reduction in coal production emissions occurred from 1970-2012 (mainly in the late 1980s), while gas production in this period increased by 30% (but declining more recently; EUROSTAT 2017). Consequently, the EU28 increasingly relied on oil and gas imports and expanded its transmission and gas distribution network with corresponding increase in CH<sub>4</sub> leakage along the entire distribution chain. Aside from the USA, the Middle East is also a global world player on the oil and gas market, shifting from oil production (40% decrease over 1976-1985) to gas production (9.3-fold increase from 1985 to 2012), mainly driven by Iran, Saudi Arabia and Qatar. African countries with the highest CH<sub>4</sub> emissions from fossil fuel production are in decreasing order of importance Algeria and Nigeria (emissions from oil and gas production) and South Africa (emissions from coal mining). Nigeria in particular has approximately doubled its CH<sub>4</sub> emissions from oil (and gas) production over the last 4 decades.

In Latin America, Mexico and Venezuela both showed increasing CH<sub>4</sub> emissions from oil and gas production by a factor of 1.6 over the 4 decades. Russia's gas and oil production

shows the world's largest CH<sub>4</sub> venting and leakage emissions, overtaking the USA in importance in 1985. Several studies, e.g. Lyon et al. (2015) or Peischl et al. (2015), suggest that CH<sub>4</sub> emissions from this sector could be higher than currently estimated (see also section 2.2 for global studies).

Methane can be trapped underground when organic strata are converted over time into coal. Fugitive emissions of CH<sub>4</sub> may therefore occur during mining operations and venting is part of normal safety operations. Coal mining has become important for China, which since 1982 has become the largest bituminous coal producer in the world, overtaking the USA. China is also the largest coal importer since 2011 (overtaking Japan), as domestic coal produced in mainly the western and northern inland provinces of China faced a transportation bottleneck, lacking southbound rail lines (Tu, 2012) towards the southern coast that has the highest coal demand. CH<sub>4</sub> emissions from coal mining activities in China increase by 6.1 times from 1970 to 2012, representing 32% of Chinese CH<sub>4</sub> emissions in 2012, with emission factors in the oil and gas production and distribution sectors are subject to particularly high uncertainties.

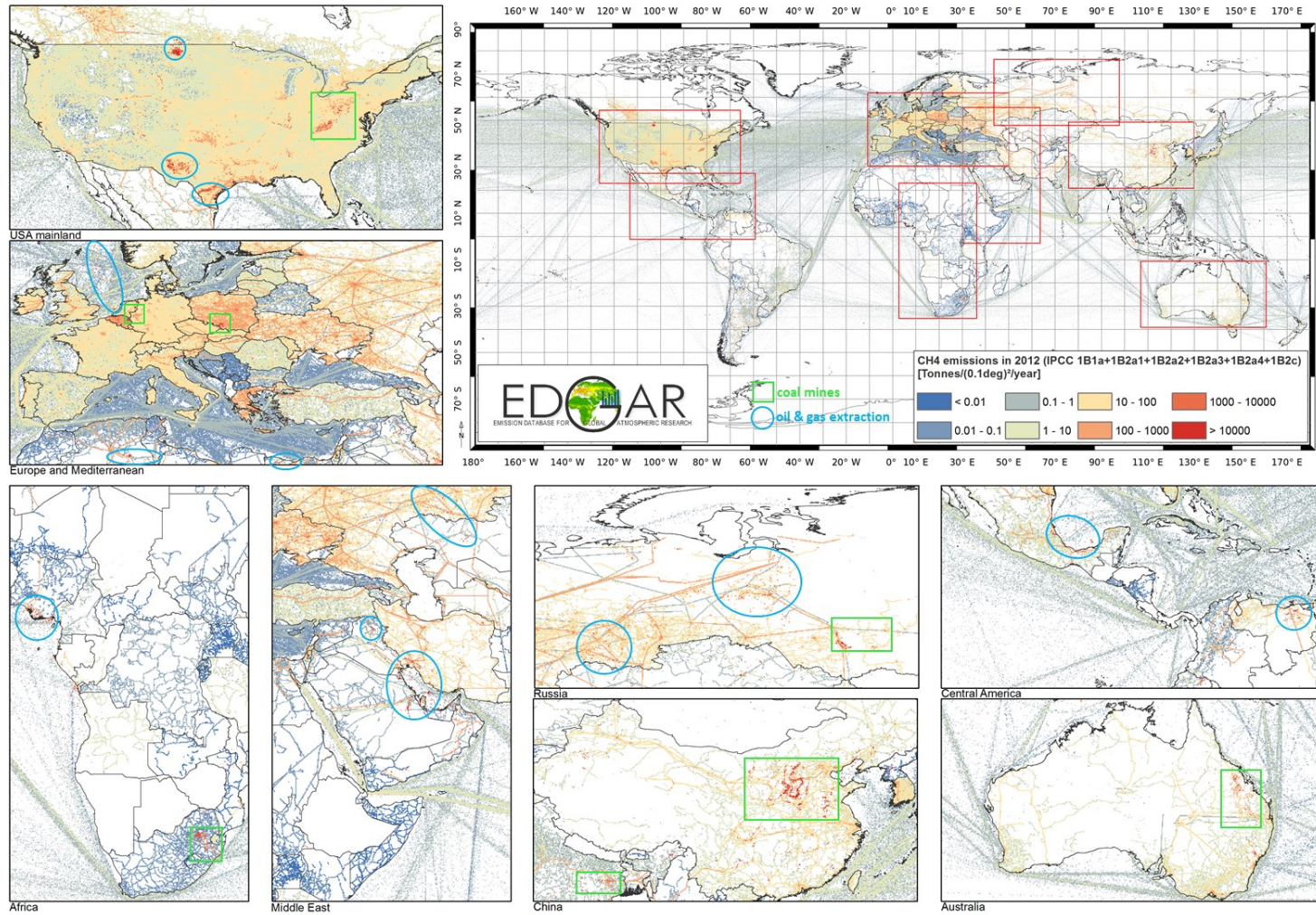
### **3.2.3 Solid waste and waste water emissions**

Solid waste and waste-water CH<sub>4</sub> emissions globally amount to 69 Tg CH<sub>4</sub> yr<sup>-1</sup> (or 19% of the global total) in 2012. Landfills emissions decreased in EU28 by 31% from 1970 to 2012, in particular in Germany, Great Britain and the Netherlands. Over the same time period, we find 20% reduction also in the USA while emissions strongly increased in China, India, Middle East, Russia and Turkey. Emissions from waste water handling in the EU28 from 1970 to 2012, ranged from 1.7 to 1.9 Tg CH<sub>4</sub> yr<sup>-1</sup>, while emissions increased in China and India by 1.9 and 2.4 times from 1970-2012, respectively.

### **3.2.4 Other remaining sources**

Other remaining sources are related to production processes of chemicals, iron and steel, the manufacturing industry, fossil fuel fires (e.g. Kuwait fires), transformation industry and ground transport (road, inland shipping, and rail) residential and other sectors in 2012 amount to 14.6 Tg CH<sub>4</sub> yr<sup>-1</sup> (4.1% of the global total of which 3.9% from the residential sector).

**Figure 3.5.** CH<sub>4</sub> emissions from fossil fuel production in 2012 with zoom on areas with intense coal mining (green frame) and gas & oil production activities with venting (blue circle). Ship tracks show minor CH<sub>4</sub> leakage during crude oil and natural gas liquids tanker transport



Source: EDGARv4.3.2

### 3.3 Future CH<sub>4</sub> emissions

Future methane emissions will depend on a range of economic, technological, societal and political developments. In section 3.3.1 we first provide an overview of available mitigation options in several key-sectors and provide a ranking of current methane emissions in the fossil fuel production sector. In section 3.3.2 we select and discuss a range of scenarios to explore a range of possible future methane trajectories currently used by the air pollution and climate communities.

#### 3.3.1 Mitigation potentials

Table 3.2 provides an overview of technological control measures in a number of key-sectors, based on the recent assessment of sectoral CH<sub>4</sub> emission reduction potentials provided by the Arctic Monitoring and Assessment (AMAP) Report (Höglund-Isaksson et al., 2015), and EDGAR data. Below we discuss a selection of control measures and mitigation options based on the relevance for European and global emissions. It is important to notice that the mitigation options can be separated in two broad sets of factors. Production/consumption factors where less energy, waste, and animal/crop production lead to lower emissions, and technological control measures improvements can lead to lower emissions per unit of production.

**Table 3.2.** Technically feasible control measures for CH<sub>4</sub> emissions in a number of key-sectors.

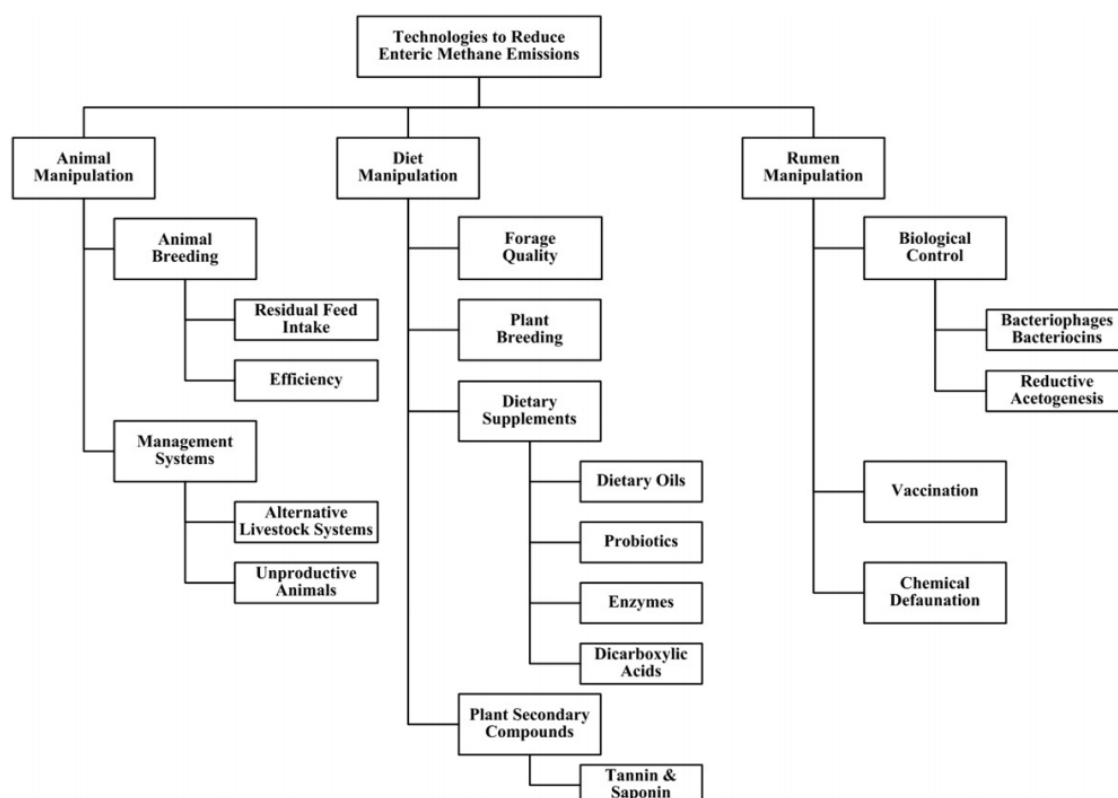
Sector	Control measure
<b>Livestock</b>	Enteric fermentation: diet changes, vaccination
	Improving animal health and productivity: genetic improvement, diet changes
	Manure management: anaerobic digestion, direct injection in soils of liquid manure.
<b>Rice cultivation</b>	Mixed: interrupted flooding and alternate wetting and drying, alternative hybrids, sulfate amendments
<b>Agricultural waste burning</b>	Ban on burning.
<b>Solid waste</b>	Maximum separation and treatment, no landfill of biodegradable waste
<b>Wastewater</b>	Extended treatment with gas recovery and utilization
<b>Coal mining</b>	Pre-mining degasification
	Ventilation air oxidizer with improved ventilation systems
<b>Conventional natural gas production</b>	Recovery and utilization of vented associated gas
	Good practice: reduced unintended leakage
<b>Unconventional natural gas production</b>	Good practice: reduced unintended leakage
<b>Long-distance gas transmission in pipelines</b>	Leakage control, especially at the pumping units
<b>Gas distribution networks</b>	Leakage control and replacement of grey cast iron networks
<b>Oil production and refinery</b>	Recovery and utilization of vented associated gas
	Good practice: reduced unintended leakage

Source: Höglund-Isaksson et al. (2012; 2015)

### Agricultural sector.

Emission reductions in agricultural production with different methods and consumer's food preference changes are the potential ways of reducing CH<sub>4</sub>. As discussed in section 3.2.1, global emissions from rice have declined by 22% between 1970-2012, while production increased with a factor of 2.3. For rice, management practices for cultivation as well as changes in varieties can further reduce CH<sub>4</sub> emissions (Yan et al., 2009; Li et al., 2002; Adhya, et al., 2014; Peng et al., 2016). An important source of CH<sub>4</sub> emissions is ruminant enteric fermentation, which can be reduced e.g. through adjustment of animal's diets and vaccination (Eckard et al., 2010; Hristov et al., 2013), see Fig. 3.6. Manure management, e.g. using anaerobic digesters, provides a further opportunity to reduce methane emissions.

**Figure 3.6.** Control measures for enteric CH<sub>4</sub> in ruminants



Source: Literature review by Eckard et al., 2010

There are relatively few studies that provide quantitative evaluation of *global* mitigation potential. Optimistic mitigation scenarios discussed in section 3.3.2 project a decrease in CH<sub>4</sub> emissions in the agricultural sector of only 40% or less by 2030. A scenario study by Höglund-Isaksson (2012) indicates by 2030 a modest mitigation potential of technological options amounting to globally 13 Tg CH<sub>4</sub> yr<sup>-1</sup> (or 9% of the agricultural total) for agricultural rice and livestock production together, which can be split between a 3% reduction in the livestock sector and a 31% reduction in emissions from rice.

For the *EU28*, the JRC EcAMPA2 study (Pérez Domínguez et al., 2016) performed an economic evaluation of about 12 agricultural GHG mitigation technologies, including methane farm-scale and community-based anaerobic digestion methods, vaccination, and changes in the composition of animals diets (feed) that specifically affect CH<sub>4</sub> emissions. ECAMPA2 indicated that subsidies to support GHG reduction targets, could avoid production losses, as well as emission leakage to foreign regions.

Among the technologies affecting CH<sub>4</sub> emissions, anaerobic digestion, feed additives and vaccination, accounted in ECAMPA2 for ca. 30% of the overall emission GHG reductions. ECAMPA2 results are highly dependent on the implementability of these technologies and other uncertainties<sup>16</sup>.

Increasing animal health and productivity (in terms of protein produced) are identified by FAO as successful strategies to mitigate GHG emissions (Gerber et al., 2013; Hristov et al., 2013). Increases in productivity, especially in Eastern Europe, are indeed projected in Europe to contribute to declining CH<sub>4</sub> emissions (EU Agricultural Outlook, 2017).

Another option to reduce CH<sub>4</sub> emissions from the agricultural sector is through change in consumers' food preferences towards reducing consumption of meat and milk products (Hedenus et al., 2014; Westhoek et al., 2015). Life-cycle analysis indicates large differences in GHG emissions for the same product, and substantial mitigation opportunities along the whole supply chain (Poore and Nemecek, 2018). Vegetable substitutes always cause less GHG emissions than the lowest impact animal product. In Europe, a shift by -50% in meat and dairy consumption would reduce CH<sub>4</sub> emissions by 45% and overall GHG agricultural emissions by ca. 20-40%. While worldwide per capita animal products protein consumption was increasing from 22 g capita<sup>-1</sup> day<sup>-1</sup> in 1970 to 32 g capita<sup>-1</sup> day<sup>-1</sup> in 2012 (FAOSTAT, 2014), the animal products protein consumption in the EU28 is plateauing around 60 g capita<sup>-1</sup> day<sup>-1</sup> since 2000, which is about 60% of the total protein consumption, and on average substantially above the recommended daily protein intake<sup>17</sup>. In this context, large efforts will be needed to achieve substantial reductions in meat and dairy consumption.

#### *Waste and wastewater.*

Large regional differences between developed and developing countries of CH<sub>4</sub> emission factors from wastewater in EDGAR4.3.2 are shown in Table 3.3. For example in large parts of Europe domestic wastewater sanitation is common practice, where sewage is treated in dedicated plants. Industrial wastewater is treated on-site in waste water treatment plants. In developing countries public or open pit latrines or improved latrines are emitting much more CH<sub>4</sub>.

EPA (2013) identifies several abatement measures to control landfill emissions. The global abatement potential in the solid waste landfill sector by 2030 is estimated to be approximately at 61% of the baseline emissions, of which 12% at relatively low or zero costs, and 49% at increasingly higher costs.

---

<sup>16</sup> Follow-up work will address in more detail the effects of emission leakage, cost, benefits and uptake barriers for mitigation measures. The assumed GWP100 for CH<sub>4</sub> in ECAMPA2 was 21, while for policy negotiations a value of 25 is used. Using the more recent IPCC AR5 (Myhre et al., 2013) GWP-100 value of 28 would increase the relevance of CH<sub>4</sub> by 33 %. See section2.

<sup>17</sup> Recommended daily protein intake range from 0.80 to 0.83 g per kilogram of body weight for both men and women with modest levels of physical activity. An adult of 70 kg would need ca. 56-58 g protein. <https://ec.europa.eu/jrc/en/health-knowledge-gateway/promotion-prevention/nutrition/protein>. Accessed August 2018.

**Table 3.3.** Implied waste water emission factors in ton CH<sub>4</sub>/kton organic degradable material (BOD).

Waste Water	
Eastern Africa	317.6
Western Africa	315.7
India + <sup>a</sup>	220.5
Southern Africa	180.7
South-eastern Asia	178.7
Turkey	167.5
Mexico	161.7
Northern Africa	147.5
Rest Central America	128.4
Asia-Stan <sup>b</sup>	123.7
China + <sup>c</sup>	113.7
Indonesia + <sup>d</sup>	107.9
Middle East	91.1
Rest South America	90.1
Brazil	79.9
Korea	65.2
Russia + <sup>e</sup>	47.8
Ukraine + <sup>f</sup>	42.0
Central Europe	35.4
Oceania	18.3
OECD Europe	17.6
USA	8.2

<sup>a</sup> India +: India, Afghanistan, Bangladesh, Bhutan, Sri Lanka, Maldives, Nepal, Pakistan

<sup>b</sup> Asia-Stan: Kazakhstan, Kyrgyzstan, Tajikistan, Turkmenistan, Uzbekistan

<sup>c</sup> China +: China, Hong Kong, Taiwan, Macao, Mongolia

<sup>d</sup> Indonesia +: Indonesia, Papua New Guinea, East Timor

<sup>e</sup> Russia +: Russian Federation, Armenia, Azerbaijan, Georgia

<sup>f</sup> Ukraine +: Ukraine, Belarus, Republic of Moldova

Source: EDGAR4.3.2.

#### *Fossil fuel production.*

Globally there is considerable technical abatement potential for methane emissions from fossil fuel production in several production sectors and using several technologies. Table 3.4 provides an overview of regional variation in production-based emission factors using EDGAR4.3.2 data. For coal production, regional differences of implied emission factors vary by a factor of 8 or more. Coal extraction is assumed to be more efficient in Europe and USA than in China and Russia due to the coal quality (more hard coal and good quality bituminous coal; Janssens-Maenhout et al., 2017a). Recovery of CH<sub>4</sub> from underground mining before starting up the operation is nowadays implemented by most of the main producer countries, however large-scale recovery/oxidation of ventilation air during operation is not routinely installed, nor is it applied to surface open-cast mining. Future work can include recent data base information on Chinese coal mine characteristics, released in the framework of the 2019 IPCC refinement of national GHG inventory report guidelines (IPCC, 2006).

**Table 3.4.** Fuel exploitation metrics in 2012 ranked from high-to-low. Coal, combined oil and gas production, gas transmission and distribution. n.a. (not applicable).

Coal production ton CH <sub>4</sub> TJ <sup>-1</sup>		Venting from oil and gas production ton CH <sub>4</sub> TJ <sup>-1</sup>		Gas transmission ton CH <sub>4</sub> km <sup>-1</sup> yr <sup>-1</sup>		Gas distribution ton CH <sub>4</sub> km <sup>-1</sup> yr <sup>-1</sup>	
Korea	0.58	Western Africa	0.38	India +	7.0	Central Europe	2.6
Northern Africa	0.57	Asia-Stan	0.18	Turkey	7.0	Ukraine +	2.1
Eastern Africa	0.57	Southern Africa	0.17	Rest Central America	7.0	Russia +	2.1
Western Africa	0.55	Northern Africa	0.14	Rest South America	7.0	Asia-Stan	1.4
Middle East	0.52	Eastern Africa	0.12	South-eastern Asia	7.0	Oceania	1.4
South- eastern Asia	0.49	Canada	0.11	Indonesia +	7.0	OECD Europe	0.9
Brazil	0.47	Indonesia +	0.09	China +	7.0	Indonesia +	0.8
Ukraine +	0.42	Rest South America	0.08	Eastern Africa	7.0	Middle East	0.8
Asia-Stan	0.30	Middle East	0.08	Middle East	7.0	Northern Africa	0.8
Russia +	0.29	USA	0.07	Western Africa	7.0	Canada	0.7
China +	0.27	Russia +	0.07	Asia-Stan	7.0	India +	0.7
Indonesia +	0.25	South- eastern Asia	0.06	Mexico	7.0	South-eastern Asia	0.7
India +	0.21	Mexico	0.05	Brazil	7.0	China +	0.7
Central Europe	0.20	Ukraine +	0.04	Northern Africa	7.0	Brazil	0.7
Southern Africa	0.20	Brazil	0.03	Southern Africa	7.0	Rest South America	0.7
Turkey	0.18	China +	0.03	Korea	7.0	Rest Central America	0.7
USA	0.15	Central Europe	0.03	Russia +	6.4	Korea	0.6
OECD Europe	0.14	Oceania	0.01	Oceania	3.4	Mexico	0.6
Oceania	0.14	Rest Central America	0.01	Canada	2.9	Turkey	0.5
Mexico	0.12	India +	0.01	USA	2.8	USA	0.4
Rest South America	0.09	Turkey	<0.01	Central Europe	2.8	Japan	0.2
Canada	0.07	OECD Europe	<0.01	Ukraine +	2.5	Southern Africa	n.a.
Rest Central America	<0.01	Japan	<0.01	OECD Europe	1.4	Eastern Africa	n.a.
Japan	<0.01	Korea	n.a.	Japan	0.3	Western Africa	n.a.

Source: EDGAR4.3.2

CH<sub>4</sub> emissions from venting of oil/gas extraction sites per production volume (expressed in energy content of the oil/gas) vary by a factor of 40, and are largest in developing regions in Africa and central Asia, while values in the range of 0.03-0.08 ton of CH<sub>4</sub>/TJ are calculated for North America, Europe, China and Russia.

Differences reflect the assumptions on type and age of infrastructure, leak detection and maintenance. Measurements around gas fields in the Netherlands, indicate that production volume alone – used as activity data in most inventories – is not necessarily a good indicator for methane emissions (Yacovitch et al., 2018), as sites that are shut down may still be emitting. As mentioned in chapter 2, similar uncertainties pertain to the United States (Alvarez et al., 2018). Unfortunately, in many cases published emission factors are not available, rendering these numbers highly uncertain, and more studies are needed to link local CH<sub>4</sub> measurements to CH<sub>4</sub> emission inventories.

Very little data is available on CH<sub>4</sub> emissions from gas transportation in pipelines (transmission). In EDGAR annual emissions range between 0.3-7 ton/km, with lowest values assigned for the OECD countries with the newest and best maintained infrastructure. CH<sub>4</sub> losses from gas distribution differ with a factor of 10 and are highest in countries with the oldest gas distribution systems. These old pipeline systems, which were leak-tight for wet gas, become leaky with a shift to dry gas. Altogether the largest mitigation potential is found in countries characterised by old production and distribution infrastructure and technology, prone to gas leakages

### 3.3.2 Emission scenarios

Projected CH<sub>4</sub> emissions for the coming decades strongly depend on the socio-economic narrative adopted, including assumptions on economic development, technological development and regional disparity as well as the political and societal willingness to abate greenhouse gas and air pollutant emissions. In this section, we focus on global scenarios, and we discuss four sets of commonly used scenario families, developed by the climate and air pollution communities. In this section a short description of the scenarios and emission results is presented, and a more comprehensive description of the scenario families and assumptions is given in Annex 2. While it is beyond the scope of this study to assess all the driving factors included in the scenarios, we will give some examples of drivers for the well-documented SSP scenario family.

The four scenario families are:

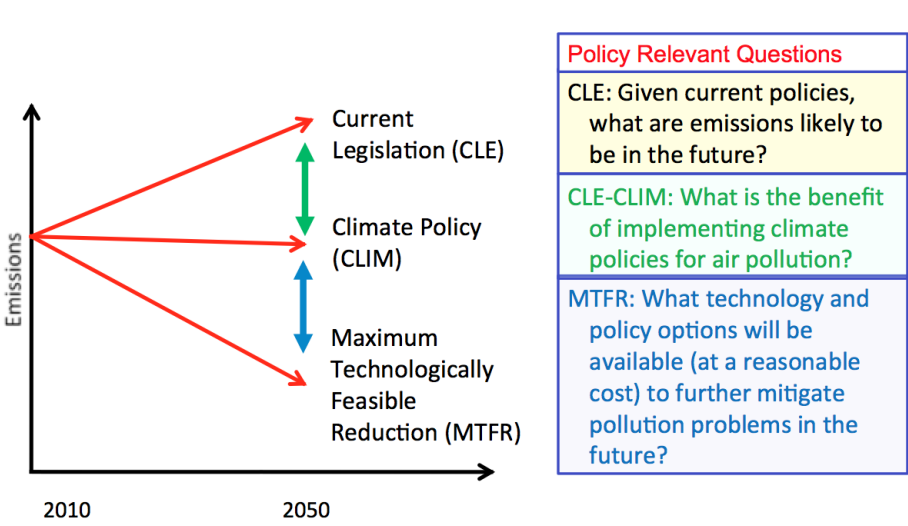
- (a) The ECLIPSE v5a scenario set project (Stohl et al., 2015; available on-line at <http://www.iiasa.ac.at/web/home/research/researchPrograms/air/ECLIPSEv5a.html>). The ECLIPSE emission set was created with the GAINS model (Amann et al., 2013), which provides emissions of long-lived greenhouse gases and short-lived pollutants in a consistent scenario framework (see Figs. 3.7 and 3.8, and Table 3.5). ECLIPSEv5a was used in a number of scientific studies, and at the basis of the analysis performed by the Task Force Hemispheric Transport of the UNECE CLRTAP.
- (b) The Representative Concentration Pathways (RCPs), which were developed for the IPCC's fifth Assessment Report (AR5, van Vuuren et al., 2011) and widely used in the scientific literature of the past decade. We discuss the marker scenarios RCP8.5, RCP6.0, and RCP2.6, corresponding to median global temperature increases by the end of the century of 4.2 °C, 2.7 °C and 1.6 °C, respectively (see Table 3.6, Fig. 3.9)
- (c) The "Shared Socioeconomic Pathways" (SSP) scenario family. The SSPs are part of a new framework that the climate change research community has adopted to facilitate the integrated analysis of future climate impacts, vulnerabilities, adaptation, and mitigation and informing the forthcoming IPCC 6<sup>th</sup> assessment report (AR6). The framework is built around a matrix that combines climate forcing on one axis (as represented by the RCPs) and socio-

economic conditions on the other. Together, these two axes describe situations in which mitigation, adaptation and residual climate damage can be evaluated (see Box 2). Of the full set of possible SSP CH<sub>4</sub> trajectories, we choose 3 scenarios, encompassing the fuller range of outcomes: SSP3-Baseline-without climate policies, SSP2-60 Middle of the road scenario, and the SSP1-26 climate mitigation scenario (Table 3.7 and Fig. 3.10).

(d) To inform European policy makers, the Global Energy and Climate (GECO, Kitous et al., 2017) scenario's provide regular assessments on climate issues and are based on socio-economic projections of the European Commission. The most recent assessment focussed on the full implementation of the pledges under Paris Agreement and the co-benefits for air quality (Table 3.8 and Fig. 3.11)

Considerable efforts have been made to better document and understand the underlying assumptions on driving factors. Figure 3.7 shows a conceptual example of the ECLIPSE scenarios computed with the GAINS model that is representative for some of the other modelling frameworks. Typically emission scenarios make assumptions on the full or partial implementation of Current air quality LEgislation (CLE). An additional scenario assumption can be that in the future the currently best available technologies will be fully implemented- called MTFR (Maximum Technologically Feasible Reduction). Climate policies (e.g. Paris agreement pledges, or 1.5 or 2 degree objectives) will impact GHG emissions, and have co-benefits for air pollutants. The actual differences between CLE and MTFR will be determined by economic factors (mitigation costs), and political and societal preparedness to implement these technologies. Generally technological developments such as new, currently not existing, technologies that may further reduce emissions are not included in MTFR, but they may be partly driving other scenarios.

**Figure 3.7.** Eclipse v5a Air pollution benchmark scenarios



Source: TF-HTAP (Dentener et al., 2010)

Figures 3.8 to 3.11 show that different scenario assumptions lead to very different developments of emissions changes in the energy, waste and agriculture sectors. Table 3.9 groups the scenarios in high, medium and low emission scenarios until 2050. The high scenarios are typically characterised by emissions increases of 150 to 250%. Global emissions in the middle group of scenarios remain close to those in 2010. In the low-emission scenario group emissions reductions of 50% or more are typical. Figure 3.12 shows the overall emission trajectories from 2010 to 2050 and a comparison with EDGAR global emissions prior to 2013. Emissions in the high-emissions group typically

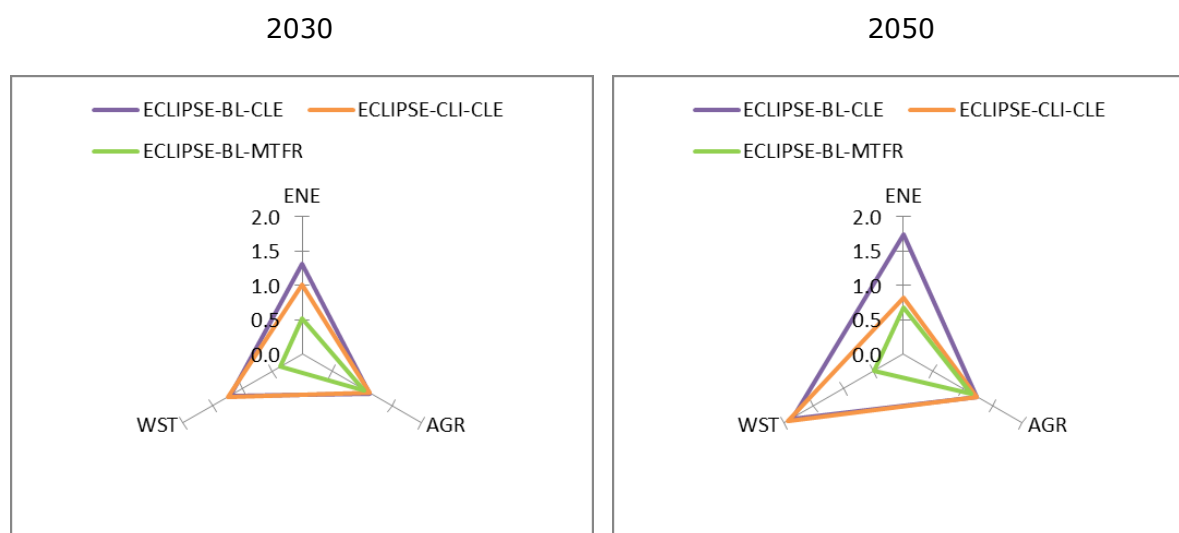
increase by 100-300 Tg CH<sub>4</sub> yr<sup>-1</sup> until 2050, the medium scenarios stabilise around their 2010 values of ca. 300 Tg CH<sub>4</sub> yr<sup>-1</sup>, and the low emissions typically decline to 200-250 Tg CH<sub>4</sub> yr<sup>-1</sup>. RCP and SSP scenarios were calibrated to the reference year 2000, with 2010 being projected, thereby missing effects of policies implemented between 2000 and 2010. In contrast, ECLIPSE and GECO projections start from 2010, and control policies before 2010 are included. This somewhat reduces the mitigation potential in the ECLIPSE scenarios compared to RCP and SSP. Interestingly, emissions in the ECLIPSE-MTFR scenario increase after 2030 due to the assumption about no further technological development. The continued decline after 2030 in the RCPs and SSPs scenarios is result from assumptions on further technological development.

**Table 3.5.** Description of ECLIPSE v5a scenarios.

<b>ECLIPSE</b>	Description
ECLIPSE-BL-CLE	The Baseline (or reference)-Current Legislation scenario takes Business-as-usual projections from the Energy Technology Projections study by the International Energy Agency (IEA, 2012) and Food and Agricultural Organization (FAO) projections of livestock- comparable to the RCP6.0 (van Vuuren et al., 2011) emission trajectory (until 2050) used by IPCC AR5 report (see table 3.6). For the EU, the air pollutant scenario is consistent with the Thematic Strategy on Air Pollution (2013).
ECLIPSE-CLI-CLE	This scenario combines IEA's "2 degrees CLIMATE" energy projections with Current Legislation on air pollution measures. The climate projections target 450 ppm CO <sub>2</sub> eq concentrations (IEA, 2012) through energy efficiency improvements and lower coal use, etc. The CO <sub>2</sub> emission trajectory is comparable to the RCP2.6 pathway used in IPCC AR5. The scenario focuses on emission reductions in fossil fuel production, while no ambitious CH <sub>4</sub> emission reductions are foreseen for the agricultural and waste sectors. Air pollutant abatement measures are like in BL-CLE.
ECLIPSE-BL-MTFR	Implementation of all currently existing technology options to mitigate CH <sub>4</sub> and other pollutant emissions, irrespective of their costs. Baseline agricultural and energy projections are used for activity/production/consumption levels to highlight the impact of technological choices.

Source: Maas and Grennfelt, 2016, IIASA web site

**Figure 3.8.** ECLIPSE v5a relative change in CH<sub>4</sub> emissions by 2030 and 2050 in the energy (ENE), waste (WST) and agricultural (AGR) sectors, for 3 selected scenarios, relative to year 2010. A minor potential for emission reductions in the agricultural sector was included in ECLIPSE climate scenarios



Source: JRC elaboration of ECLIPSE v5a emission data

The difference in CH<sub>4</sub> emissions between high and low scenarios in 2030 is of the order of 200 Tg CH<sub>4</sub> yr<sup>-1</sup> doubling to 400 Tg CH<sub>4</sub> yr<sup>-1</sup> in 2050 (Fig. 3.13). 40 to 50% of this difference is attributed to Asia, followed by the Middle East and Africa (20%) and OECD countries (10 - 15%). For agriculture these changes are 1.3-1.7 (high), 0.9-1.3 (middle), 0.6-1.1 (low). For the waste sector these values are 1.7-2.0 (high), 0.8-1.9 (middle) and 0.2-1.0 (low). While in the SSP3-REF scenario global population increases by 43% from 2010 to 2050, the corresponding waste and agricultural CH<sub>4</sub> emissions go up even stronger by 70%. In contrast, the SSP1-26 population in 2050 is 23% higher than in 2010, but with 40% lower agricultural emissions due to lower per capita demand of livestock products (Popp et al., 2017) and constant waste emissions.

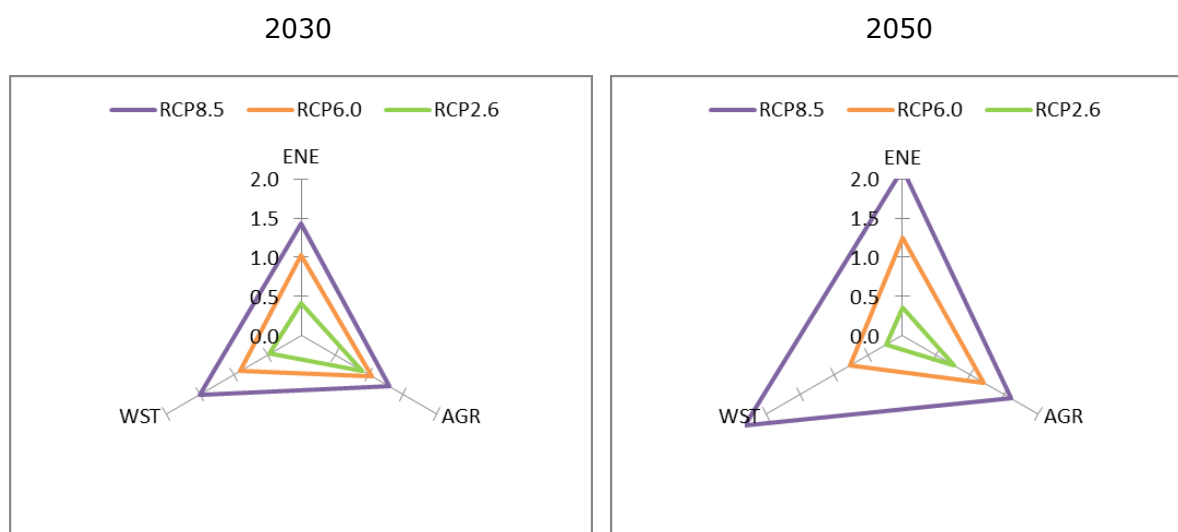
**Table 3.6.** Description of RCP scenarios. In all three scenarios, Kuznets<sup>18</sup>-curve assumptions were made for air pollutants, leading to relatively similar air pollutant emissions across scenarios.

RCP	Description
RCP8.5	RCP8.5 (8.5 Wm <sup>-2</sup> ) is characterised by increasing greenhouse gas emissions over time representative for literature scenarios leading to high greenhouse gas concentration levels. For RCP8.5 global median temperature increase is 4.2 °C with a 5-95 percentile range between 3.2 and 5.4 °C by 2100 (IPCC AR5). CO <sub>2</sub> emission projections are 75.6 and 105.5 Tg CO <sub>2</sub> yr <sup>-1</sup> in 2050 and 2100, respectively.
RCP6.0	Stabilisation scenario (6.0 Wm <sup>-2</sup> ) where total radiative forcing is stabilised after 2100 without overshoot by employment of a range of technologies and strategies for reducing greenhouse gas emissions. By the end of the century, RCP6.0 would correspond to a median global temperature increase of 2.7 °C (range 2.1 to 3.9 °C). CO <sub>2</sub> emission projections are 45.9 and 50.7 Tg CO <sub>2</sub> yr <sup>-1</sup> in 2050 and 2100, respectively.
RCP2.6	The emission pathway is representative of scenarios in the literature leading to greenhouse gas concentration levels near or below the present day values. It is a so-called "peak" scenario: radiative forcing level first reaches a value around 3.1 Wm <sup>-2</sup> mid-century, returning to 2.6 Wm <sup>-2</sup> by 2100, compatible with a less than 2 °C global temperature rise compared to pre-industrial (median 1.6 °C, range 0.8-2.4 °C). In order to reach such radiative forcing levels, greenhouse gas emissions (and indirectly emissions of air pollutants) are reduced substantially over time. CO <sub>2</sub> emissions evolve from 35.6 Tg CO <sub>2</sub> yr <sup>-1</sup> in 2010, 12.9 in 2050 to -1.5 Tg CO <sub>2</sub> yr <sup>-1</sup> in 2100.

Source: IIASA <https://tntcat.iiasa.ac.at/RcpDb>

<sup>18</sup> The environmental Kuznets relationship assumes that economic growth initially leads to deterioration in the environment and emissions, but after a substantial economic growth, society and policy automatically start to invest in improving pollution levels. The Kuznets mechanism is strongly disputed in the literature, as empirical evidence is rather limited, and pollution is not simply a function of GDP, but of many other factors- including policy strength.

**Figure 3.9.** Relative change in CH<sub>4</sub> emissions per sector, relative to year 2010 for the 3 selected RCP scenarios.



Source: JRC elaboration of RCP emission data

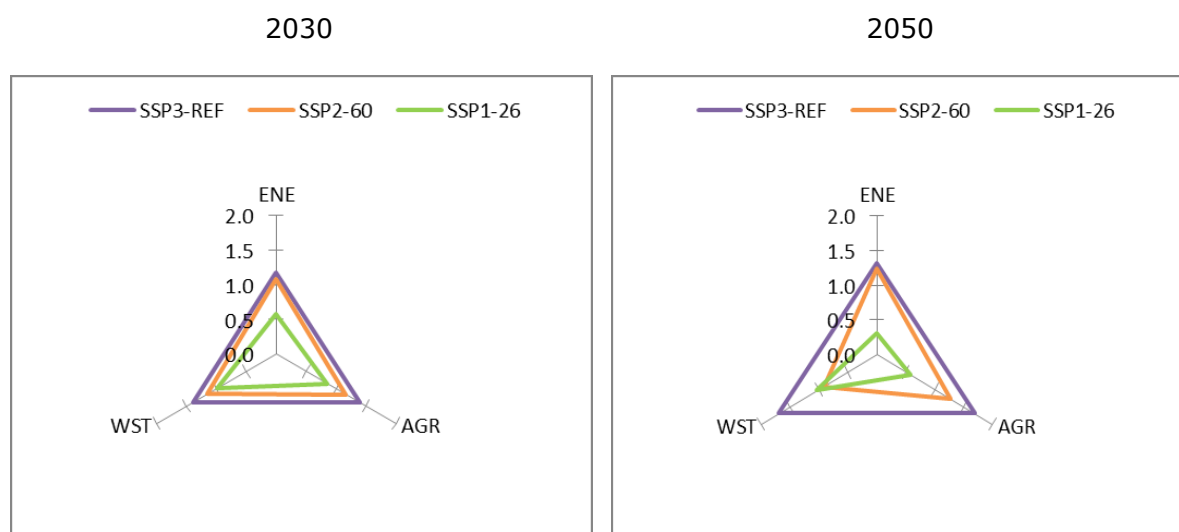
In terms of global sectoral emissions amounts, these numbers correspond to absolute differences of high and low emission scenarios between 100 and 170 Tg CH<sub>4</sub> yr<sup>-1</sup> for the energy sector (see Annex A2), 40-150 Tg CH<sub>4</sub> yr<sup>-1</sup> in the waste sector and 4-170 Tg CH<sub>4</sub> yr<sup>-1</sup> for agriculture, reflecting important differences in assumptions on activity levels and mitigation potential of these sectors. Globally the mitigation potential over all sectors between high and low emission scenarios ranges from 250 to 490 Tg CH<sub>4</sub> yr<sup>-1</sup> across scenario families (Fig. 3.13).

**Table 3.7.** Description of SSP scenarios. See also Table 3.6 for the RCP scenarios.

SSP	Description
SSP3-REF	The SSP3-baseline regional rivalry scenario, with no additional climate mitigation objectives, leading to radiative forcing of almost 8.0 Wm <sup>-2</sup> by the end of the century. With a wide range of uncertainty, future CO <sub>2</sub> emissions cluster around the corresponding RCP8.5 trajectories, see Table 3.6 and Riahi et al., (2017). An indicative global temperature increase by 2100 is 4.1 °C.
SSP2-60	Middle of the road scenario, medium challenges to mitigation and adaptation and reaching a climate forcing of 6 Wm <sup>-2</sup> by the end of the century. Future CO <sub>2</sub> emissions cluster around the equivalent RCP6.0 trajectories see Table 3.6 and Riahi et al. (2017). An indicative global temperature increase by 2100 is 3.2 °C.
SSP1-26	Sustainable trajectories lead to lower emissions, radiative forcing and climate change. The world shifts gradually, but pervasively, towards a more sustainable path. Future CO <sub>2</sub> emissions are declining less strongly than the corresponding RCP2.6 emissions (Riahi et al., 2017). An indicative temperature global increase by 2100 is 1.8 °C.

Source: <https://tntcat.iiasa.ac.at/SspDb>

**Figure 3.10.** Relative change in emissions per sector, relative to year 2010 for the 3 selected SSP scenarios.



Source: JRC elaboration of SSP emission data

Thus in the scenarios explored in this study, a wide range of assumptions on the implementation of mitigation measures and to some extent also demand for fuel and food, are the primary reason for the wide diversity of future emissions. This diversity is more prominent for the energy and waste sectors than for agriculture.

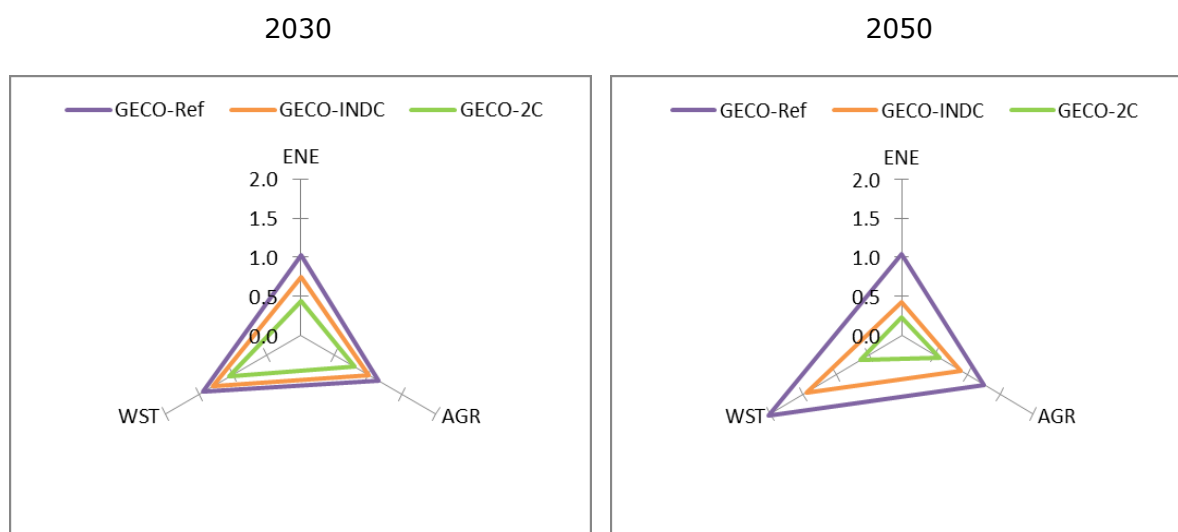
Comparing 2050 to 2010, relative sectoral emission changes (table 3.9) in the energy sector range from a factor 1-1.7 in the group of high emission scenarios, to 0.4-0.8 in the middle and 0.2-0.7 in the low scenarios. Focusing on SSP-scenarios, the CH<sub>4</sub> 2050-to-2010 emission ratios in the scenarios are typically lower than those stemming from the corresponding primary energy usage, especially for the low emission scenarios. For instance in the SSP1-26 marker scenario, primary energy from oil and gas increases by 10% in 2050 compared to 2010, coal use reduces by 54%, while the corresponding methane emissions decline by 70%. For the pessimistic SSP3-REF scenario oil and gas primary energy use increases by 60%, coal by 128%, while CH<sub>4</sub> emissions increase only by 30%.

**Table 3.8.** Description of GECO2017 scenarios

GECO2017	CLIMATE POLICIES
GECO-REF	Adopted energy and climate policies worldwide for 2020; thereafter, CO <sub>2</sub> and other GHG emissions driven by income growth, energy prices and expected technological development with no supplementary incentivising for low-carbon technologies.
GECO-INDC	All the Intended Nationally Determined Contributions (INDCs) put forward by countries (for 2030) are implemented. Beyond 2030 global GHG intensity of GDP decreases at the same rate as for 2020-2030.
GECO-2C	Global GHG trajectory over 2010-2100 compatible with a likely chance (above 66%) of temperature rise staying below 2°C above pre-industrial levels.

Source: Kitous et al., 2017

**Figure 3.11.** Relative change in emissions per sector, relative to year 2010 for the 3 selected GECO-2017 scenarios.



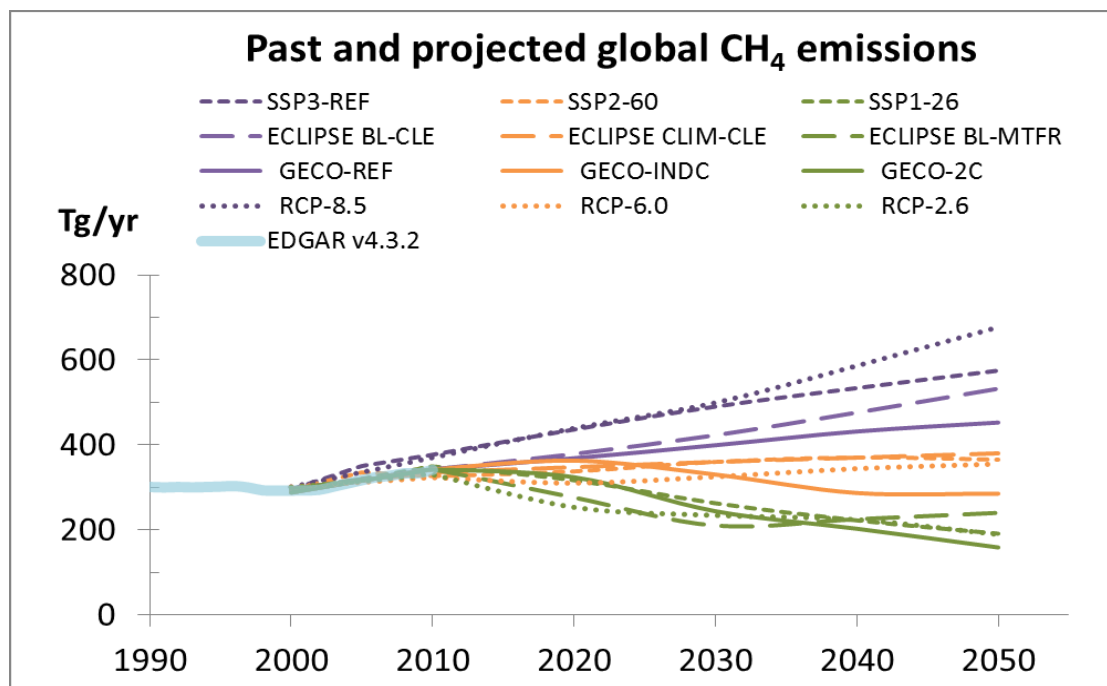
Source: JRC elaboration of emission data

**Table 3.9.** Ratio of global methane emissions in 2050 relative to 2010 of the 3 major sectors in 12 scenarios- grouped in high emission (H, purple), Middle of the Road (M, brown) and low emission- high effort (L, green).

Scenario	Energy	Agriculture	Waste
H ECLIPSE BL-CLE	1.7	1.2	1.9
H RCP8.5	2.1	1.6	2.3
H SSP3-Ref	1.3	1.7	1.7
H GECO REF	1.0	1.3	2.0
M ECLIPSE-CLIM-CLE	0.8	1.2	1.9
M RCP6.0	1.2	1.2	0.8
M SSP2-60	1.2	1.3	0.9
M GECO-INDC	0.4	0.9	1.5
L ECLIPSE BL-MFTR	0.7	1.1	0.5
L RCP2.6	0.4	0.8	0.2
L SSP1-26	0.3	0.6	1.0
L GECO-2C	0.2	0.6	0.6

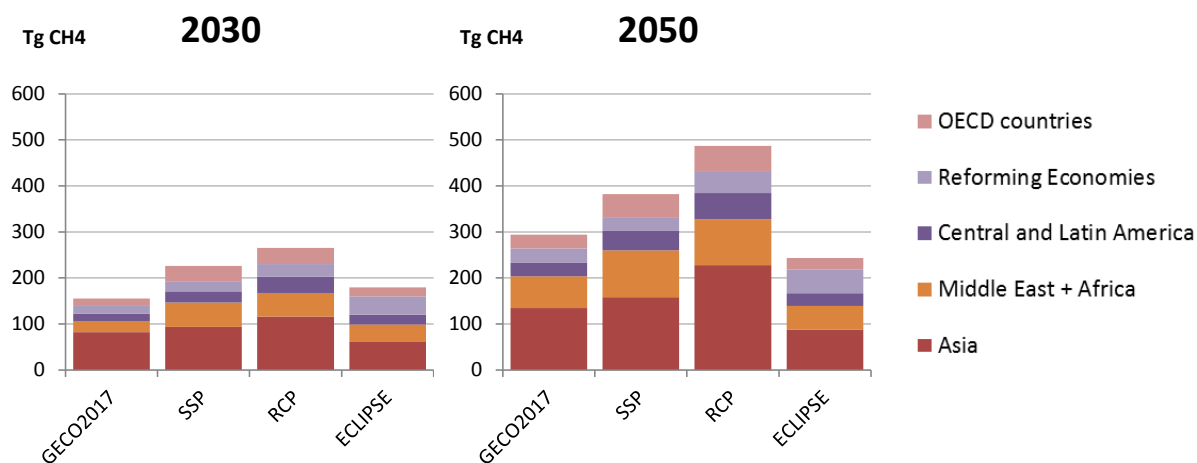
Source: JRC elaboration of emission data

**Figure 3.12.** Historical (1990 – 2010) global anthropogenic CH<sub>4</sub> emission trends from EDGAR v4.3.2 and projected (2000 – 2050) trends from four scenario families. Scenarios have been colour-coded to easily distinguish the “high emission”, “middle of the road” and “low emission-high mitigation effort” members in each family.



Source: JRC elaboration of emission data

**Figure 3.13.** Maximum difference in anthropogenic CH<sub>4</sub> emissions in 2030 and 2050 between highest and lowest scenario member for the four selected scenario families. GECO2017 and ECLIPSE have a lower mitigation range, due to inclusion of policies prior to 2010.



Source: JRC elaboration of emission data

## 4 Air quality impacts of CH<sub>4</sub> emissions

Previous studies have indicated that methane mitigation can be a cost-effective means of long-term and international air quality management, with additional benefits for climate (Aakre et al., 2018; Fiore et al., 2002; West et al., 2006, 2012), see section 2.3.2.

In this section we explore the impact of projected CH<sub>4</sub> emission trends until 2050 on background ozone, and its impacts on human health and crop yields. Other vegetation (e.g. forests) can likewise be affected by ozone (Sitch et al., 2007; Paoletti, 2006, de Vries et al., 2017), but this was not analysed in this study. We use the four scenario families discussed in section 3.3, to provide insight on the range and magnitudes of possible benefits associated with CH<sub>4</sub> mitigation policies.

For a practical application of pollutant concentration responses to changing emissions, including CH<sub>4</sub>, JRC has developed the TM5-FASt Screening Tool (TM5-FASST, Van Dingenen et al., 2018). The methodology used in this report builds upon results obtained by dedicated model ensemble experiments in the framework of the first and second phase of the Task Force on Hemispheric Transport of Air Pollutants (HTAP1, HTAP2) and is described in Annexes 4 and 5.

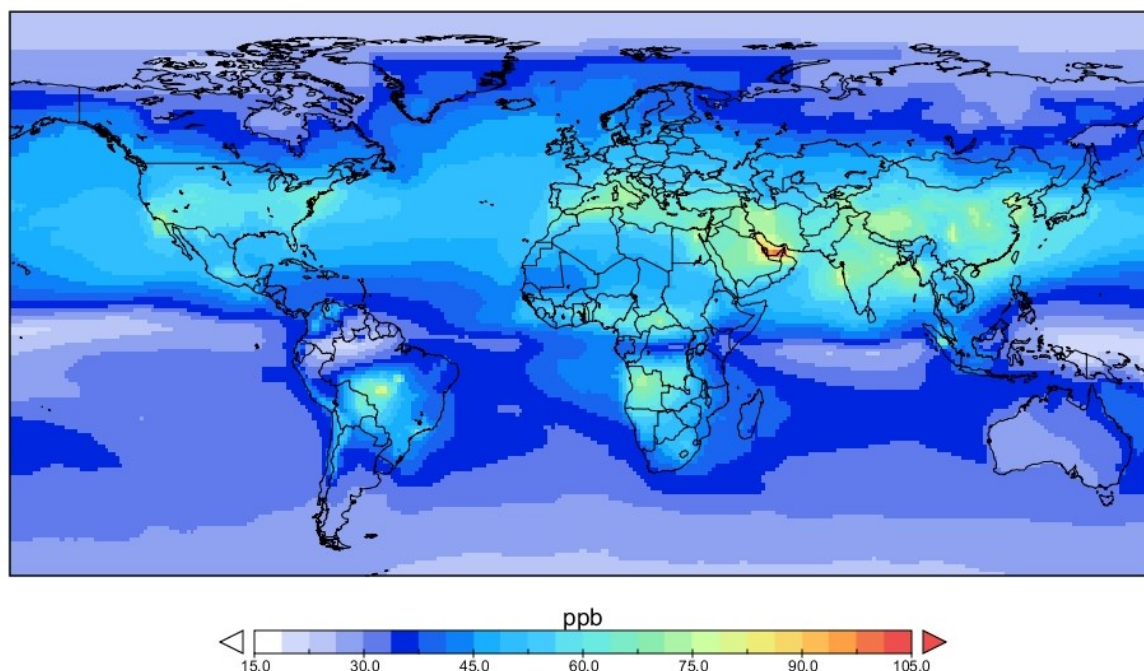
### 4.1 Current O<sub>3</sub> exposure patterns

In this work we evaluate the health-relevant O<sub>3</sub> exposure metric 6mDMA1, i.e. the highest 6-monthly mean of daily maximum 1 hourly ozone value, applying the widely-accepted O<sub>3</sub> health exposure-impact relationship by Jerrett et al. (2009), see section 4.3 and Annex 5.

Figure 4.1 displays the spatial pattern of the 6mDMA1 ozone metric calculated with TM5-FASST for 2010. A broad band of 6mDMA1 above 60 ppb stretches over the Northern Hemisphere mid-latitudes, Middle East, South and East Asia, with peak values of 75 ppb. Over South America and Africa maxima of 70-80 ppb are related to large-scale open biomass burning. A comparison with observations is shown in Annex 5.

Highlighting the contribution of anthropogenic CH<sub>4</sub> emissions to 6mDMA1, we analysed for all TM5-FASST regions and countries a situation considering only natural CH<sub>4</sub> emissions, but leaving other emissions at their 2000 values. For Europe country-averaged contribution to 6mDMA1 was lower by 9% to 16% (5 to 8 ppb) and by 7% to 18% (3 to 8 ppb) worldwide. These estimates are consistent with estimates made by West et al. (2006) and Fiore et al. (2008). We note that along with CH<sub>4</sub> also changes in VOC, and CO and especially NO<sub>x</sub> emissions may affect the lifetime and ozone production efficiency of CH<sub>4</sub>. Assessing these non-linear interactions is beyond the scope of this study.

**Figure 4.1.** Year 2010 Ozone exposure metric 6mDMA1 calculated with TM5-FASST (ECLIPSE v5a).



Source: JRC TM5-FASST

## 4.2 Future trends in background O<sub>3</sub> from CH<sub>4</sub> emissions

We have applied the regional HTAP CH<sub>4</sub>-ozone response sensitivities, taking into account the 12 year response time of CH<sub>4</sub> (see Annex 4) to estimate the change in ground-level ozone concentrations associated with the changes in projected global CH<sub>4</sub> emissions. To isolate the effect of CH<sub>4</sub> on O<sub>3</sub>, we assume that changing CH<sub>4</sub> emissions do not affect O<sub>3</sub> formation from its other precursors<sup>19</sup>. HTAP analysis by Wild et al. (2012), Maas and Grennfelt (2016) and Turnock et al. (2018) of a variety of air pollution scenarios shows that air pollution emission controls can also exert sizeable impacts in and downwind of the air pollutant emission regions. For instance, for Europe, stringent North American emission controls (MFR) will be beneficial. We refer for more information to these publications.

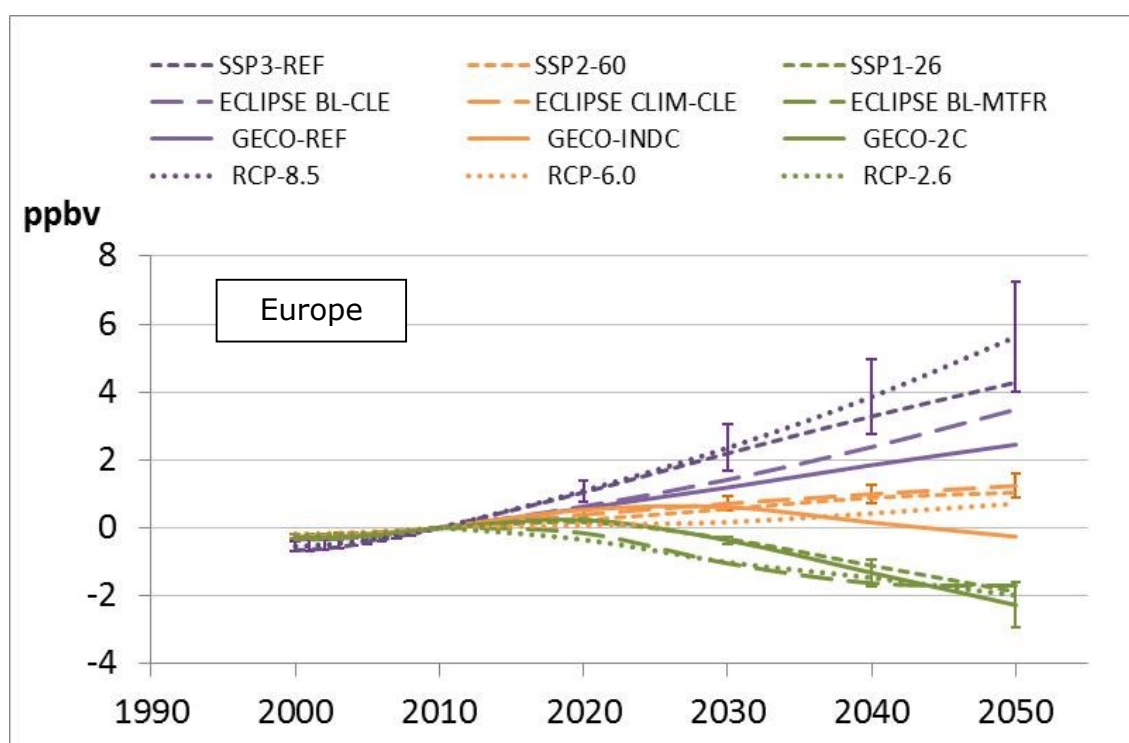
Figure 4.2 shows the development between 2010-2050 of the 6mDMA1 ozone exposure metric in Europe relative to year 2010, as a response to changing global CH<sub>4</sub> emissions for the scenarios discussed in section 3. For Europe (HTAP2 region definition: see Annex 3), the largest difference between the highest and lowest emission scenario of each family produces changes in 6mDMA1 O<sub>3</sub> exposure of between 1.6 and 3.4 ppb in 2030 and between 4.7 and 7.6 ppb in 2050, the latter corresponding to about 8-12% of the 6mDMA1 in 2010. Although the high mitigation scenarios lead to a similar outcome across all scenario families by 2050, the differing implementation rates of emission controls lead to a faster decrease in the 2010 – 2040

<sup>19</sup> The HTAP CH<sub>4</sub>-O<sub>3</sub> response sensitivities used in the present analysis are representative for year 2000 emissions (see Annex 4). The impact of changing NO<sub>x</sub>, VOC, and CO emissions on CH<sub>4</sub> concentrations and CH<sub>4</sub> – O<sub>3</sub> response sensitivities goes via a complex set of reactions influencing O<sub>3</sub> and the OH radical. As a rule of thumb increasing NO<sub>x</sub> emissions increase the levels of OH and decrease the chemical residence time of CH<sub>4</sub>. In contrast, increasing CO and VOC emissions decrease levels of OH, and increase the residence time of CH<sub>4</sub>. As NO<sub>x</sub>, VOC, and CO are to some extent co-controlled, some previous studies have suggested a relative stability of the global OH amounts, while other studies suggest larger variability. A more quantitative assessment of this is beyond the scope of this study, but we do not expect large impacts of this assumption.

period in the ECLIPSE MTR and RCP-26 scenarios than in the GECO-2C and SSP1-26 projections.

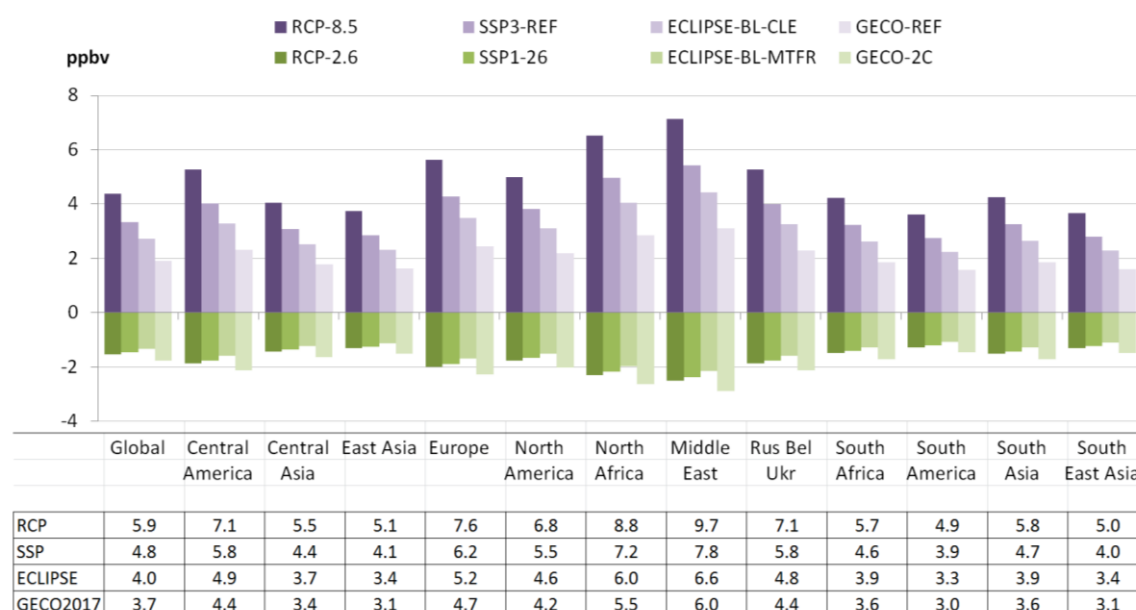
Differences in global and regional 6mDMA1 O<sub>3</sub> exposure due to the use of the most and least stringent emission scenarios for the year 2050 (relative to year 2010) are shown in Fig. 4.3. Averaged over all scenario families, the difference between a high mitigation and a high emission scenario path leads globally to a difference of 4.6 (±1.0) ppb in ozone exposure, with regional extremes of 7.5 (±1.6) ppb in the Middle East. These regional differences in ozone sensitivities to methane emissions are based on response sensitivities obtained under current NO<sub>x</sub> and VOC regimes, and are further affected by different physical conditions (sunlight, temperature, humidity, and land cover).

**Figure 4.2.** Projected change in ozone exposure metric 6mDMA1 over Europe, relative to year 2010, as a consequence of the global CH<sub>4</sub> emission trends in Fig. 3.12. The error bars represent 1 standard deviation over the range of O<sub>3</sub> – CH<sub>4</sub> response sensitivities obtained in the HTAP model ensemble (shown for RCP-85, ECLIPSE-CLIM-CLE and GECO-2C only), and show that the O<sub>3</sub> signal from the emission scenarios is larger than model uncertainty.



Source: JRC TM5-FASST

**Figure 4.3.** Projected change in regional mean ozone exposure metric 6mDMA1 in 2050, relative to year 2010, for the highest and lowest global CH<sub>4</sub> emission scenarios in each family. The data table below the figure gives the total range width between the highest and lowest emission scenario of each family (i.e. sum of absolute values of purple and green bar for each scenario).



Source: JRC TM5-FASST

### 4.3 Future health impacts from CH<sub>4</sub>-induced O<sub>3</sub>

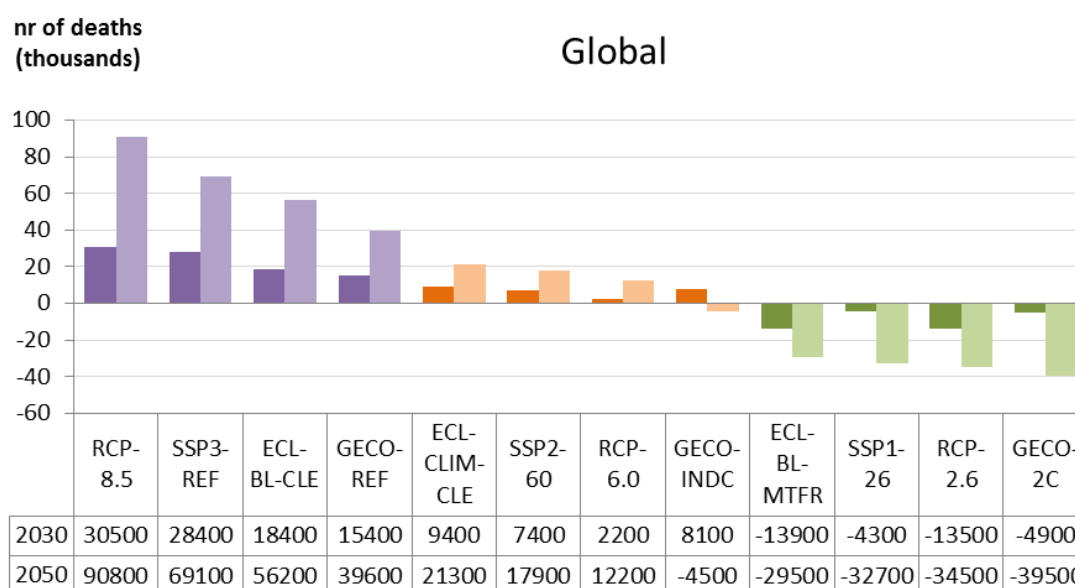
O<sub>3</sub> exposure is associated with a range of health impacts, including mortality from respiratory disease. WHO's most recent review of evidence on health aspects of air pollution (REVIHAAP, 2013) reports a number of cohort studies suggesting an effect of ozone on long-term mortality.

Here we include an estimate of the CH<sub>4</sub>-related O<sub>3</sub> health impacts from long-term exposure, following Jerrett et al. (2009), using as exposure metric 6mDMA1 with a threshold of 33.3 ppb for zero effect. Recent estimates of the present-day premature deaths associated with ground-level ozone range from 254,000 to 470,000 (see Annex 5). An important aspect is the effect of growing population and changing base-mortalities (e.g. ageing) in future scenarios, which may make it difficult to single out the signal of O<sub>3</sub> on health impacts. In general, demographic developments in emerging economies will increase impacts of air pollution – even with unchanged or even declining pollution. In contrast to earlier studies on impacts of CH<sub>4</sub> emission reductions on O<sub>3</sub> (e.g. West et al., 2006), where population change by 2030 contributed to the increasing mortalities, in this work we compare O<sub>3</sub>-related mortalities for the year 2050 population<sup>20</sup>, exposed to the ozone distributions produced by each scenario in 2050, relative to the 2050 population exposed to 2010 O<sub>3</sub> levels.

Worldwide, relative to year 2010 exposure levels, the high CH<sub>4</sub> emission scenarios (Fig. 4.4) would lead in 2050 to an estimated additional 40,000 to 91,000 O<sub>3</sub> mortalities, whereas the low emission-high mitigation scenarios would decrease mortalities by 30,000 to 40,000 units. The 2050 global and regional differences in mortality between the highest and lowest emission scenario in each family are given in Table 4.1

<sup>20</sup> Projections by the United Nations (2015) (median prediction interval)

**Figure 4.4.** Change in global mortalities from exposure to O<sub>3</sub> from global CH<sub>4</sub> emissions in 2030 (dark shaded bars) and 2050 (light shaded bars), relative to exposure of the same population to year 2010 O<sub>3</sub> levels<sup>21</sup>. Purple: high emission scenarios; orange: middle-of-the-road scenarios, green: low emission-high mitigation scenarios.



Source: JRC TM5-FASST

The number of premature mortalities from CH<sub>4</sub>-related background ozone in the EU in 2050 is projected to increase by 3600 to 8300 annual deaths in the high emission scenarios and decrease by 2100 to 2800 annual deaths for the high mitigation effort scenarios, compared to a population exposed to 2010 O<sub>3</sub> levels (Fig. 4.5).

The European contribution to global CH<sub>4</sub> emissions declined from ca. 12% in 1970, 6% in 2012 and will be further declining to 3-5% in 2030-2050. Because CH<sub>4</sub>-related ozone is independent of the location of the CH<sub>4</sub> emission, Europe's share in its own as well as in the global CH<sub>4</sub>-related O<sub>3</sub> mortality burden is 3 to 5% across all scenarios in 2030 and 2050. The contribution of European CH<sub>4</sub> emission controls to European O<sub>3</sub> concentrations is proportional to the emissions and currently amounts to about 0.3 ppb (or 500 premature deaths). Reducing EU28 CH<sub>4</sub> emissions by 10%, 20%, or 50%, saves 50, 100 and 250 deaths annually, and globally 540, 1040, and 2700.

Table 4.2 shows the relative shares of the global mortality burden in 2030 and 2050 for 12 receptor regions. Europe "receives" 9% of the global health impact in 2030 and 7 to 9% in 2050. The imbalance between emission and impact share is mainly due to the relatively high population density in Europe, in combination with a somewhat higher O<sub>3</sub> response to CH<sub>4</sub> emissions compared to other world regions (see Fig. A4.2 and Table A4.2 in Annex 4).

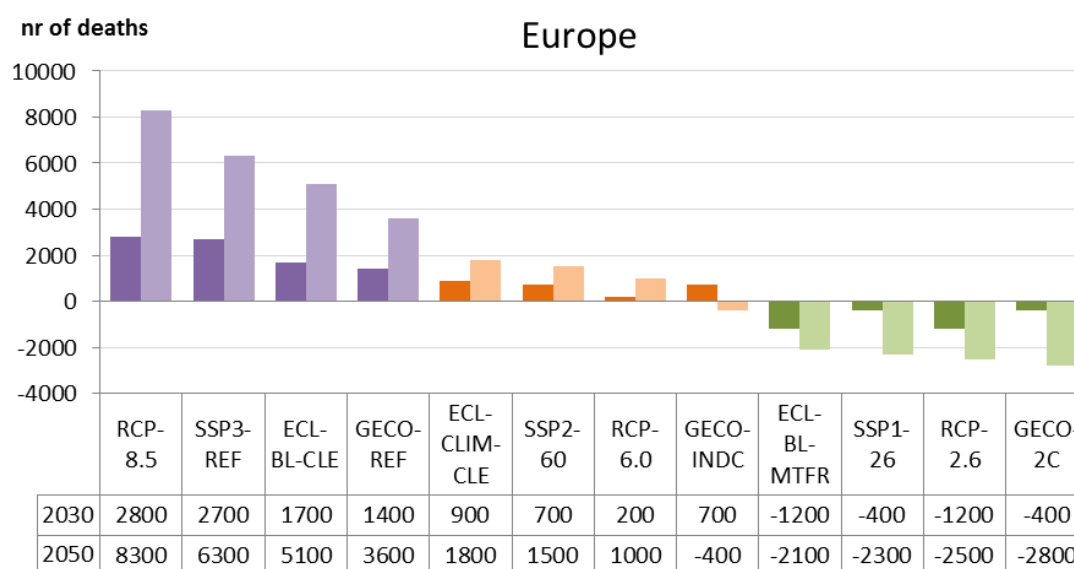
Table 4.3 and 4.4 summarize the impacts from global CH<sub>4</sub> emission scenarios for the globe and Europe respectively. In relative terms, the high emission scenarios would lead to an increase in global O<sub>3</sub>-related mortality with 3 to 5% in 2030, and 5 to 11% in 2050 compared to a year 2010 situation. The mitigation scenarios project a global decrease in mortalities of -2 to -1% in 2030 and -5 to -3% in 2050. For Europe, the contribution of CH<sub>4</sub>-related O<sub>3</sub> mortalities is higher: 8 to 15% (2030) and 18 to 42%

<sup>21</sup> Using the population of 2030 and 2050 in combination with 2010 O<sub>3</sub> exposure levels as a reference eliminates the effect of the changing population and age structure on changing mortality rates which would mask part of the O<sub>3</sub> impact

(2050) for the high emission scenarios, while the mitigation scenarios project a -7 to -2% (2030) and -14% to -11% (2050) decrease compared to 2010.

We note that recent re-evaluation of mortality risks associated with long-term ozone exposure (Malley et al., 2017; Turner et al., 2016) suggest a factor of 2.3 higher global estimate of O<sub>3</sub> mortalities than those applied in this work. However, these new studies are not yet evaluated by WHO. This represents a major uncertainty in this study, and would also double the impact of CH<sub>4</sub> on O<sub>3</sub> health impacts.

**Figure 4.5.** Change in mortalities in HTAP2 Europe region (see Annex 3) from exposure to O<sub>3</sub> from global CH<sub>4</sub> emissions in 2030 (left bar) and 2050 (right bar), relative to exposure of the same population to year 2010 O<sub>3</sub> levels. Purple: high emission scenarios; orange: middle-of-the-road scenarios, green: high mitigation scenarios.



Source: JRC TM5-FASST

**Table 4.1.** Year 2050 O<sub>3</sub> differences in mortality between highest and lowest emission scenario in each scenario family for HTAP2 world regions (see Annex 3), relative to year 2010.

Mortality difference (thousands)	Global	Europe	North America	Middle East	Russia Belarus & Ukraine	Central Asia	East Asia	South Asia	South East Asia	North Africa	Sub-Saharan Africa	South America	Central America
RCP	125	10.7	5.2	2.8	0.8	9.4	13.9	52	17	2.1	6.3	2.6	1.9
SSP	102	8.6	4.2	2.3	0.6	7.6	11.3	43	14	1.7	5.2	2.1	1.5
ECLIPSE	86	7.2	3.5	1.9	0.5	6.4	9.5	36	12	1.5	4.4	1.8	1.3
GECO2017	79	6.4	3.1	1.8	0.5	5.9	8.8	33	11	1.4	4.2	1.7	1.2

Source: JRC TM5-FASST

**Table 4.2.** Regional shares of global O<sub>3</sub> mortalities in 2030 and 2050 for high CH<sub>4</sub> emission scenarios (H) middle-of-the road scenarios (M) and low-emission-high mitigation scenarios (L) for the HTAP2 world regions (Annex 3)

	Europe	North-America	Middle East	Russia , Belarus & Ukraine	Central Asia	East Asia	South Asia	South East Asia	North Africa	Sub-Sahara-Africa	South Am.	Central Am.
2030												
H	9.3%	4.5%	2.0%	0.7%	7.3%	13%	41%	13%	1.5%	4.4%	2.0%	1.4%
M	9.0%	4.3%	2.0%	0.7%	7.3%	13%	41%	13%	1.5%	4.5%	2.0%	1.5%
L	8.6%	4.1%	2.1%	0.7%	7.3%	13%	41%	13%	1.6%	4.8%	2.2%	1.6%
2050												
H	9.1%	4.4%	2.1%	0.6%	7.5%	11%	42%	14%	1.6%	4.8%	2.0%	1.4%
M	8.3%	4.0%	2.2%	0.6%	7.6%	11%	42%	14%	1.7%	5.0%	2.0%	1.5%
L	7.2%	3.5%	2.5%	0.6%	7.5%	11%	42%	14%	1.9%	5.7%	2.4%	1.7%

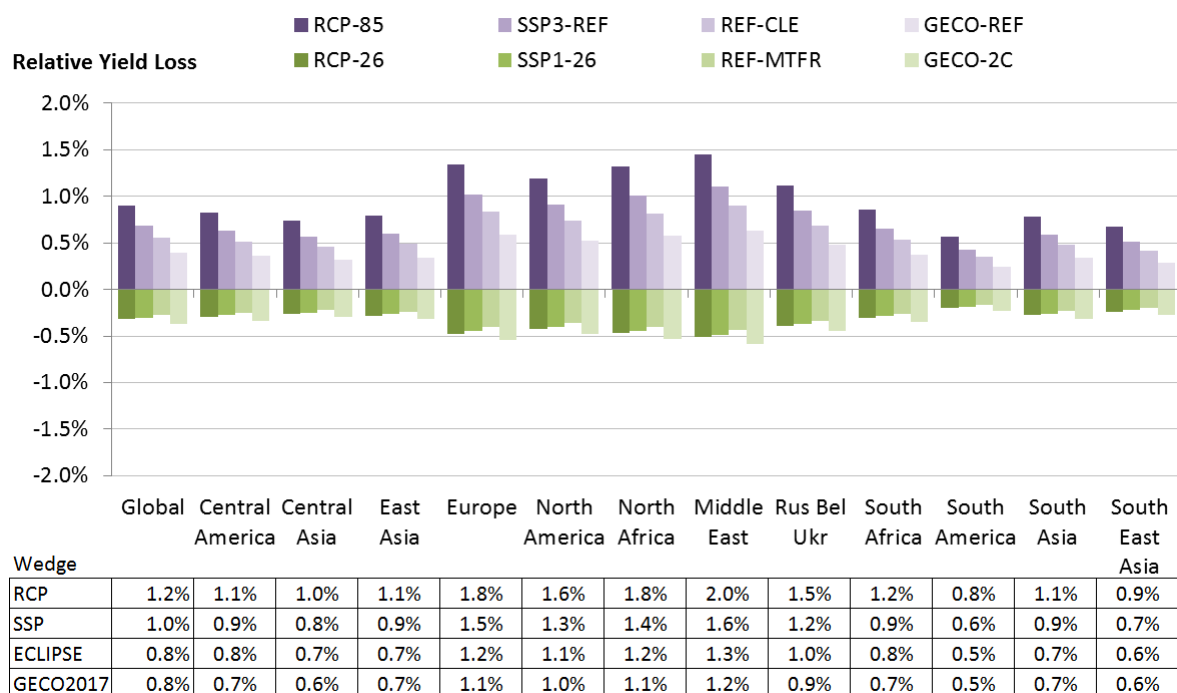
Source: JRC TM5-FASST

#### 4.4 Future crop impacts from CH<sub>4</sub>-induced O<sub>3</sub>

Annex 5 provides details on the metrics and methods used to calculate yield losses due to ozone. Global yield losses (based on year 2000 crop shares and geographical distributions) for 2010 emissions are 45, 6.5, 65, and 25 million metric tons for four major crops- wheat, maize, rice and soy bean respectively. Considering average global market prices and production in the period 2000 - 2010, these numbers translate into a global economic damage for the four crops considered in the range \$30–\$40 billion US\$.

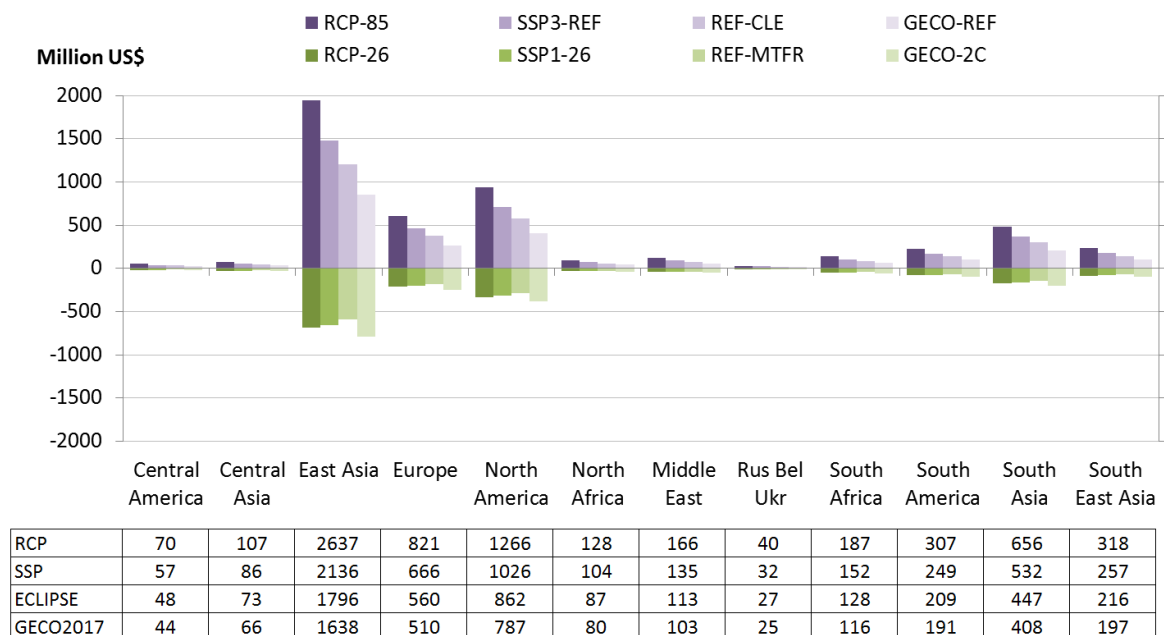
We estimate the change in year 2050 relative crop yield loss (for four major crops wheat, maize, rice and soy bean), based on year 2000 crop shares and geographical distributions (Fig. 4.6). We do not consider discounting or supply/demand feedbacks on the market. In general, the difference between a high and a stringent CH<sub>4</sub> emission trajectory results in a crop yield benefit of the order of 1 to 2% (global mean: 1%). Based on year 2000-2010 average crop production and producer prices these yield benefits correspond to a difference in global economic value for the four crops of 4 to US\$ 7 billion of which 40% in East Asia, 20% in North America and 12% in Europe (Fig. 4.7). Putting these crop economic losses in perspective of losses in the year 2010, the high emission scenarios project an global increase in economic loss of 4 to 8% by 2030 and 8 to 19% by 2050). For the high mitigation scenarios economic losses decrease with –4% to –1% (2030) and -8% to -6% (2050). In Europe these relative impacts are more significant: an increase of the crop economic loss with 8 to 15% (2030) and 16 to 35% (2050) for the high mitigation scenarios, and a decrease with -7 to -2% (2030) and -15 to -11% for the high mitigation scenarios.

**Figure 4.6.** Year 2050 Relative yield loss of 4 major crops relative to year 2010 exposure due to CH<sub>4</sub>-induced O<sub>3</sub> for 12 world regions (HTAP2- Annex 3), for the highest and lowest emission scenario in each family. (Negative loss corresponds to a gain in crop yield). The data table shows the value of the difference between best and worst case scenario in each family.



Source: JRC TM5-FASST

**Figure 4.7.** Estimated change in economic cost from crop losses (based on year 2010 production and producer prices) in 2050 relative to year 2010 for the considered scenarios. The data table gives the difference between best and worst-case scenario in each family.

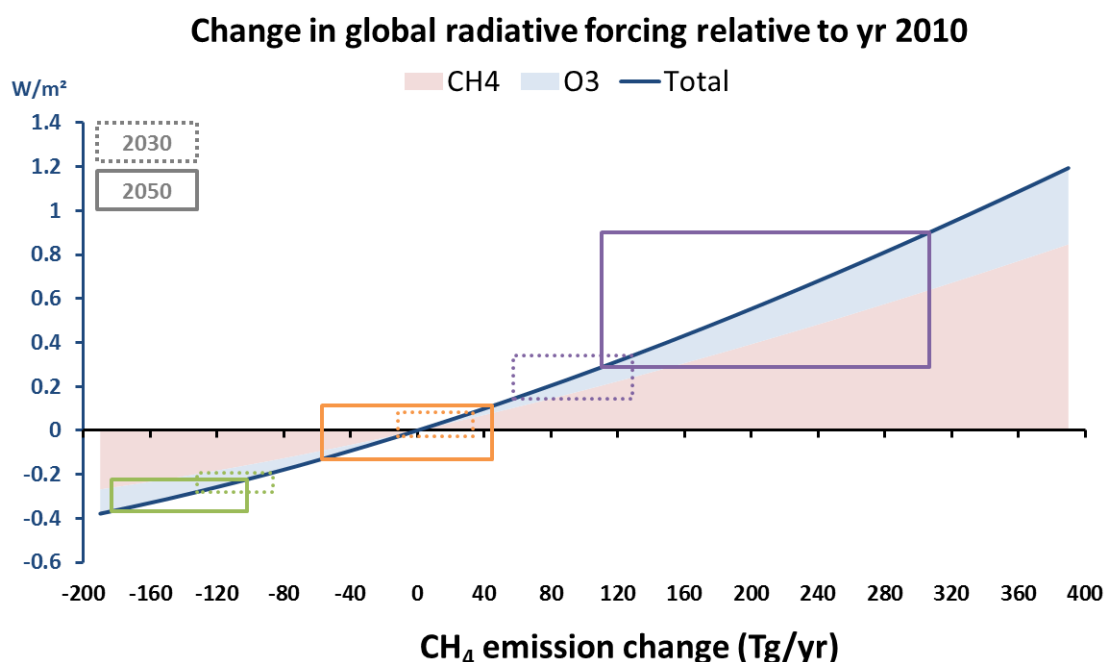


Source: JRC TM5-FASST

## 4.5 Role of CH<sub>4</sub> in closing the GHG emissions gap

Although this report focuses on the air quality impacts of CH<sub>4</sub> mitigation, we also briefly discuss some climate-related impacts of the considered scenarios, in terms of changes in global radiative forcing and equivalent CO<sub>2</sub> (CO<sub>2e</sub>) emissions. Figure 4.8 shows, relative to year 2000, the change in global radiative forcing as a function of CH<sub>4</sub> emission changes, together with the ranges projected in the different scenario families discussed above. The total forcing includes the well-known direct contribution of CH<sub>4</sub> emission changes, as well as the long-term feedback on large scale O<sub>3</sub>.

**Figure 4.8.** Ranges of the change in radiative forcing (blue line, left axis) for the low (green), middle (orange) and high (purple) CH<sub>4</sub> emission scenario groups in 2030 and 2050 relative to the year 2010. The red shaded area shows the contribution of CH<sub>4</sub> only, the blue shaded area the contribution of O<sub>3</sub> via long-term CH<sub>4</sub> chemistry feedback.



Source: JRC evaluation of scenarios (this work)

The relevance of CH<sub>4</sub> mitigation efforts can be put in perspective applying its global warming potential of 28 (Myhre et al., 2013) to evaluate the CO<sub>2e</sub> emissions. Relative to the year 2010, the most stringent emission scenarios (i.e. MTFR or a 2° scenario) lead to a CO<sub>2e</sub> emission reduction of 2.4 to 3.7 Gt annually in 2030 and 2.9 to 5.1 Gt in 2050 whereas the high emission scenarios lead to an emission increase of 1.6 to 3.6 Gt CO<sub>2e</sub> in 2030 (3.1 to 8.6 Gt in 2050).

The UNEP Emission Gap Report 2017 (UNEP, 2017) indicates that, in order to meet the year 2100 2° target, by 2030, additionally to the NDCs 11 to 13.5 GtCO<sub>2e</sub> emission reductions have to be achieved. The stringent emission control scenarios in our analysis foresee a reduction of -2 to -4GtCO<sub>2e</sub> relative to the GECO INDC scenario by 2030, hence contributing 15 to 33% to the required emission gap closure. In contrast, under non-ambitious CH<sub>4</sub> mitigation scenarios, the total mitigation effort needed for reducing emissions of other GHGs would increase by 2 to 4Gt CO<sub>2e</sub>.

## 4.6 Summary of impacts

Finally, Table 4.3 summarizes the health and crop impacts for the globe and for EU28, as well as global climate metrics, as a consequence of global CH<sub>4</sub> emission reductions under the highest and lowest emission scenario families.

**Table 4.3.** Summary of global and European health, crop and climate impacts of global high and low CH<sub>4</sub> emission scenarios. Impacts are for global CH<sub>4</sub> emission changes relative to the year 2010.

Year	High emission scenarios		High mitigation scenarios	
Change in global CH <sub>4</sub> emissions relative to 2010 (Tg CH <sub>4</sub> yr <sup>-1</sup> ):				
2030	57 to 129		-132 to -87	
2050	111 to 307		-183 to -102	
Change in ozone exposure metric 6mDMA1 relative to 2010 (ppb) from CH <sub>4</sub>				
2030	Global	Europe	Global	Europe
	0.9 to 1.8	1.2 to 2.4	-0.8 to -0.3	-1.0 to -0.3
	2050	1.9 to 4.4	2.5 to 5.6	-1.8 to -1.3
Change in CH <sub>4</sub> -related O <sub>3</sub> mortalities relative to 2010 exposure levels (thousands):				
2030	Global	Europe	Global	Europe
	15 to 30	1.4 to 2.8	-14 to -5	-1.2 to -0.4
	2050	40 to 90	3.6 to 8.1	-40 to -30
Percentage change in CH <sub>4</sub> -related O <sub>3</sub> mortalities relative to 2010 exposure levels:				
2030	Global	Europe	Global	Europe
	3% to 5%	8% to 15%	-2% to -1%	-7% to -2%
	2050	5% to 11%	18% to 42%	-5% to -3%
Change in crop economic loss relative to 2010 (million US\$)				
2030	Global	Europe	Global	Europe
	1,050 to 2,075	130 to 250	-920 to -290	-110 to -35
	2050	2,160 to 5,000	265 to 600	-2,000 to -1,500
Percentage change in crop economic loss relative to the loss in 2010				
2030	Global	Europe	Global	Europe
	4% to 8%	8% to 15%	-4% to -1%	-7% to -2%
	2050	8% to 19%	16% to 37%	-8% to -6%
Change in gobal radiative forcing relative to 2010 (mW m <sup>-2</sup> )				
2030	140 to 340		-280 to -190	
2050	290 to 900		-370 to -220	
Change in GWP100 CO <sub>2e</sub> emissions relative to 2010 (GtCO <sub>2e</sub> )				
2030	1.6 to 3.6		-3.7 to -2.4	
2050	3.1 to 8.6		-2.1 to -2.9	

Source: JRC TM5-FASST analysis, this work

## 5 Conclusions and way forward

This report presented an analysis of the role of CH<sub>4</sub> emission abatement to reduce global and European surface ozone and their related impacts. Guided by the earlier defined science questions we draw the following conclusions.

### 5.1 Current understanding of observed changes of CH<sub>4</sub> and O<sub>3</sub> concentrations

After a short period (2000-2008) of stagnation, CH<sub>4</sub> concentrations are again increasing and have reached a level of 1860 ppb in 2018, compared to 1705 ppb in 1990. These trends are based on a relatively accurate GHG observing system and not disputed.

Extrapolating these observed concentration trends a few years ahead to 2020, CH<sub>4</sub> concentrations will be much closer to the concentrations projected by the most pessimistic RCP8.5 scenario compared to an optimistic 2 °C compatible scenario, suggesting that for CH<sub>4</sub> global mitigation efforts are not well on track.

There are several scientific hypotheses on what is causing the renewed trend- with recent literature providing evidence for increasing fossil-fuel production and agricultural emissions. Other studies point to the large uncertainties in natural emissions, specifically from tropical wetlands, which may contribute to inter-annual variability and thus short-term trend fluctuations. More exact knowledge on the drivers of the recent CH<sub>4</sub> trends will be essential for informing both climate and air pollution policies.

In contrast to global CH<sub>4</sub> concentration trends, our knowledge of long-term historic global surface O<sub>3</sub> changes is relatively limited, and relies on inaccurate observations at the beginning of the 20<sup>th</sup> century and a very limited set of more accurate surface stations that stretch back to the 1970s. Global atmospheric chemistry transport models, that include state-of-the art knowledge on changes in O<sub>3</sub> precursor gas emissions (including methane), meteorology and natural processes (such as ozone transported from the stratosphere), can only partly reproduce the observed annual O<sub>3</sub> trends at surface stations and the free troposphere since the 1970s, but models and observations do agree on relatively constant *annual* O<sub>3</sub> concentrations since the 2000s in large parts of Europe and the USA. Observations clearly show that peak O<sub>3</sub> values in summer have gone down in large parts of Europe and the US, resulting from reductions of O<sub>3</sub> precursor emissions. Observations also show that O<sub>3</sub> is strongly increasing in East Asia. In winter O<sub>3</sub> concentrations are increasing almost everywhere. The contribution of CH<sub>4</sub> to O<sub>3</sub> trends can only be estimated by models. Based on observed CH<sub>4</sub> concentrations and relatively well known degradation chemistry of CH<sub>4</sub> derived from field and laboratory studies, the literature finding that methane changes have contributed 1.8 [range 1-3] ppb to *annual* O<sub>3</sub> concentration changes from 1960-2000 is relatively well understood. This represents less than 15% of the annual O<sub>3</sub> changes observed at a limited number of rural surface stations and 20-40% trends observed in the free troposphere. Our TM5-FASST analysis indicates a country-averaged contribution of 9% to 16% of anthropogenic CH<sub>4</sub> emissions to the health-relevant O<sub>3</sub> exposure metric 6mDMA1, within Europe, and from 7% to 18% worldwide.

Based on long-term observations at the coastal inflow station at Mace Head, Ireland, it has been postulated that baseline O<sub>3</sub> flowing into Europe was strongly increasing. However, these trends have also been flattening in the 2000s and O<sub>3</sub> may be slightly decreasing in the recent few years. Model analysis suggests that emission reductions of air pollutants in the Eastern US may have partly contributed to this recent flattening of O<sub>3</sub> trend.

## 5.2 Current knowledge on the geographical distribution of CH<sub>4</sub> emissions and on the contributing sources

The total global amount of CH<sub>4</sub> emissions, from both natural and anthropogenic sources, can be accurately determined from the combined information on observed atmospheric CH<sub>4</sub> concentrations and chemical destruction in the troposphere and amounts to 558 [540-568] Tg CH<sub>4</sub> yr<sup>-1</sup> for the period 2003-2012. Natural sources contribute by ca. 40% to global methane emissions, and human activities contribute by 60%. The separate contributions of natural and anthropogenic emissions in different world regions can be derived from emission inventories and natural emission process models, while inverse models, that combine information derived from observations, emissions, and atmospheric transport, can determine regional emissions. Uncertainties of global and regional natural versus anthropogenic emission estimates are higher than for the global emission budget.

Anthropogenic CH<sub>4</sub> emissions are both reported to the United Nations Framework Convention on Climate Change (UNFCCC) and also independently calculated by the EDGAR4.3.2 emission database, which couples official internationally reported activity data for the most important sources with detailed information on emission factors. In this work we also compare to the GAINS emission database provided by IIASA. According to both databases, China and surrounding regions are in 2012 the dominant and growing emitters of anthropogenic CH<sub>4</sub>. South Asia, Central and South America, Africa, South East Asia, the former Soviet Union, and North America have relatively similar contributions, fluctuating between 9% and 13%. The EU28 contributes by about 6% to the global CH<sub>4</sub> emissions.

In coal, oil and gas producing countries fossil fuel production and distribution tends to be a dominating sector. While in Europe fossil fuel related methane emissions (especially from coal mining) have decreased, in other countries gas and oil production have become more important since 1970, leading to higher global methane emissions from this sector. Our analysis has identified substantial opportunities to further reduce global fossil-fuel production related CH<sub>4</sub> emissions, although the EU reduction potential may be more limited. However, as the EU28 increasingly relies on oil and gas imports and expanded its transmission and gas distribution network, increases in CH<sub>4</sub> leakage along the entire production and distribution chain add to emissions. Due to a lack of observations, large uncertainties are associated with this sector.

In Europe, agriculture is the largest contributor to CH<sub>4</sub> emissions. Livestock, especially enteric fermentation in ruminants, but also manure management, are important contributors to agricultural CH<sub>4</sub> emissions.

While CH<sub>4</sub> emissions from rice are not very important in the EU, in Asian countries, rice production is also an important source of CH<sub>4</sub>, with scope for further reductions.

According to EDGAR, solid waste and waste-water CH<sub>4</sub> emissions globally contribute by 19% to the global total emissions. There are large regional differences between developed and developing countries of per capita CH<sub>4</sub> emission factors from waste and wastewater. Improving sanitary standards in developing countries, and implementing western standards for domestic and industrial wastewater sanitation, will not only help reducing CH<sub>4</sub> emissions, but also contribute to achieving Sustainable Development Goal SDG6. Likewise landfill CH<sub>4</sub> emissions have been decreasing in OECD countries, while they are still increasing elsewhere, indicating a large mitigation potential.

### **5.3 Policy-relevant CH<sub>4</sub> emission scenarios until 2050 and contributions to O<sub>3</sub> concentrations in Europe and other parts of the world**

The air pollutant and climate research communities have used integrated assessment models, along with socio-economic, technological and policy assumptions, to develop scenarios of air pollutants and greenhouse gases emissions, including methane. In total we have analysed methane emissions of twelve scenarios, which can be characterised by unambitious, middle-of-the-road and ambitious developments regarding sustainability, climate and air pollutant mitigation. The high emission-unambitious- group of scenarios, i.e. the RCP8.5 and SSP3-REF used for IPCC's climate analysis, the ECLIPSE-REF-CLE used in CLRTAP convention, and the European Commission's GECO-REF, is typically characterised by increasing emissions by 150 to 250%, i.e. from ca. 300 Tg CH<sub>4</sub> yr<sup>-1</sup> in 2010 to more than 600 Tg CH<sub>4</sub> yr<sup>-1</sup> by 2050. In the middle-of-the-road group of scenarios (including the GECO analysis of determined national contributions under the Paris Agreement) global emissions remain more or less unchanged from 2010 emissions. In the low-emission scenario group, i.e. RCP26, SSP1-26, ECLIPSE-MFTR, and GECO-2C, CH<sub>4</sub> emission reductions of 50% or more are typical, going down between 2010 and 2050 by 90 to 170 Tg CH<sub>4</sub> yr<sup>-1</sup>. The range between pessimistic high-emission scenarios and optimistic low-emission scenarios amounts to ca. 170 to 445 Tg CH<sub>4</sub> yr<sup>-1</sup> by 2050. Differences between high and low scenarios in the energy sector vary between 100 and 170 Tg CH<sub>4</sub> yr<sup>-1</sup>, in the waste sector 40-150 Tg CH<sub>4</sub> yr<sup>-1</sup>, and 4-170 Tg CH<sub>4</sub> yr<sup>-1</sup> for agriculture, reflecting important differences in scenario assumptions on activity levels and mitigation potential.

In this work we use health impact assessment methods recommended by the World Health Organization, based on the 6mDMA1 O<sub>3</sub> exposure metric. Due to differences in meteorological conditions and atmospheric chemistry, O<sub>3</sub> responses to methane emissions may vary by ca. 65% across world regions. For Europe, the difference in O<sub>3</sub> response to high and low emission scenarios ranges between 4.7 and 7.6 ppb in 2050. This would correspond to about 9-14% of the current 6mDMA1 O<sub>3</sub> levels. Low ambition, high emission scenarios (SSP3-REF, RCP8.6 and GECO-REF) indicate O<sub>3</sub> increases by 2.5-4.2 ppb. High-ambition, low emission scenarios would lower O<sub>3</sub> by 1.5-1.7 ppb. Averaged over all scenario families, the benefit of avoiding high CH<sub>4</sub> emission pathways, and implementing ambitious mitigation strategies lead globally to an O<sub>3</sub> reduction of 4.6 (±1.0) ppb. O<sub>3</sub> responses in some regions, like the Middle East and South Asia are particularly sensitive to CH<sub>4</sub> emissions.

### **5.4 Benefits for human health, crops and climate of CH<sub>4</sub> emission reductions in the EU alone, and through collaboration with other parties**

Although not the focus of this report, it is important to realize that CH<sub>4</sub> and the O<sub>3</sub> produced from it, are both important climate gases. The significance for climate of CH<sub>4</sub> emission mitigation can be demonstrated by relating it to the so-called emission gap (UNEP, 2017). By 2030 the additional emission reductions associated with ambitious CH<sub>4</sub> scenarios would close 15 to 33% of the emission gap between the total commitments outlined in the countries NDCs under the Paris Agreement and the emission trajectories needed reach the 2 °C target by 2100. For the pessimistic CH<sub>4</sub> scenarios, in the somewhat hypothetical case that CH<sub>4</sub> and other greenhouse gas emissions are decoupled, additional efforts would be needed to mitigate other greenhouse gases.

Worldwide between 80,000 and 125,000 mortalities can be avoided in 2050 when avoiding the most pessimistic CH<sub>4</sub> scenario and implementing the most stringent CH<sub>4</sub> emission reduction scenarios. By 2050, the EU28 share in the global CH<sub>4</sub> emissions and hence to the global CH<sub>4</sub>-related O<sub>3</sub> mortality burden is 5% across all scenarios, whereas a higher percentage (6% to 7%) of the health impact improvements due to

the global CH<sub>4</sub> emissions are received by the EU28. This is mainly due to the relatively high population density in Europe exposed to ozone.

Reduction of methane emissions also leads to less exposure of crops to ozone. Other vegetation such as forests can likewise be affected by ozone, but this was not analysed in this study. By 2050 the yields of 4 major crops may increase by 0.3 to 0.4% globally under low emissions scenarios, with a difference between highest and lowest emission scenarios of about 1%, representing an economic benefit of 4 to 7 billion US\$.

Impacts of short-lived air pollutants (PM<sub>2.5</sub>, NO<sub>2</sub>) are strongly linked to the emission location and emission controls are largely driven by countries' self-interest. In contrast, the transboundary nature of the air quality impacts of CH<sub>4</sub> emissions justifies international cooperation to reduce these emissions. This cooperation may be found under the UNFCCC Paris Agreement, or regional conventions such as the UNECE Convention Long Range Transport of Air Pollution (see Maas and Grennfelt, P., 2016), or the Arctic Council. Aakre et al. (2018), using the TM5-FASST tool also utilised in this report, argue that collaborations between 3 to 6 key regions ('clubs'), may realize a substantial portion of the global mitigation potential, and overcome some of the difficulties associated with global agreements.

In this context the availability of scientific assessment tools, encompassing the full cycle from CH<sub>4</sub> emissions to impacts as well as the evaluation of economic costs and benefits is essential in building trust and confidence between the collaborating partners.

## **5.5 Promising economic sectors to effectively achieve CH<sub>4</sub> emission reductions**

This report shows that there is a substantial global mitigation potential in the three major emitting sectors- energy, waste and wastewater, and agriculture. For instance, currently, in the waste and fossil fuel production sectors there are large differences in emission factors (a factor of 10 or more) between developed and developing countries. A huge potential for emission reductions in many developing regions can be unlocked.

These mitigation potentials are reflected in the emission scenarios analysed in this report, where compared to 2010, energy related emissions in 2050 can increase by up to 70% in the group of high emission scenarios, are lower by 30-80% for the low-emission scenarios. Lower energy consumption, fuel substitution, but also upgrading old gas and oil production and gas distribution infrastructure are important factors.

Likewise, waste related emissions may increase by 70% to 130% by 2050 relative to 2010 for high emission scenarios, and decrease up to 80% for the low scenarios. Alignment with several sustainable development goals in developing countries may help to realize these emission reductions.

For agriculture, FAO suggested that general improvement in animal health and efficiency of milk and meat production is a straightforward strategy to mitigate agricultural CH<sub>4</sub> emissions. Especially in Eastern Europe, but also outside Europe, substantial emission reductions per unit production may still be achieved. Worldwide, and especially in Asia, further improvements in rice production may reduce CH<sub>4</sub> emissions. There are a number of technological options to reduce CH<sub>4</sub> emissions from agriculture, but there is not yet much experience with wide-spread implementation and possible implementation barriers. Economic studies suggest that subsidies for implementing emission reduction technologies (such as for CH<sub>4</sub> anaerobic digesters, feed supplements, and vaccination), may help to avoid loss of production and emission leakage to countries outside of the EU. There is mounting evidence that substantial reductions of the current animal products protein consumption, which is since ca. 2000 plateauing at a level 60 g/capita/day, have a large potential to reduce CH<sub>4</sub> emissions. Dietary change will have additional advantages for reducing nitrogen emissions to water and air (including the GHG N<sub>2</sub>O), and will have additional health benefits from

reducing the daily protein and saturated fat intake. Scenarios that assume reductions of meat and dairy consumption by 50%, indeed suggest a large reduction potential of CH<sub>4</sub> emissions by up to 45%, but the societal change in food attitudes will require time.

The set of scenario studies for the agricultural sector explored in this study indicate a somewhat smaller range of future agricultural emission changes than for the energy and waste sectors. Agricultural CH<sub>4</sub> emissions increase by 30-70% for the high emission scenarios; change by -10 to 30% under the middle scenarios, and decline by 20-40% for the low emission scenarios. Important drivers of change in these scenarios are population growth, per capita meat (protein) consumption, improvements in the animal production methods, and mitigation technologies.

Literature reviews have indicated that a number of the methane emission reduction technologies may have negative, zero or small positive costs, making them attractive targets for policies. However, there are large differences in estimated cost curves, making the economic cost related to “deep” mitigation of methane uncertain.

Further uncertainties are related to barriers for uptake, including sociological, technological and knowledge gaps between regions. The mitigation potentials will be regionally different, depending on the current predominance of sectoral emissions. E.g. energy emissions are dominating in Russia, USA and China, agriculture is important in the EU, India and China, while reducing CH<sub>4</sub> from waste and wastewater is required for sustainable development in developing countries.

## **5.6 The way forward**

Methane is an important target gas for emission abatements, with benefits for O<sub>3</sub> air quality and climate. To assess more accurately the potential of CH<sub>4</sub> abatements to improve ozone air quality, crop production and climate, the following considerations are important:

Funding for continuation of long-term background ozone and methane observations is under pressure, while they are essential to characterise long-term background changes and imperative to test models- a prerequisite for most of the points below. Bottom-up emission inventories are highly uncertain, in particular for fugitive emissions from fossil fuels. Top-down inverse modelling emission estimates can be used to improve CH<sub>4</sub> inventories, but they are highly dependent on observations, from facility scale to regional. Our understanding of large-scale O<sub>3</sub> trends in the last decades is severely hampered by the lack of reliable remote and rural stations, and tropospheric ozone satellite observations are not yet of sufficient quality to substitute in-situ observations.

The forthcoming 2019 Refinement to the 2006 IPCC guidelines for National Emission Inventories will facilitate a more accurate assessment of global methane emissions and also of emission reduction potentials- these new insights need to be included in scientific inventories as well.

Substantial work on understanding realistic mitigation potentials, cost-barriers etc. is needed. Further understanding and clarifying the specific commitments in the Nationally Determined Contributions with regard to CH<sub>4</sub> and promoting the understanding of the air quality benefits of CH<sub>4</sub> to the parties in the Paris Agreement are recommended. Initial analysis of a NDC scenario indicates that CH<sub>4</sub> may stabilize around the current values, an improvement of the pessimistic base-line scenarios, but not sufficient to reach the below 2 °C goal.

The mismatch of global models to understand ozone trends over the last 4-5 decades may be partly due to quality issues with ozone observations, but also point to limitations of models. Although we have relatively good knowledge on the specific contributions of methane to ozone, improving the understanding of the overall ozone budget (ozone production from anthropogenic emissions, natural emissions, stratospheric inflow and deposition processes), will also provide a scientifically more convincing case for the role of methane in determining ozone trends. Continuation of

model development and systematic testing of parameterisations and processes in global and regional models will help in further understanding ozone trends.

Recent publications suggest a substantially higher health impact of ozone, with consequences for the contribution by CH<sub>4</sub> as well. It is recommended that WHO reviews this new evidence and if appropriate gives guidance on its possible inclusion in health impacts assessment methodologies. Current EU and WHO (WHO, 2006) ozone 8-hourly mean O<sub>3</sub> guidelines use thresholds of 120 µg/m<sup>3</sup> and 100 µg/m<sup>3</sup> (ca 60 and 50 ppb), respectively. Especially the latter is close to the concentrations measured at locations where O<sub>3</sub> is transported into Europe. If those concentrations would again increase due to increasing methane emissions, there is limited possibility for local emission controls. Accurate quantification of the factors that may drive ozone away from or towards these limit values remains essential.

Estimates of ozone on crop yields, quantity and quality of production are based on fairly simplified impact methods, which are gradually replaced by more advanced approaches that measure and model ozone fluxes into crops. The understanding of the interplay of ozone, climate change, CO<sub>2</sub> and climate change adaptation is very limited and needs to be addressed to properly understand the relative benefits of methane emission reductions. Similar analysis is needed for the impact on (semi-)natural vegetation.

Europe's CH<sub>4</sub> emissions declined by 31% from 1970 to 2012, in particular driven by emission reductions in the period after 1990. In a perspective of increasing global emissions, the relative contribution of Europe to the global emissions declined from ca. 12% in 1970, to 11% in 1990, and 6.4% in 2012, and is projected to amount 3-5% in the period 2030-2050. The contribution of European CH<sub>4</sub> emission controls to European O<sub>3</sub> concentrations is proportional to the emissions and is about 0.3 ppb (or 500 premature deaths). Reducing EU28 CH<sub>4</sub> emissions by 10%, 20%, or 50%, saves 50, 100 and 250 deaths annually, and globally 540, 1040, and 2700. Since the benefits of CH<sub>4</sub> of emission reductions are globally distributed, global mitigation strategies are most effective in reaching substantial health benefits within and outside world regions. The largest scope for future CH<sub>4</sub> emission reductions is outside Europe, specifically in Asia, the middle East and Africa, which together account for 60-70% of the global difference between the high and low emission trajectories.

International scientific collaboration on understanding the benefit of CH<sub>4</sub> emission abatement on O<sub>3</sub> air quality, and implementing the findings in a shared policy perspective, is key to making progress.

## References

- Aakre, S., Kallbekken, S., Van Dingenen, R., Victor, D.G., 2018. Incentives for small clubs of Arctic countries to limit black carbon and methane emissions. *Nat. Clim. Change* 8, 85.
- Adhya, T. K., B. Lundquist, T. Searchinger, R. Wassmann, X. Yan, 2014, World Resources Institute, Installment 8 of 'Creating a Sustainable Food Future', Wetting and drying: reducing greenhouse gas emissions and saving water from rice production, Working Paper, 2014.
- Alvarez, R.A. D.Zavala-Araiza, D. R. Lyon, D. T. Allen, Z.R. Barkley, A.R. Brandt, K.J. Davis, S.C. Herndon, D.J. Jacob, A. Karion, E.A. Kort, B.K. Lamb, T. Lauvaux, J.D. Maasackers, A.J. Marchese, M.Omara, Stephen W. Pacala, J. Peischl, A.L. Robinson, P.B. Shepson, C. Sweeney, A.Townsend-Small, S.C. Wofsy, S.P. Hamburg, 2018. Assessment of methane emissions from the U.S. oil and gas supply chain, *Science*
- Amann, M., Klimont, Z., Wagner, F., 2013. Regional and global emissions of air pollutants: Recent trends and future scenarios, *Annual Review of Environment and Resources*.
- Beig, G., Singh, V., 2007. Trends in tropical tropospheric column ozone from satellite data and MOZART model. *Geophys. Res. Lett.* 34.
- Bergamaschi, P., A. Danila, R. F. Weiss, P. Ciais, R. L. Thompson, D. Brunner, I. Levin, Y. Meijer, F. Chevallier, G. Janssens-Maenhout, H. Bovensmann, D. Crisp, S. Basu, E. Dlugokencky, R. Engelen, C. Gerbig, D. Günther, S. Hammer, S. Henne, S. Houweling, U. Karstens, E. A. Kort, M. Maione, A. J. Manning, J. Miller, S. Montzka, S. Pandey, W. Peters, P. Peylin, B. Pinty, M. Ramonet, S. Reimann, T. Röckmann, M. Schmidt, M. Strogies, J. Sussams, O. Tarasova, J. van Aardenne, A. T. Vermeulen, F. Vogel, 2018, JRC Science for Policy Report, 2018, Luxembourg: Publications Office of the European Union, ISBN 978-92-79-88938-7
- Butler, J. H., and S. A. Montzka, 2017. The NOAA annual greenhouse gas index (AGGI), <https://www.esrl.noaa.gov/gmd/aggi/aggi.html>, last access: 19 September 2017.
- Brunekreef, B., Holgate, S.T., 2002. Air pollution and health. *The Lancet* 360, 1233–1242.
- Bruhwyler, L. M., Basu, S., Bergamaschi, P., Bousquet, P., Dlugokencky, E., Houweling, S., Ishizawa, M., Kim, H.-S., Locatelli, R., Maksyutov, S., Montzka, S., Pandey, S., Patra, P. K., Petron, G., Saunio, M., Sweeney, C., Schwietzke, S., Tans, P., Weatherhead, E. C., 2017. U.S. CH<sub>4</sub> emissions from oil and gas production: Have recent large increases been detected? *J. Geophys. Res. Atmospheres* 122, 4070–4083.
- Chang, K.-L., Petropavlovskikh, I., Cooper, O.R., Schultz, M.G., Wang, T., 2017. Regional trend analysis of surface ozone observations from monitoring networks in eastern North America, Europe and East Asia. *Elem Sci Anth* 5.
- Cohen, A. J., Brauer, M., Burnett, R., Anderson, H. R., Frostad, J., Estep, K., Balakrishnan, K., Brunekreef, B., Dandona, L., Dandona, R., Feigin, V., Freedman, G., Hubbell, B., Jobling, A., Kan, H., Knibbs, L., Liu, Y., Martin, R., Morawska, L., Pope, C. A., III, Shin, H., Straif, K., Shaddick, G., Thomas, M., van Dingenen, R., van Donkelaar, A., Vos, T., Murray, C. J. L. and Forouzanfar, M. H., 2017. Estimates and 25-year trends of the global burden of disease attributable to ambient air pollution: an analysis of data from the Global Burden of Diseases Study 2015, *The Lancet*, 389(10082), 1907–1918.
- Colette, A., Andersson, C., Manders, A., Mar, K., Mircea, M., Pay, M.-T., Raffort, V., Tsyro, S., Cuvelier, C., Adani, M., Bessagnet, B., Bergström, R., Briganti, G., Butler, T., Cappelletti, A., Couvidat, F., D'Isidoro, M., Doumbia, T., Fagerli, H., Granier, C., Heyes, C., Klimont, Z., Ojha, N., Otero, N., Schaap, M., Sindelarova, K., Stegehuis, A.

I., Roustan, Y., Vautard, R., van Meijgaard, E., Vivanco, M. G., and Wind, P., 2017: EURODELTA-Trends, a multi-model experiment of air quality hindcast in Europe over 1990–2010, *Geosci. Model Dev.*, 10, 3255–3276.

Cooper, O.R., Parrish, D.D., Ziemke, J., Balashov, N.V., Cupeiro, M., Galbally, I.E., Gilge, S., Horowitz, L., Jensen, N.R., Lamarque, J.-F., Naik, V., Oltmans, S.J., Schwab, J., Shindell, D.T., Thompson, A.M., Thouret, V., Wang, Y., Zbinden, R.M., 2014. Global distribution and trends of tropospheric ozone: An observation-based review. *Elem Sci Anth*, 2–29

Dalsøren, S.B., Myhre, G., Hodnebrog, O., Myhre, C.L., Stohl, A., Pissò, I., Schwietzke, S., Höglund-Isaksson, L., Helmig, D., Reimann, S., Sauvage, S., Schmidbauer, N., Read, K.A., Carpenter, L.J., Lewis, A.C., Punjabi, S., Wallasch, M., 2018 Discrepancy between simulated and observed ethane and propane levels explained by underestimated fossil emissions *Nature Geoscience*, 11 (3), pp. 178–184

Denier van der Gon, H. A. C., Kuenen, J. J. P., Janssens-Maenhout, G., Döring, U., Jonkers, S., and Visschedijk, 2017. A.: TNO CAMS high resolution European emission inventory 2000–2014 for anthropogenic CO<sub>2</sub> and future years following two different pathways, *Earth Syst. Sci. Data Discuss.*, 2017, 1–30.

Dentener, F., Keating, T., Akimoto, H., Pirrone, N., Dutchak, S., Zuber, A., Convention on Long-range Transboundary Air Pollution, United Nations, UNECE Task Force on Emission Inventories and Projections (Eds.), 2010. Hemispheric transport of air pollution 2010: prepared by the Task Force on Hemispheric Transport of Air Pollution acting within the framework of the Convention on Long-range Transboundary Air Pollution, *Air pollution studies*. United Nations, New York ; Geneva.

Dentener, F., Stevenson, D., Cofala, J., Mechler, R., Amann, M., Bergamaschi, P., Raes, F., Derwent, R., 2005. The impact of air pollutant and methane emission controls on tropospheric ozone and radiative forcing: CTM calculations for the period 1990–2030. *Atmos Chem Phys* 5, 1731–1755.

Derwent, R.G., Manning, A.J., Simmonds, P.G., Spain, T.G., O'Doherty, S., 2018. Long-term trends in ozone in baseline and European regionally-polluted air at Mace Head, Ireland over a 30-year period. *Atmos. Environ.* 179, 279–287.

de Vries, W., Posch, M., Simpson, D., Reinds, G.J., 2017. Modelling long-term impacts of changes in climate, nitrogen deposition and ozone exposure on carbon sequestration of European forest ecosystems, *Sci Total Environ.* 605–606:1097–1116.

Dlugokencky, E. J., Bruhwiler, L., White, J. W. C., Emmons, L. K., Novelli, P. C., Montzka, S. A., Masarie, K. A., Lang, P. M., Crotwell, A. M., Miller, J. B., Gatti, L. V., 2009. Observational constraints on recent increases in the atmospheric CH<sub>4</sub> burden. *Geophys. Res. Lett.* 36.

Eckard, R. J., Grainger, C., and de Klein, C. A. M., 2010 Options for the abatement of methane and nitrous oxide from ruminant production: A review, *Livestock Science*, 130, 47–56.

EU Agricultural Outlook for the EU Agricultural Markets and income, 2017–2030, 2017. [https://ec.europa.eu/agriculture/sites/agriculture/files/markets-and-prices/medium-term-outlook/2017/2017-fullrep\\_en.pdf](https://ec.europa.eu/agriculture/sites/agriculture/files/markets-and-prices/medium-term-outlook/2017/2017-fullrep_en.pdf), European Commission, Brussels.

EEA, European Environment Agency, 2018. Annual European Union greenhouse gas inventory 1990–2016 and inventory report 2018, <https://www.eea.europa.eu/publications/european-union-greenhouse-gas-inventory-2018>

EPRTTR: European Pollutant Transfer Register, database version v4.2, 2012. <http://prtr.ec.europa.eu>

EMEP/EEA emission inventory guidebook, 2013. European Environment Agency. <https://www.eea.europa.eu/publications/emep-eea-guidebook-2013>.

EPA, Global mitigation of Non-CO<sub>2</sub> Greenhouse Gases, 2010-2030, 2013. United States Environmental Protection Agency, Office of Atmospheric Programs, Washington DC, EPA-430-13-011.

EUROSTAT, 2017; [http://ec.europa.eu/eurostat/statistics-explained/index.php/Energy\\_production\\_and\\_imports](http://ec.europa.eu/eurostat/statistics-explained/index.php/Energy_production_and_imports) for EU28 gas numbers since 2005, accessed 10.06.2018.

FAO, 2017. The charcoal transition: greening the charcoal value chain to mitigate climate change and improve local livelihoods, by J. van Dam. Rome, Food and Agriculture Organization of the United Nations.

FAOSTAT: Statistics Division of the Food and Agricultural Organisation of the UN, Rome. <http://www.fao.org/faostat/en/#data>, accessed 2014.

Fiore, A.M., Dentener, F.J., Wild, O., Cuvelier, C., Schultz, M.G., Hess, P., Textor, C., Schulz, M., Doherty, R.M., Horowitz, L.W., MacKenzie, I.A., Sanderson, M.G., Shindell, D.T., Stevenson, D.S., Szopa, S., Van Dingenen, R., Zeng, G., Atherton, C., Bergmann, D., Bey, I., Carmichael, G., Collins, W.J., Duncan, B.N., Faluvegi, G., Folberth, G., Gauss, M., Gong, S., Hauglustaine, D., Holloway, T., Isaksen, I.S.A., Jacob, D.J., Jonson, J.E., Kaminski, J.W., Keating, T.J., Lupu, A., Marmer, E., Montanaro, V., Park, R.J., Pitari, G., Pringle, K.J., Pyle, J.A., Schroeder, S., Vivanco, M.G., Wind, P., Wojcik, G., Wu, S., Zuber, A., 2009. Multimodel estimates of intercontinental source-receptor relationships for ozone pollution. *J. Geophys. Res. - Atmospheres* 114, D04301

Fiore, A.M., Jacob, D.J., Field, B.D., Streets, D.G., Fernandes, S.D., Jang, C., 2002. Linking ozone pollution and climate change: The case for controlling methane. *Geophys. Res. Lett.* 29, 25-1-25-4.

Fiore, A.M., West, J.J., Horowitz, L.W., Naik, V., Schwarzkopf, M.D., 2008. Characterizing the tropospheric ozone response to methane emission controls and the benefits to climate and air quality. *J. Geophys. Res. Atmospheres* 113, D08307

Fleming, Z. L., Doherty, R. M., Schneidemesser, E. von, Malley, C. S., Cooper, O. R., Pinto, J. P., Colette, A., Xu, X., Simpson, D., Schultz, M. G., Lefohn, A. S., Hamad, S., Moolia, R., Solberg, S. and Feng, Z. (2018). Tropospheric Ozone Assessment Report: Present-day ozone distribution and trends relevant to human health, *Elem Sci Anth*, 6(1)

Forster, P., Ramaswamy, V., Artaxo, P., Bernsten, T., Betts, R., Fahey, D.W., Haywood, J., Lean, J., Lowe, D.C., Myhre, G., Nganga, J., Prinn, R., Raga, G., Schulz, M., Van Dorland, R., 2007. Changes in Atmospheric Constituents and in Radiative Forcing., in: *Climate Change 2007: The Physical Science Basis. Contribution of Working Group I to the Fourth Assessment Report of the Intergovernmental Panel on Climate Change*. Cambridge University Press, Cambridge, United Kingdom and New York, NY, USA.

Fowler, D., Pilegaard, K., Sutton, M.A., Ambus, P., Raivonen, M., Duyzer, J., Simpson, D., Fagerli, H., Fuzzi, S., Schjoerring, J.K., Granier, C., Neftel, A., Isaksen, I.S.A., Laj, P., Maione, M., Monks, P.S., Burkhardt, J., Daemmgen, U., Neirynck, J., Personne, E., Wichink-Kruit, R., Butterbach-Bahl, K., Flechard, C., Tuovinen, J.P., Coyle, M., Gerosa, G., Loubet, B., Altimir, N., Gruenhage, L., Ammann, C., Cieslik, S., Paoletti, E., Mikkelsen, T.N., Ro-Poulsen, H., Cellier, P., Cape, J.N., Horváth, L., Loreto, F., Niinemets, U., Palmer, P.I., Rinne, J., Misztal, P., Nemitz, E., Nilsson, D., Pryor, S., Gallagher, M.W., Vesala, T., Skiba, U., Brüggemann, N., Zechmeister-Boltenstern, S., Williams, J., O'Dowd, C., Facchini, M.C., de Leeuw, G., Flossman, A., Chaumerliac, N., Erisman, J.W., 2009. Atmospheric composition change: Ecosystems-Atmosphere interactions. *Atmos. Environ.* 43, 5193-5267.

Gaudel, A., Cooper, O.R., Ancellet, G., Barret, B., Boynard, A., Burrows, J.P., Clerbaux, C., Coheur, P.-F., Cuesta, J., Cuevas, E., Doniki, S., Dufour, G., Ebojie, F., Foret, G.,

Garcia, O., Muños, M.J.G., Hannigan, J.W., Hase, F., Huang, G., Hassler, B., Hurtmans, D., Jaffe, D., Jones, N., Kalabokas, P., Kerridge, B., Kulawik, S.S., Latter, B., Leblanc, T., Flochmoën, E.L., Lin, W., Liu, J., Liu, X., Mahieu, E., McClure-Begley, A., Neu, J.L., Osman, M., Palm, M., Petetin, H., Petropavlovskikh, I., Querel, R., Rahpoe, N., Rozanov, A., Schultz, M.G., Schwab, J., Siddans, R., Smale, D., Steinbacher, M., Tanimoto, H., Tarasick, D.W., Thouret, V., Thompson, A.M., Trickl, T., Weatherhead, E., Wespes, C., Worden, H.M., Vigouroux, C., Xu, X., Zeng, G., Ziemke, J., 2018. Tropospheric Ozone Assessment Report: Present-day distribution and trends of tropospheric ozone relevant to climate and global atmospheric chemistry model evaluation. *Elem Sci Anth* 6, 39.

GBD 2015 Disease and Injury Incidence and Prevalence Collaborators, 2016. Global, regional, and national incidence, prevalence, and years lived with disability for 310 diseases and injuries, 1990–2015: a systematic analysis for the Global Burden of Disease Study 2015, *Lancet* 2016; 388: 1545–602.

Gerber, P.J., Steinfeld, H., Henderson, B., Mottet, A., Opio, C., Dijkman, J., Falcucci, A., Tempio, G. 2013. Tackling climate change through livestock – A global assessment of emissions and mitigation opportunities. Food and Agriculture Organization of the United Nations (FAO), Rome.

Gomez-Sanabria, A., L. Höglund-Isaksson, P. Rafaj and W. Schöpp, 2018. Carbon in global waste and wastewater flows - its potential as energy source under alternative future waste management regimes. *Advances in Geosciences* 45:105-113.

Hartmann, D.L., A.M.G. Klein Tank, M. Rusticucci, L.V. Alexander, S. Brönnimann, Y. Charabi, F.J. Dentener, E.J. Dlugokencky, D.R. Easterling, A. Kaplan, B.J. Soden, P.W. Thorne, M. Wild and P.M. Zhai, 2013: Observations: Atmosphere and Surface. In: *Climate Change 2013: The Physical Science Basis. Contribution of Working Group I to the Fifth Assessment Report of the Intergovernmental Panel on Climate Change* [Stocker, T.F., D. Qin, G.-K. Plattner, M. Tignor, S.K. Allen, J. Boschung, A. Nauels, Y. Xia, V. Bex and P.M. Midgley (eds.)]. Cambridge University Press, Cambridge, United Kingdom and New York, NY, USA.

Hedenus, F., Wirsén, S., and Johansson, D. J. A., 2014. The importance of reduced meat and dairy consumption for meeting stringent climate change targets, *Climatic Change*, 124, 79-91, 10.1007/s10584-014-1104-5.

Höglund-Isaksson, L., 2012. Global anthropogenic methane emissions 2005-2030: technical mitigation potentials and costs. *Atmospheric Chemistry and Physics*, 12:9079-9096.

Höglund-Isaksson, L., A. Thomson, K. Kupiainen, S. Rao, and G. Janssens-Maenhout, 2015. Chapter 5: Anthropogenic methane sources, emissions and future projections. In *AMAP Assessment 2015: Methane as an Arctic climate forcer*, Arctic Monitoring and Assessment Programme (AMAP), Oslo.

Höglund-Isaksson, L., 2017. Bottom-up simulations of methane and ethane emissions from global oil and gas systems 1980 to 2012, *Environ. Res. Lett.*, Vol. 12 No.2

Houweling, S., Badawy, B., Baker, D.F., Basu, S., Belikov, D., Bergamaschi, P., Bousquet, P., Broquet, G., Butler, T., Canadell, J.G., Chen, J., Chevallier, F., Ciais, P., Collatz, G.J., Denning, S., Engelen, R., Enting, I.G., Fischer, M.L., Fraser, A., Gerbig, C., Gloor, M., Jacobson, A.R., Jones, D.B., Heimann, M., Khalil, A., Kaminski, T., Kasibhatla, P.S., Krakauer, N.Y., Krol, M., Maki, T., Maksyutov, S., Manning, A., Meesters, A., Miller, J.B., Palmer, P.I., Patra, P., Peters, W., Peylin, P., Poussi, Z., Prather, M.J., Randerson, J.T., Röckmann, T., Rödenbeck, C., Sarmiento, J.L., Schimel, D.S., Scholze, M., Schuh, A., Suntharalingam, P., Takahashi, T., Turnbull, J., Yurganov, L., Vermeulen, A., 2012. Iconic CO<sub>2</sub> time series at risk, *Science*, 337(6098):1038-40.

Hristov, A. N., Oh, J., Firkins, J. L., Dijkstra, J., Kebreab, E., Waghorn, G., Makkar, H. P. S., Adesogan, A. T., Yang, W., Lee, C., Gerber, P. J., Henderson, B., and Tricarico, J. M., 2013. SPECIAL TOPICS — Mitigation of methane and nitrous oxide emissions from animal operations: I. A review of enteric methane mitigation options, *Journal of Animal Science*, 91, 5045-5069

IEA- World Energy Outlook, 2012. International Energy Agency, Paris, France.

IEA- World Energy Outlook, 2017. International Energy Agency, Paris, France.

IIASA, FAO, 2012. Global Agro-Ecological Zones V3.0 [WWW Document]. URL <http://www.gaez.iiasa.ac.at/> (accessed 11.11.16).

IPCC: 2006. IPCC Guidelines for National Greenhouse Gas Inventories. Eggleston, S., Buendia, L., Miwa, K., Ngara, T., Tanabe, K. (eds.). IPCC-TSU NGGIP, IGES, Hayama, Japan. [www.ipcc-nggip.iges.or.jp/public/2006gl/index.html](http://www.ipcc-nggip.iges.or.jp/public/2006gl/index.html).

IRRI: World Rice statistics, 2007. Distribution of rice crop area by environment. International Rice Research Institute, <http://www.irri.org/science/ricestat/>, latest access: 2009.

Janssens-Maenhout, G., Crippa, M., Guizzardi, D., Dentener, F., Muntean, M., Pouliot, G., Keating, T., Zhang, Q., Kurokawa, J., Wankmüller, R., Denier van der Gon, H., Kuenen, J.J.P., Klimont, Z., Frost, G., Darras, S., Koffi, B., Li, M., 2015. HTAP\_v2.2: a mosaic of regional and global emission grid maps for 2008 and 2010 to study hemispheric transport of air pollution. *Atmos Chem Phys* 15, 11411–11432.

Janssens-Maenhout, G., Crippa, M., Guizzardi, D., Muntean, M., Schaaf, E., Dentener, F., Bergamaschi, P., Pagliari, V., Olivier, J.G.J., Peters, J.A.H.W., van Aardenne, J.A., Monni, S., Doering, U., Petrescu, A.M.R., 2017a. EDGARv4.3.2 Global Atlas of the three major Greenhouse Gas Emissions for the period 1970-2012, *Earth Syst. Sci. Data Discuss*, in review.

Janssens-Maenhout, G., Crippa, M., Guizzardi, D., Muntean, M., Schaaf, E., Olivier, J.G.J., Peters, J.A.H.W., Schure, K.M., 2017b. Fossil CO<sub>2</sub> and GHG emissions of all world countries, EUR 28766 EN, Publications Office of the European Union, Luxembourg, ISBN 978-92-79-73207-2, doi:10.2760/709792, JRC107877.

Jerrett, M., Burnett, R.T., Arden, P.I., Ito, K., Thurston, G., Krewski, D., Shi, Y., Calle, E., Thun, M., 2009. Long-term ozone exposure and mortality. *N. Engl. J. Med.* 360, 1085–1095.

Kitous, A., Keramidas, K., Vandyck, T., Saveyn, B., Van Dingenen, R., Spadaro, J., Holland, M., 2017. Global Energy and Climate Outlook 2017: How climate policies improve air quality, JRC Science for Policy report. Joint Research Centre, Luxembourg: Publications Office of the European Union.

Klimont, Z., Kupiainen, K., Heyes, C., Purohit, P., Cofala, J., Rafaj, P., Borken-Kleefeld, J. and Schöpp, W., 2017. Global anthropogenic emissions of particulate matter including black carbon, *Atmospheric Chem. Phys.*, 17(14), 8681–8723.

Kuenen, J. J. P., Visschedijk, A. J. H., Jozwicka, M., and Denier van der Gon, H. A. C., 2014. TNO-MACC\_II emission inventory; a multi-year (2003-2009) consistent high-resolution European emission inventory for air quality modelling, *Atmos. Chem. Phys.*, 14, 10963-10976.

Leip, A., G. Billen, J. Garnier, B. Grizzetti, L. Lassaletta, S. Reis, D. Simpson, M. A. Sutton, W. de Vries, F. Weiss, 2015. Impacts of European livestock production: nitrogen, sulphur, phosphorus and greenhouse gas emissions, land-use, water eutrophication and biodiversity. *Environ. Res. Lett.* 10-115004.

Lelieveld, J., Lechtenböhmer, S., Assonov, S. S., Brenninkmeijer, C. A. M., Dienst, C., Fischeidick, M. and Hanke, T., 2005. Greenhouse gases: Low methane leakage from gas pipelines, *Nature*, 434(7035), 841–842

- Lyon, DR, Zavala-Araiza D, Alvarez, RA, Harriss, R., Palacios, V., Lan, X., Talbot, R., Lavoie, T., Shepson, P., Yacovitch, T.I., Herndon, S.C., Marchese, A.J., Zimmerle, D., Robinson, A.L., Hamburg, S.P., 2015. Constructing a Spatially Resolved Methane Emission Inventory for the Barnett Shale Region, *Environ. Sci. Technol* 49, 81478157.
- Li, C., Qiu, J., Frohling, S., Xiao, X., Salas, W., Moore, B., Boles, S., Huang, Y., Sass, R., 2002b. Reduced methane emissions from large-scale changes in water management of China's rice paddies during 1980–2000. *Geophys. Res. Lett.* 29, 33-1-33–4.
- Liang, C.-K., West, J. J., Silva, R. A., Bian, H., Chin, M., Dentener, F. J., Davila, Y., Emmons, L., Folberth, G., Flemming, J., Henze, D., Im, U., Jonson, J. E., Kucsera, T., Keating, T. J., Lund, M. T., Lenzen, A., Lin, M., Pierce, R. B., Park, R. J., Pan, X., Sekiya, T., Sudo, K. and Takemura, T., 2018. HTAP2 multi-model estimates of premature human mortality due to intercontinental transport of air pollution, *Atmos. Chem. Phys.*, 18, 10497-10520.
- Liu, Z., Guan, D., Wei, W., Davis, S. J., Ciais, P., Bai, J., Peng, S., Zhang, Q., Hubacek, K., Marland, G., Andres, R. J., Crawford-Brown, D., Lin, J., Zhao, H., Hong, C., Boden, T. A., Feng, K., Peters, G. P., Xi, F., Liu, J., Li, Y., Zhao, Y., Zeng, N., and He, K., 2015. Reduced carbon emission estimates from fossil fuel combustion and cement production in China, *Nature*, 524, 335-338.
- Maas, R., Grennfelt, P.(eds). Towards Cleaner Air, Scientific Assessment Report 2016. EMEP Steering Body and Working Group on Effects of the Convention on Long-Range Transboundary Air Pollution, Oslo.
- Malley, C.S., Henze, D.K., Kuylensstierna, J.C.I., Vallack, H., Davila, Y., Anenberg, S.C., Turner, M.C., Ashmore, M., 2017. Updated Global Estimates of Respiratory Mortality in Adults  $\geq 30$  Years of Age Attributable to Long-Term Ozone Exposure. *Environ. Health Perspect.* 125, 087021.
- Marcogaz: Technical statistics 01-01-2013, technical sheet of Marcogaz technical association of the European natural gas industry, *Technical\_statistics\_01-01-2013\_revision\_on\_15-09-2014\_-\_WEB\_VERSION.pdf*, 2013.
- Mills, G., Pleijel, H., Braun, S., Büker, P., Bermejo, V., Calvo, E., Danielsson, H., Emberson, L., Fernández, I.G., Grünhage, L., Harmens, H., Hayes, F., Karlsson, P.-E., Simpson, D., 2011. New stomatal flux-based critical levels for ozone effects on vegetation. *Atmos. Environ.* 45, 5064–5068.
- Montzka, S.A., Krol, M., Dlugokencky, E., Hall, B., Jöckel, P., Lelieveld, J., 2011. Small interannual variability of global atmospheric hydroxyl. *Science* 331, 67–69.
- Murray, C.J., Ezzati, M., Lopez, A.D., Rodgers, A., Vander Hoorn, S., 2003. Comparative quantification of health risks: conceptual framework and methodological issues. *Popul. Health Metr.* 1, 1.
- Myhre, G., Shindell, D., Bréon, F.-M., Collins, W., Fuglestad, J., Huang, J., Koch, D., Lamarque, J.-F., Lee, D., Mendoza, B., 2013. Anthropogenic and natural radiative forcing, in: *Climate Change 2013: The Physical Science Basis. Contribution of Working Group I to the Fifth Assessment Report of the Intergovernmental Panel on Climate Change* [Stocker, T.F., D. Qin, G.-K. Plattner, M. Tignor, S.K. Allen, J. Boschung, A. Nauels, Y. Xia, V. Bex and P.M. Midgley (Eds.). Cambridge University Press, Cambridge, United Kingdom and New York, NY, USA, pp. 658–740.
- Myhre, G., Aas, W., Cherian, R., Collins, W., Faluvegi, G., Flanner, M., Forster, P., Hodnebrog, O., Klimont, Z., Lund, M.T., Mülmenstädt, J., Lund Myhre, C., Olivé, D., Prather, M., Quaas, J., Samset, B.H., Schnell, J.L., Schulz, M., Shindell, D., Skeie, R.B., Takemura, T., Tsyro, S., 2017. Multi-model simulations of aerosol and ozone radiative forcing due to anthropogenic emission changes during the period 1990–2015. *Atmospheric Chem. Phys.* 17, 2709–2720.

Nisbet, E.G., Dlugokencky, E.J., Manning, M.R., Lowry, D., Fisher, R.E., France, J.L., Michel, S.E., Miller, J.B., White, J.W.C., Vaughn, B., Bousquet, P., Pyle, J.A., Warwick, N.J., Cain, M., Brownlow, R., Zazzeri, G., Lanoisellé, M., Manning, A.C., Gloor, E., Worthy, D.E.J., Brunke, E.-G., Labuschagne, C., Wolff, E.W., Ganesan, A.L., 2016, Rising atmospheric methane: 2007–2014 growth and isotopic shift, *Global Biogeochem. Cycles*, 30.

Paoletti, E., 2006. Impact of ozone on Mediterranean forests: A review, *Environmental Pollution*, 2, 463–474.

Parrish, D.D., Petropavlovskikh, I., Oltmans, S.J., 2017. Reversal of Long-Term Trend in Baseline Ozone Concentrations at the North American West Coast. *Geophys. Res. Lett.* 44, 10, 675–10, 681.

Pérez Domínguez, I., Fellman, T., Weiss, F., Witzke, P., Barreiro-Hurlé, J., Himics, M., Jansson, T., Salputra, G., Leip, A., 2016. An economic assessment of GHG mitigation policy options for EU agriculture (EcAMPA 2), EUR 27973 EN, JRC Science for Policy Report. Publication Office of the European Union.

Pleijel, H., Broberg, M.C., Uddling, J., Mills, G., 2018. Current surface ozone concentrations significantly decrease wheat growth, yield and quality. *Sci. Total Environ.* 613–614, 687–692.

Peischl, J., Ryerson, T.B., Aikin, K.C., de Gouw, J.A., Gilman, J.B., Holloway, J.S., Lerner, B.M., Nadkarni, R., Neuman, J.A., Nowak, J.B., Trainer, M., Warneke, C., Parrish, D.D., 2015. Quantifying atmospheric methane emissions from the Haynesville, Fayetteville, and northeastern Marcellus shale gas production regions. *J. Geophys. Res. Atmospheres* 120, 2119–2139.

Peng, S., Piao, S., Bousquet, P., Ciais, P., Li, B., Lin, X., Tao, S., Wang, Z., Zhang, Y., and Zhou, F., 2016. Inventory of anthropogenic methane emissions in mainland China from 1980 to 2010, *Atmos. Chem. Phys.*, 16, 14545–14562.

Poore, J., Nemecek, T., 2018. Reducing food's environmental impacts through producers and consumers. *Science* 360, 987–992.

Popp, A., Calvin, K., Fujimori, S., Havlik, P., Humpenöder, F., Stehfest, E., Bodirsky, B.L., Dietrich, J.P., Doelman, J.C., Gusti, M., Hasegawa, T., Kyle, P., Obersteiner, M., Taboada, A., Takahashi, K., Valin, H., Waldhoff, S., Weindl, I., Wise, M., Kriegler, E., Lotze-Campen, H., Fricko, O., Riahi, K., van Vuuren, D.P., 2017. Land-use futures in the shared socio-economic pathways. *Glob. Environ. Change* 42, 331–345.

Prather, M., Ehhalt, D., Dentener, F., Derwent, R., Dlugokencky, E., Holland, E., Isaksen, I., Katima, J., Kirchhoff, V., Matson, P., Midgley, P., Wang, M., Bernsten, T., Bey, I., Brasseur, G., Buja, L., Pitari, G., Et, A., 2001. Chapter 4: Atmospheric Chemistry and Greenhouse Gases. Cambridge University Press.

Prather, M., Flato, G., Friedlingstein, P., Jones, C., Lamarque, J.F., Liao, H., Rasch, P. (Eds.), 2013. IPCC, 2013: Annex II: Climate System Scenario Tables, in: *Climate Change 2013: The Physical Science Basis. Contribution of Working Group I to the Fifth Assessment Report of the Intergovernmental Panel on Climate Change* [Stocker, T.F., D. Qin, G.-K. Plattner, M. Tignor, S.K. Allen, J. Boschung, A. Nauels, Y. Xia, V. Bex and P.M. Midgley (Eds.)]. Cambridge University Press, Cambridge, United Kingdom and New York, NY, USA, p. 52.

Prather, M.J., C.D. Holmes, 2017, Explaining methane's role in climate change. *Proceedings of the National Academy of Sciences* May 2017, 114 (21) 5324–5326; DOI: 10.1073/pnas.1704884114.

Reidmiller, D.R., Fiore, A.M., Jaffe, D.A., Bergmann, D., Cuvelier, C., Dentener, F.J., Duncan, B.N., Folberth, G., Gauss, M., Gong, S., Hess, P., Jonson, J.E., Keating, T., Lupu, A., Marmer, E., Park, R., Schultz, M.G., Shindell, D.T., Szopa, S., Vivanco, M.G.,

Wild, O., Zuber, A., 2009. The influence of foreign vs. North American emissions on surface ozone in the US. *Atmospheric Chem. Phys.* 9, 5027–5042

REVIHAAP, 2013. Review of evidence on health aspects of air pollution - REVIHAAP Project. World Health Organisation (WHO) Regional Office for Europe, Bonn, Germany.

Riahi, K., van Vuuren, D.P., Kriegler, E., Edmonds, J., O'Neill, B.C., Fujimori, S., Bauer, N., Calvin, K., Dellink, R., Fricko, O., Lutz, W., Popp, A., Cuaresma, J.C., Kc, S., Leimbach, M., Jiang, L., Kram, T., Rao, S., Emmerling, J., Ebi, K., Hasegawa, T., Havlik, P., Humpenöder, F., Da Silva, L.A., Smith, S., Stehfest, E., Bosetti, V., Eom, J., Gernaat, D., Masui, T., Rogelj, J., Strefler, J., Drouet, L., Krey, V., Luderer, G., Harmsen, M., Takahashi, K., Baumstark, L., Doelman, J.C., Kainuma, M., Klimont, Z., Marangoni, G., Lotze-Campen, H., Obersteiner, M., Tabeau, A., Tavoni, M., 2017. The Shared Socioeconomic Pathways and their energy, land use, and greenhouse gas emissions implications: An overview. *Glob. Environ. Change* 42, 153–168.

Rigby, M., Montzka, S.A., R.G. Prinn, J.W. C. White, D. Young, S.O'Doherty, M.F. Lunt, A. L. Ganesan, A.J. Manning, P.G. Simmonds, P.K. Salameh, C.M. Harth, J.Mühle, R.F. Weiss, P.J. Fraser, L.P. Steele, P. B. Krummel, A. McCulloch, S. Park, 2017. Proceedings of the National Academy of Sciences May 2017, 114 (21) 5373-5377.

Saunio, M., Bousquet, P., Poulter, B., Peregon, A., Ciais, P., Canadell, J.G., Dlugokencky, E.J., Etiope, G., Bastviken, D., Houweling, S., Janssens-Maenhout, G., Tubiello, F.N., Castaldi, S., Jackson, R.B., Alexe, M., Arora, V.K., Beerling, D.J., Bergamaschi, P., Blake, D.R., Brailsford, G., Brovkin, V., Bruhwiler, L., Crevoisier, C., Crill, P., Covey, K., Curry, C., Frankenberg, C., Gedney, N., Höglund-Isaksson, L., Ishizawa, M., Ito, A., Joos, F., Kim, H.-S., Kleinen, T., Krummel, P., Lamarque, J.-F., Langenfelds, R., Locatelli, R., Machida, T., Maksyutov, S., McDonald, K.C., Marshall, J., Melton, J.R., Morino, I., Naik, V., O'Doherty, S., Parmentier, F.-J.W., Patra, P.K., Peng, C., Peng, S., Peters, G.P., Pison, I., Prigent, C., Prinn, R., Ramonet, M., Riley, W.J., Saito, M., Santini, M., Schroeder, R., Simpson, I.J., Spahni, R., Steele, P., Takizawa, A., Thornton, B.F., Tian, H., Tohjima, Y., Viovy, N., Voulgarakis, A., Weele, M. van, Werf, G.R. van der, Weiss, R., Wiedinmyer, C., Wilton, D.J., Wiltshire, A., Worthy, D., Wunch, D., Xu, X., Yoshida, Y., Zhang, B., Zhang, Z., Zhu, Q., 2016a. The global methane budget 2000–2012. *Earth Syst. Sci. Data* 8, 697–751.

Saunio, M., Jackson, R.B., Bousquet, P., Poulter, B., Canadell, J.G., 2016b. The growing role of methane in anthropogenic climate change. *Environ. Res. Lett.* 11, 120207.

Saunio, M., Bousquet, P., Poulter, B., Peregon, A., Ciais, P., Canadell, J.G., Dlugokencky, E.J., Etiope, G., Bastviken, D., Houweling, S., Janssens-Maenhout, G., Tubiello, F.N., Castaldi, S., Jackson, R.B., Alexe, M., Arora, V.K., Beerling, D.J., Bergamaschi, P., Blake, D.R., Brailsford, G., Bruhwiler, L., Crevoisier, C., Crill, P., Covey, K., Frankenberg, C., Gedney, N., Höglund-Isaksson, L., Ishizawa, M., Ito, A., Joos, F., Kim, H.-S., Kleinen, T., Krummel, P., Lamarque, J.-F., Langenfelds, R., Locatelli, R., Machida, T., Maksyutov, S., Melton, J.R., Morino, I., Naik, V., O'Doherty, S., Parmentier, F.-J.W., Patra, P.K., Peng, C., Peng, S., Peters, G.P., Pison, I., Prinn, R., Ramonet, M., Riley, W.J., Saito, M., Santini, M., Schroeder, R., Simpson, I.J., Spahni, R., Takizawa, A., Thornton, B.F., Tian, H., Tohjima, Y., Viovy, N., Voulgarakis, A., Weiss, R., Wilton, D.J., Wiltshire, A., Worthy, D., Wunch, D., Xu, X., Yoshida, Y., Zhang, B., Zhang, Z., Zhu, Q., 2017. Variability and quasi-decadal changes in the methane budget over the period 2000–2012. *Atmospheric Chem. Phys.* 17, 11135–11161.

Schaefer, H., Fletcher, S.E.M., Veidt, C., Lassey, K.R., Brailsford, G.W., Bromley, T.M., Dlugokencky, E.J., Michel, S.E., Miller, J.B., Levin, I., Lowe, D.C., Martin, R.J., Vaughn, B.H., White, J.W.C., 2016. A 21st-century shift from fossil-fuel to biogenic methane emissions indicated by  $^{13}\text{CH}_4$ . *Science* 352, 80–84.

Schwietzke, S., Sherwood, O.A., Bruhwiler, L.M.P., Miller, J.B., Etiope, G., Dlugokencky, E.J., Michel, S.E., Arling, V.A., Vaughn, B.H., White, J.W.C., Tans, P.P., 2016. Upward revision of global fossil fuel methane emissions based on isotope database. *Nature* 538, 88–91.

Schultz, M.G., Schröder, S., Lyapina, O., Cooper, O., Galbally, I., Petropavlovskikh, I., von Schneidemesser, E., Tanimoto, H., Elshorbany, Y., Naja, M., Seguel, R., Dauert, U., Eckhardt, P., Feigenspahn, S., Fiebig, M., Hjellbrekke, A.-G., Hong, Y.-D., Kjeld, P.C., Koide, H., Lear, G., Tarasick, D., Ueno, M., Wallasch, M., Baumgardner, D., Chuang, M.-T., Gillett, R., Lee, M., Molloy, S., Moolla, R., Wang, T., Sharps, K., Adame, J.A., Ancellet, G., Apadula, F., Artaxo, P., Barlasina, M., Bogucka, M., Bonasoni, P., Chang, L., Colomb, A., Cuevas, E., Cupeiro, M., Degorska, A., Ding, A., Frölich, M., Frolova, M., Gadhavi, H., Gheusi, F., Gilge, S., Gonzalez, M.Y., Gros, V., Hamad, S.H., Helmig, D., Henriques, D., Hermansen, O., Holla, R., Huber, J., Im, U., Jaffe, D.A., Komala, N., Kubistin, D., Lam, K.-S., Laurila, T., Lee, H., Levy, I., Mazzoleni, C., Mazzoleni, L., McClure-Begley, A., Mohamad, M., Murovic, M., Navarro-Comas, M., Nicodim, F., Parrish, D., Read, K.A., Reid, N., Ries, L., Saxena, P., Schwab, J.J., Scorgie, Y., Senik, I., Simmonds, P., Sinha, V., Skorokhod, A., Spain, G., Spangl, W., Spoor, R., Springston, S.R., Steer, K., Steinbacher, M., Suharguniyawan, E., Torre, P., Trickl, T., Weili, L., Weller, R., Xu, X., Xue, L., Zhiqiang, M., 2017. Tropospheric ozone assessment report: database and metrics data of global surface ozone observations. 5:58.

Shindell, D., Kuylensstierna, J., Vignati, E., van Dingenen, R., Amann, M., Klimont, Z., Anenberg, S., Muller, N., Janssens-Maenhout, G., Raes, F., Schwartz, J., Faluvegi, G., Pozzoli, L., Kupiainen, K., Hoglund-Isaksson, L., Emberson, L., Streets, D., Ramanathan, V., Hicks, K., Oanh, N., Milly, G., Williams, M., Demkine, V., Fowler, D., 2012. Simultaneously Mitigating Near-Term Climate Change and Improving Human Health and Food Security. *Science* 335, 183–189.

Shindell, D.T., Fuglestad, J.S., Collins, W.J., 2017. The social cost of methane: Theory and applications. *Faraday Discuss.* 200, 429–451.

Silva, R. A., West, J. J., Zhang, Y., Anenberg, S. C., Lamarque, J.-F., Shindell, D. T., Collins, W. J., Dalsoren, S., Faluvegi, G., Folberth, G., Horowitz, L. W., Tatsuya Nagashima, Naik, V., Rumbold, S., Skeie, R., Sudo, K., Takemura, T., Daniel Bergmann, Cameron-Smith, P., Cionni, I., Doherty, R. M., Eyring, V., Josse, B., MacKenzie, I. A., Plummer, D., Righi, M., Stevenson, D. S., Strode, S., Szopa, S. and Zeng, G., 2013. Global premature mortality due to anthropogenic outdoor air pollution and the contribution of past climate change, *Environ. Res. Lett.*, 8(3), 034005.

Simmonds, P.G., Derwent, R.G., Manning, A.L., Spain, G., 2004. Significant growth in surface ozone at Mace Head, Ireland, 1987-2003. *Atmos. Environ.* 38, 4769–4778.

Sitch, S., Cox, P.M., Collins, W.J., Huntingford, C., 2007. Indirect radiative forcing of climate change through ozone effects on the land-carbon sink. *Nature* 448: 791-794

Stevenson, D.S., Dentener, F.J., Schultz, M.G., Ellingsen, K., van Noije, T.P.C., Wild, O., Zeng, G., Amann, M., Atherton, C.S., Bell, N., Bergmann, D.J., Bey, I., Butler, T., Cofala, J., Collins, W.J., Derwent, R.G., Doherty, R.M., Drevet, J., Eskes, H.J., Fiore, A.M., Gauss, M., Hauglustaine, D.A., Horowitz, L.W., Isaksen, I.S.A., Krol, M.C., Lamarque, J.-F., Lawrence, M.G., Montanaro, V., Müller, J.-F., Pitari, G., Prather, M.J., Pyle, J.A., Rast, S., Rodriguez, J.M., Sanderson, M.G., Savage, N.H., Shindell, D.T., Strahan, S.E., Sudo, K., Szopa, S., 2006. Multimodel ensemble simulations of present-day and near-future tropospheric ozone. *J. Geophys. Res. Atmospheres* 111.

Stevenson, D.S., Young, P.J., Naik, V., Lamarque, J.-F., Shindell, D.T., Voulgarakis, A., Skeie, R.B., Dalsoren, S.B., Myhre, G., Berntsen, T.K., Folberth, G.A., Rumbold, S.T., Collins, W.J., MacKenzie, I.A., Doherty, R.M., Zeng, G., Van, N., Strunk, A., Bergmann, D., Cameron-Smith, P., Plummer, D.A., Strode, S.A., Horowitz, L., Lee, Y.H., Szopa, S., Sudo, K., Nagashima, T., Josse, B., Cionni, I., Righi, M., Eyring, V., Conley, A.,

Bowman, K.W., Wild, O., Archibald, A., 2013. Tropospheric ozone changes, radiative forcing and attribution to emissions in the Atmospheric Chemistry and Climate Model Intercomparison Project (ACCMIP). *Atmospheric Chem. Phys.* 13, 3063–3085.

Stohl, A., Aamaas, B., Amann, M., Baker, L.H., Bellouin, N., Berntsen, T.K., Boucher, O., Cherian, R., Collins, W., Daskalakis, N., Dusinska, M., Eckhardt, S., Fuglestad, J.S., Harju, M., Heyes, C., Hodnebrog, Ø., Hao, J., Im, U., Kanakidou, M., Klimont, Z., Kupiainen, K., Law, K.S., Lund, M.T., Maas, R., MacIntosh, C.R., Myhre, G., Myriokefalitakis, S., Olivié, D., Quaas, J., Quennehen, B., Raut, J.-C., Rumbold, S.T., Samset, B.H., Schulz, M., Seland, Ø., Shine, K.P., Skeie, R.B., Wang, S., Yttri, K.E., Zhu, T., 2015. Evaluating the climate and air quality impacts of short-lived pollutants. *Atmospheric Chem. Phys.* 15, 10529–10566.

Thematic Strategy Airpollution, 2013. Policy scenarios for the revision of the thematic strategy of air pollution, TSAP report #10, version 1.2, International Institute for Applied Systems Analysis IIASA, Laxenburg, Austria.  
<http://ec.europa.eu/environment/air/pdf/TSAP-Report-10.pdf>

Tu, K.J.: Understanding China's Rising Coal Imports. Carnegie. Internet:  
<http://carnegieendowment.org/2012/02/16/understanding-china-s-rising-coal-imports>, 2012.

Turner, M.C., Jerrett, M., Pope, C.A., Krewski, D., Gapstur, S.M., Diver, W.R., Beckerman, B.S., Marshall, J.D., Su, J., Crouse, D.L., Burnett, R.T., 2016. Long-Term Ozone Exposure and Mortality in a Large Prospective Study. *Am. J. Respir. Crit. Care Med.* 193, 1134–1142.

Turner, A.J., C. Frankenberg, P.O. Wennberg, D.J. Jacob, 2017. Decadal trends in atmospheric methane and OH, *Proceedings of the National Academy of Sciences* May 2017, 114 (21) 5367–5372.

Turnock, S., Wild, O., Dentener, F., Davila, Y., Emmons, L., Flemming, J., Folberth, G., Henze, D., Jonson, J., Keating, T., Kengo, S., Lin, M., Lund, M., Tilmes, S., O'Connor, F., 2018. The Impact of Future Emission Policies on Tropospheric Ozone using a Parameterised Approach. *Atmos. Chem. Phys.*, 18, 8953–8978

UNEP, 2017. The Emissions Gap Report 2017. United Nations Environment Programme (UNEP), Nairobi.

UNFCCC, National Inventory Report, submissions of the greenhouse gas inventories for Annex I countries.  
[http://unfccc.int/national\\_reports/annex\\_i\\_ghg\\_inventories/national\\_inventories\\_submissions/items/7383.php](http://unfccc.int/national_reports/annex_i_ghg_inventories/national_inventories_submissions/items/7383.php), 2014, 2016.

United Nations (2015). Probabilistic Population Projections based on the World Population Prospects: The 2015 Revision. Population Division, DESA.  
<http://esa.un.org/unpd/ppp/>

Van Dingenen, R., Dentener, F., Crippa, M., Leitao, J., Marmer, E., Rao, S., Solazzo, E., Valentini, L., 2018. TM5-FASST: a global atmospheric source-receptor model for rapid impact analysis of emission changes on air quality and short-lived climate pollutants. *Atmos Chem Phys Discuss*, 2018, 1–55.

Van Dingenen, R., Dentener, F.J., Raes, F., Krol, M.C., Emberson, L., Cofala, J., 2009. The global impact of ozone on agricultural crop yields under current and future air quality legislation. *Atmos. Environ.* 43, 604–618.

van Vuuren, D.P., Edmonds, J., Kainuma, M., Riahi, K., Thomson, A., Hibbard, K., Hurtt, G.C., Kram, T., Krey, V., Lamarque, J.-F., Masui, T., Meinshausen, M., Nakicenovic, N., Smith, S.J., Rose, S.K., 2011. The representative concentration pathways: An overview. *Clim. Change* 109, 5–31.

Wang, Y., Jacob, D.J., 1998. Anthropogenic forcing on tropospheric ozone and OH since preindustrial times. *J. Geophys. Res. Atmospheres* 103, 31123–31135.

- Wang, X., Mauzerall, D.L., 2004. Characterizing distributions of surface ozone and its impact on grain production in China, Japan and South Korea: 1990 and 2020. *Atmos. Environ.* 38, 4383–4402.
- West, J.J., Fiore, A.M., 2005. Management of Tropospheric Ozone by Reducing Methane Emissions. *Environ. Sci. Technol.* 39, 4685–4691.
- West, J.J., Fiore, A.M., Horowitz, L.W., Mauzerall, D.L., 2006. Global health benefits of mitigating ozone pollution with methane emission controls. *Proc. Natl. Acad. Sci.* 103, 3988–3993.
- West, J.J., Fiore, A.M., Horowitz, L.W., 2012. Scenarios of methane emission reductions to 2030: Abatement costs and co-benefits to ozone air quality and human mortality. *Clim. Change* 114, 441–461.
- Westhoek, H., Lesschen, J. P., Leip, A., Rood, T., Wagner, S., De Marco, A., Murphy-Bokern, D., Pallière, C., Howard, C. M., Oenema, O. and Sutton, M. A.: Nitrogen on the table: the influence of food choices on nitrogen emissions, greenhouse gas emissions and land use in Europe, Centre for Ecology & Hydrology, Edinburgh, UK. [online] Available from: <http://edepot.wur.nl/368693>
- Wild, O., Fiore, A.M., Shindell, D.T., Doherty, R.M., Collins, W.J., Dentener, F.J., Schultz, M.G., Gong, S., MacKenzie, I.A., Zeng, G., others, 2012. Modelling future changes in surface ozone: a parameterized approach. *Atmospheric Chem. Phys.* 12, 2037–2054.
- WHO - World Health Organisation, WHO Air quality guidelines for particulate matter, ozone, nitrogen dioxide and sulfur dioxide, Global update 2005, WHO/SDE/PHE/OEH/06.02, Geneva, 2006.
- Worden, J.R., Bloom, A.A., Pandey, S., Jiang, Z., Worden, H.M., Walker, T.W., Houweling, S., Röckmann, T., 2017. Reduced biomass burning emissions reconcile conflicting estimates of the post-2006 atmospheric methane budget. *Nat. Commun.* 8, 2227.
- World coal association, Spatial proxies for the coal mining activities, <http://www.worldcoal.org/coal/coalmining/>, 2016.
- Yacovitch, T.I., Neininger, B., Herndon, S.C., Gon, H.D. van der, Jonkers, S., Hulskotte, J., Roscioli, J.R., Zavala-Araiza, D., 2018. Methane emissions in the Netherlands: The Groningen field. *Elem Sci Anth* 6.
- Yan, X., Akiyama, H., Yagi, K., and Akimoto, H.: Global estimations of the inventory and mitigation potential of methane emissions from rice cultivation conducted using the 2006 Intergovernmental Panel on Climate Change Guidelines, *Global Biogeochemical Cycles*, 23, n/a-n/a, 10.1029/2008gb003299, 2009.
- Ziemke, J.R., Chandra, S., Labow, G.J., Bhartia, P.K., Froidevaux, L., Witte, J.C., 2011. A global climatology of tropospheric and stratospheric ozone derived from Aura OMI and MLS measurements. *Atmospheric Chem. Phys.* 11, 9237–9251.

## List of abbreviations and definitions

AMAP: Arctic Monitoring and Assessment Programme

CAPRI: Common Agricultural Policy Regional Impact Analysis Model

CCAC: Climate and Clean Air Coalition

CH<sub>4</sub>: Methane. Simplest alkane, and component of natural gas. Contributes to greenhouse Gas Warming and ozone production.

CLRTAP: Convention Long Range Transport Air Pollution under the UN Economic Commission for Europe. <https://www.unece.org/env/lrtap/welcome.html>

EDGAR: *Emission* Database for Global Atmospheric Research. *edgar.jrc.ec.europa.eu*. JRC in-house worldwide database of air pollutant and GHG emissions.

EcAMPA: Economic assessment of GHG mitigation policy options for EU agriculture

ECLIPSE: emission dataset created with the GAINS emission scenario evaluation model.

EDGAR: Emissions Database for Global Atmospheric Research maintained at JRC.

EEA: European Environment Agency

EMEP: European Monitoring and Evaluation Programme

EU28: the 28 Member States of the European Union. EU15 pertains to the original EU Member States: Belgium, Denmark, Germany, Ireland, Greece, Spain, France, Italy, Luxembourg, Netherlands, Austria, Portugal, Finland, Sweden, United Kingdom and EU13 to new EU Member States: Bulgaria, Czechia, Estonia, Croatia, Cyprus, Latvia, Lithuania, Hungary, Malta, Poland, Romania, Slovenia, Slovakia.

ETS: Emission trading System currently covering 45% of EU GHG in 31 European countries. Non-ETS comprises all sectors not covered by ETS.

FAO: Food and Agricultural organisation of the United Nations

GAINS: Greenhouse gas Air pollutant Interactions and Synergies

GECCO: Global Energy and Climate Outlook initiated by JRC and CLIMA to inform EU policy making on future scenarios.

GHG: Greenhouse gas absorbs and emits radiant energy within the thermal infrared range, and the principal cause of global warming.

GWP: Global Warming Potential, a measure of the relative importance of a kg of Greenhouse gas emission compared to carbon dioxide. Typically a timescale of 20 or 100 years is chosen.

HTAP: Hemispheric Transport of Air Pollution. Task Force of the UNECE CLRTAP. HTAP1- phase 1 (2005-2010), HTAP2- phase 2 (2011-2018)

IEA: International Energy Agency

IPCC: Intergovernmental Panel on Climate Change. [www.ipcc.ch](http://www.ipcc.ch). AR4, AR5, and AR6 refer to the 2007, 2013 and forthcoming 2021 assessment reports.

JRC: Directorate General Joint Research Centre of the European Commission.

NECD: National Emission Ceilings Directive.

NDC: Nationally Determined Contribution, efforts by each country to reduce national emissions and adapt to climate change.

O<sub>3</sub>: Ozone. A powerful oxidising gas which can cause damage in respiratory tissues of human and animals, and stomatal tissues of plants.

PM<sub>2.5</sub>: Particulate matter with an aerodynamic diameter smaller than 2.5 micrometer.

OECD: Organisation for Economic Co-operation and Development

ppb: parts per billion volume mixing ratios. 1 ppb is about equivalent to a concentration of  $2 \mu\text{g m}^{-3}$

RCP: Representative Concentration Pathways- concentrations and associated global emission scenarios to inform the IPCC AR5 report.

SSP: Shared Socioeconomic Pathways analysis framework adopted by the climate change research community to facilitate the integrated analysis of future climate impacts, vulnerabilities, adaptation, and mitigation. Informing the IPCC AR6 report.

UNFCCC: United Nations Framework Convention on Climate Change. [unfccc.int](http://unfccc.int)

WHO: World Health Organisation

WMO: World Meteorological Organisation

## List of figures

Figure ES1. Change in European O <sub>3</sub> -related premature mortalities linked to CH <sub>4</sub> emissions in 2050, relative to 2010. The 3 colours represent different scenario family characteristics (see section 3.3). High: non-ambitious high emission scenarios; Mid: Moderate ambition; Low: high ambition low-emission scenarios. Population was kept constant at projected 2050 levels to allow comparability. ....	6
Figure 2.1. Atmospheric methane measured as “dry air mole fraction” in ppb. The red dots are globally averaged monthly mean values, whereas the black line shows the long-term trend through a 12-month running mean (removing the average seasonal cycle).....	10
Figure 2.2. Evolution of O <sub>3</sub> peak concentrations (4th highest daily maxima 8-hour mean O <sub>3</sub> ; MDA8) and annual mean concentrations at the 54 EMEP European background monitoring stations with satisfactory data coverage. Thick lines indicate the network median and shaded areas the 25th and 75th percentiles. Trend lines are indicative for the periods 1990–2002 and 2002–2012 .....	12
Figure 2.3. Trends (2000–2014) of summertime (April–September) daytime average O <sub>3</sub> at available ozone monitoring stations in Europe, North America and Asia (in other world regions very few long-term ozone measurements are available). Vector colours indicate the statistical likelihood (p-values) on the linear trend for each site: blues indicate negative trends, oranges indicate positive trends and green indicates weak or no trend; more likely trends (lower p-values) have greater colour saturation .....	13
Figure 3.1. Methane emissions (kton CH <sub>4</sub> yr <sup>-1</sup> ) for (a) the globe, (b) European Union, (c) by world region (region definition Annex 3).....	16
Figure 3.2. Global CH <sub>4</sub> emissions in 2012 as reported by the EDGARv4.3.2 database with sector specific shares and regional total emissions (Mton=Tg) for major world regions. Gridcells with emissions smaller than 38 tons yr <sup>-1</sup> are not displayed. Definition of EDGAR sectors is given in Annex 1. ....	18
Figure 3.3. CH <sub>4</sub> emissions from agricultural soils (mainly rice production) in 2012 .....	21
Figure 3.4. CH <sub>4</sub> emissions from enteric fermentation in 2012 .....	22
Figure 3.5. CH <sub>4</sub> emissions from fossil fuel production in 2012 with zoom on areas with intense coal mining (green frame) and gas & oil production activities with venting (blue circle). Ship tracks show minor CH <sub>4</sub> leakage during crude oil and natural gas liquids tanker transport .....	25
Figure 3.6. Control measures for enteric CH <sub>4</sub> in ruminants .....	26
Figure 3.7. Eclipse v5a Air pollution benchmark scenarios.....	31
Figure 3.8. ECLIPSE v5a relative change in CH <sub>4</sub> emissions by 2030 and 2050 in the energy (ENE), waste (WST) and agricultural (AGR) sectors, for 3 selected scenarios, relative to year 2010. A minor potential for emission reductions in the agricultural sector was included in ECLIPSE climate scenarios .....	33
Figure 3.9. Relative change in CH <sub>4</sub> emissions per sector, relative to year 2010 for the 3 selected RCP scenarios.....	35
Figure 3.10. Relative change in emissions per sector, relative to year 2010 for the 3 selected SSP scenarios.....	36
Figure 3.11. Relative change in emissions per sector, relative to year 2010 for the 3 selected GECO-2017 scenarios. ....	37
Figure 3.12. Historical (1990 – 2010) global anthropogenic CH <sub>4</sub> emission trends from EDGAR v4.3.2 and projected (2000 – 2050) trends from four scenario families. Scenarios have been colour-coded to easily distinguish the “high emission”, “middle of the road” and “low emission-high mitigation effort” members in each family.....	38

Figure 3.13. Maximum difference in anthropogenic CH <sub>4</sub> emissions in 2030 and 2050 between highest and lowest scenario member for the four selected scenario families. GECO2017 and ECLIPSE have a lower mitigation range, due to inclusion of policies prior to 2010. ....	38
Figure 4.1. Year 2010 Ozone exposure metric 6mDMA1 calculated with TM5-FASST (ECLIPSE v5a). ....	40
Figure 4.2. Projected change in ozone exposure metric 6mDMA1 over Europe, relative to year 2010, as a consequence of the global CH <sub>4</sub> emission trends in Fig. 3.12. The error bars represent 1 standard deviation over the range of O <sub>3</sub> – CH <sub>4</sub> response sensitivities obtained in the HTAP model ensemble (shown for RCP-85, ECLIPSE-CLIM-CLE and GECO-2C only), and show that the O <sub>3</sub> signal from the emission scenarios is larger than model uncertainty. ....	41
Figure 4.3. Projected change in regional mean ozone exposure metric 6mDMA1 in 2050, relative to year 2010, for the highest and lowest global CH <sub>4</sub> emission scenarios in each family. The data table below the figure gives the total range width between the highest and lowest emission scenario of each family (i.e. sum of absolute values of purple and green bar for each scenario). ....	42
Figure 4.4. Change in global mortalities from exposure to O <sub>3</sub> from global CH <sub>4</sub> emissions in 2030 (dark shaded bars) and 2050 (light shaded bars), relative to exposure of the same population to year 2010 O <sub>3</sub> levels. Purple: high emission scenarios; orange: middle-of-the-road scenarios, green: low emission-high mitigation scenarios. ....	43
Figure 4.5. Change in mortalities in HTAP2 Europe region (see Annex 3) from exposure to O <sub>3</sub> from global CH <sub>4</sub> emissions in 2030 (left bar) and 2050 (right bar), relative to exposure of the same population to year 2010 O <sub>3</sub> levels. Purple: high emission scenarios; orange: middle-of-the-road scenarios, green: high mitigation scenarios. ....	44
Figure 4.6. Year 2050 Relative yield loss of 4 major crops relative to year 2010 exposure due to CH <sub>4</sub> -induced O <sub>3</sub> for 12 world regions (HTAP2- Annex 3), for the highest and lowest emission scenario in each family. (Negative loss corresponds to a gain in crop yield). The data table shows the value of the difference between best and worst case scenario in each family. ....	46
Figure 4.7. Estimated change in economic cost from crop losses (based on year 2010 production and producer prices) in 2050 relative to year 2010 for the considered scenarios. The data table gives the difference between best and worst-case scenario in each family. ....	46
Figure 4.8. Ranges of the change in radiative forcing (blue line, left axis) for the low (green), middle (orange) and high (purple) CH <sub>4</sub> emission scenario groups in 2030 and 2050 relative to the year 2010. The red shaded area shows the contribution of CH <sub>4</sub> only, the blue shaded area the contribution of O <sub>3</sub> via long-term CH <sub>4</sub> chemistry feedback. ....	47
Figure A1.1. Comparison of CH <sub>4</sub> emissions for EU28 as estimated by the EDGAR v4.3.2 database and TNO-MACCIII ....	75
Figure A1.2. CH <sub>4</sub> emissions (in kton CH <sub>4</sub> /year) for major world regions: fuel production and transformation, waste, fuel combustion, agriculture.....	77
Figure A2.1. Eclipse v5a Air pollution benchmark scenarios.....	78
Figure A2.2. CH <sub>4</sub> emission trends in ECLIPSE v5a by sector (top) and by world region (bottom). From left to right: REF-CLE, CLIM-CLE, REF-MTFR.....	79
Figure A2.3. CH <sub>4</sub> emission trends in RCP by sector (top) and by world region (bottom). From left to right: RCP 8.5, RCP 6.0, RCP 2.6.....	80

Figure A2.4. CH <sub>4</sub> emission trends in SSP by sector (top) and by world region (bottom). From left to right: SSP3-REF (high emission), SSP2-6.0 (middle of the road), and SSP1-2.6 (low emissions). .....	82
Figure A2.5. CH <sub>4</sub> emission trends in RCP by sector (top) and by world region (bottom). From left to right: GECO_REF, GECO_INDC, GECO_2C. ....	84
Figure A4.1. Steady-state decrease in annual mean surface O <sub>3</sub> for a 20% decrease in year 2000 CH <sub>4</sub> concentration.....	89
Figure A4.2. Global and regional averaged surface ozone concentration change per Tg CH <sub>4</sub> yr <sup>-1</sup> emission change, obtained from a CH <sub>4</sub> concentration perturbation experiments for TM5 model only (blue dots), ensemble of all HTAP1 models (open squares, with 1 standard deviation as error bar), and new HTAP2 results. ....	89
Figure A5.1. Comparison of a) 6mDMA1, b) 3mDMA1 computed by the TM5-FASST model, and c) 3mDMA1 for non-urban stations taken from the TOAR analysis by Fleming et al. (2018) .....	94

## List of tables

Table 3.1. CH <sub>4</sub> emissions (Tg CH <sub>4</sub> yr <sup>-1</sup> ) and shares (%) by region for EDGAR4.3.2 and GAINS in 2012. ....	19
Table 3.2. Technically feasible control measures for CH <sub>4</sub> emissions in a number of key-sectors. ....	25
Table 3.3. Implied waste water emission factors in ton CH <sub>4</sub> /kton organic degradable material (BOD). ....	28
Table 3.4. Fuel exploitation metrics in 2012 ranked from high-to-low. Coal, combined oil and gas production, gas transmission and distribution. n.a. (not applicable). ....	29
Table 3.5. Description of ECLIPSE v5a scenarios. ....	32
Table 3.6. Description of RCP scenarios. In all three scenarios, Kuznets-curve assumptions were made for air pollutants, leading to relatively similar air pollutant emissions across scenarios. ....	34
Table 3.7. Description of SSP scenarios.. ....	35
Table 3.8. Description of GECO2017 scenarios. ....	36
Table 3.9. Ratio of global methane emissions in 2050 relative to 2010 of the 3 major sectors in 12 scenarios- grouped in high emission (H, purple), Middle of the Road (M, brown) and low emission- high effort (L, green). ....	37
Table 4.1. Year 2050 O <sub>3</sub> differences in mortality between highest and lowest emission scenario in each scenario family for HTAP2 world regions (see Annex 3), relative to year 2010. ....	44
Table 4.2. Regional shares of global O <sub>3</sub> mortalities in 2030 and 2050 for high CH <sub>4</sub> emission scenarios (H) middle-of-the road scenarios (M) and low-emission-high mitigation scenarios (L) for the HTAP2 world regions (Annex 3). ....	45
Table 4.3. Summary of global and European health, crop and climate impacts of global high and low CH <sub>4</sub> emission scenarios. Impacts are for global CH <sub>4</sub> emission changes relative to the year 2010. ....	48
Table A1.1 EDGAR sectors relevant for CH <sub>4</sub> emissions, using following the Common Reporting Format (CRF)/Nomenclature For Reporting (NFR) described in IPCC (1996)...72	72
Table A1.2. Comparison of EDGAR4.3.2 shares (%) of agriculture, waste and fuel production/distribution in 2012 with GAINS data for 2012 (updated from Höglund-Isaksson et al., 2017; Gomez-Sanabria et al., 2018), and EEA (2018) data reported for 2012 and 2016. Dominant contributions are in bold. In EDGAR other emissions add 4% to the global total ....	76
Table A3.2.1 HTAP2 receptor region aggregation ....	86
Table A4.1 Regional annual mean steady-state O <sub>3</sub> response to a 20% reduction in global Methane concentration (ppb ± 1 standard deviation). DECR refers to experiments where CH <sub>4</sub> concentration was decreased by 20% (HTAP1 and HTAP2 experiments) , INCR to a 20% increase (HTAP2 experiments only). All HTAP2 results shown have been rescaled to -20% emission for comparison with HTAP1. ....	90
Table A4.2. Regional population-weighted average O <sub>3</sub> concentration and O <sub>3</sub> exposure metrics response to sustained 1 Tg CH <sub>4</sub> yr <sup>-1</sup> increase in CH <sub>4</sub> annual emission. ....	91
Table A4.3. Definitions of commonly used metrics used for evaluating impacts of O <sub>3</sub> on human health and crops. ....	92
Table A5.1. Premature O <sub>3</sub> related deaths in world regions and EU28, 2010. ....	93

## ANNEXES

### Annex 1. The EDGAR v4.3.2 CH<sub>4</sub> emissions

In this Annex, pertinent details about the methodology and assumption used in EDGAR v4.3.2 to estimate CH<sub>4</sub> emissions for major emitting sectors are reported. A comparison of EDGAR4.3.2 to the MACC and GAINS emission databases are in A.1.2. We refer to Janssens-Maenhout et al. (2017a,b) for further details.

#### A.1.1 Sources: Methodologies and assumptions

##### A.1.1.1 EDGAR-IPCC sector aggregation

Table A1.1 EDGAR sectors ([http://edgar.jrc.ec.europa.eu/overview.php?v=432\\_GHG](http://edgar.jrc.ec.europa.eu/overview.php?v=432_GHG)) relevant for CH<sub>4</sub> emissions, using following the Common Reporting Format (CRF)/Nomenclature For Reporting (NFR) described in IPCC (1996).

Aggregated emissions	EDGAR4.3.2	IPCC NFR
Agriculture	Agricultural soils (mainly rice production)	4C+4D
	Agricultural waste burning	4F
	Manure management	4B
	Enteric fermentation	4A
Fuel combustion	Power generation industry	1A1
Fuel Production and transformation	Fuel exploitation	1B1a+1B2a1+1B2a2+1B2a3+1B2a4+1B2c
	Oil refineries and Transformation industry	1A1b+1A1c+1A5b1+1B1b+1B2a5+1B2a6+1B2b5+2C1b
Processes	Iron and steel production	2C1a+2C1c+2C1d+2Ce+2C1f+2C2
	Combustion for manufacturing	1A2
	Chemical processes	2b
Waste	Solid waste landfills	6A+6D
	Waste water handling	6B
	Solid waste incineration	6C
Other combustion	Road transportation	1A3b
	Aviation (international/domestic)	1A3a
	Non-road transport: Railways, off-road transport, pipelines	1A3c+1A3e
	Shipping	1A3d+1C2
	Fossil fuel fires (uncontrolled coal gas and oil fires)	7A
	Energy for buildings	1A4

Source: EDGAR 4.3.2

#### **A.1.1.2 Agricultural soils and livestock**

Following the IPCC (2006) methodology we apply FAOSTAT crop and livestock data and IPCC (2006) emission factors for CH<sub>4</sub>. Livestock numbers for buffalo, camels, dairy and non-dairy cattle, goats, horses, swine, sheep, mules and asses and for poultry (turkeys, geese, chickens and ducks) are taken from FAOSTAT (2014). Except poultry, these animal categories contribute to manure and to enteric fermentation emissions. For enteric fermentation by cattle, country specific methane emission factors are calculated following IPCC methodology (IPCC, 2006), using country specific milk yield (dairy cattle) and carcass weight (other cattle) trends from FAO to estimate the trends in the emission factors. For other animal types, regional emission factors from IPCC (2006) are used.

CH<sub>4</sub> emissions from manure management are estimated by applying default IPCC emission factors for each country and temperature zone. Livestock fractions of the countries are calculated for 19 annual mean temperature zones for cattle, swine and buffalo and three climate zones for other animals (cold, temperate, warm).

The total area for rice cultivation, obtained from FAOSTAT (2014), is split between the different agro-ecological land-use types (rain fed, irrigated, deep water and upland) using data from IRRI (2007). Methane emission factors for the various production land-uses are taken from IIASA (2007).

#### **A.1.1.3 Fugitive emissions from fossil fuel production and transmission**

To compile fugitive emissions from solid fuel production and transmission, hard coal and brown coal production data are separated into surface and underground mining based on the World Coal Association (2016). Methane (CH<sub>4</sub>) emission factors for coal mining are based on average depths of coal production and include post-mining emissions, following IPCC recommendations and the EMEP/EEA (2013) Guidebook. CH<sub>4</sub> recovery from coal mining was estimated following IPCC (2006) for the 11 countries with largest coal mining in the past. According to Peng et al. (2016) and Liu et al. (2015), Chinese underground coal mines are characterised by low quality coal and, and have relatively high emission factors. The CH<sub>4</sub> emission factor used in EDGAR for China corresponds within 10% to the value reported Peng et al. (2016). EDGAR v4.3.2 revised emission factors for coal mining using local data from Peng et al. (2016), weighted by coalmine activity per province. These emission factors are at the lower end of IPCC (2006) recommendations and yield EDGAR v4.3.2 estimates of 17.2 Tg CH<sub>4</sub> yr<sup>-1</sup> in 2008 and 21.2 Tg CH<sub>4</sub> yr<sup>-1</sup> in 2012. For coal mine activities in China (split in brown and hard coal), the coal mine database of Liu et al. (2015) provides over 4200 coal mine locations. Fugitive emissions from the many abandoned smaller scale mines in China are assumed very small because they are normally flooded after closure. Taking all factors together, China is currently the largest source of CH<sub>4</sub> emissions, with an increased role for fugitive CH<sub>4</sub> emissions from coal production.

While gas transmission through large pipelines is characterised by relatively small country-specific emission factors of Lelieveld et al. (2005), much larger and material-dependent leakage rates of IPCC Guidelines (2006) were assumed for gas distribution to consumers. Gas distribution is a relative large source of uncertainty, in particular in countries with old gas distribution city networks using steel pipes now distributing dry rather than wet gas, with potentially more leakages. Based on IPCC (2006), EMEP/EEA (2009, 2013) and Marcogaz (2013), the emission factors for steel pipes and grey cast iron pipelines vary in the range of 0.1~3 ton km<sup>-1</sup> yr<sup>-1</sup> and 1~7 ton km<sup>-1</sup> yr<sup>-1</sup>, respectively, depending on the country. Since EDGAR estimates emission factors as a function of pipe length with the pipe material as a parameter, any dependence on the composition of the transported gas is accounted for by country-specific variations. PVC pipelines are only assumed to emit between 0.05~0.3 ton km<sup>-1</sup> yr<sup>-1</sup>, but for polyethylene pipelines a higher leakage rate of 0.15~2 ton km<sup>-1</sup> yr<sup>-1</sup> is assumed. The high CH<sub>4</sub> emissions during the natural gas transmission in the Russian reporting to

UNFCCC (2016) might also account for all or part of accidental CH<sub>4</sub> releases, which are not negligible according to Höglund-Isaksson (2017).

In EDGAR4.3.2 venting of CH<sub>4</sub> and flaring (CO<sub>2</sub>) during oil and gas production are considered together, representing typical churn flow, pumping up a multiphase emulsion of oil, gas, water and sand. The CH<sub>4</sub> emission factor for venting and flaring has been extracted from country specific UNFCCC reported data, and uses the average default value for other countries. EDGAR4.3.2 includes new estimates for the CH<sub>4</sub> emissions from venting of oil and gas extraction facilities, with higher values compared to the former EDGAR v4.2 dataset or to what reported by US EPA (between 2.6 and 6.6 times as global average, depending on the year), in particular during the time of the Soviet Union than previously thought, after Höglund-Isaksson (2017) used ethane-methane ratios as an indicator.

#### **A.1.1.4 Solid waste and waste water emissions**

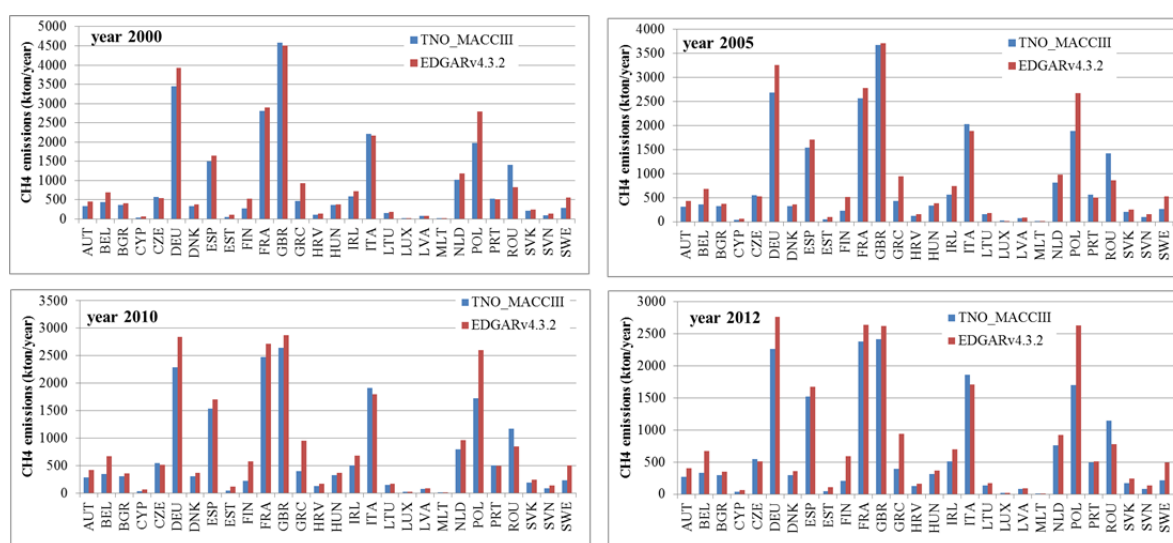
The amount of organic solid waste in landfills is determined by 3 key parameters: (a) Municipal Solid Waste (MSW) generated per year (kg/cap), (b) fraction *f* of total solid waste that is deposited on landfills, and (c) fraction of Degradable Organic Carbon (DOC) in the MSW. The per capita MSW generation rate (for 2000) and the fraction MSW disposed, incinerated and composted are specified by IPCC (2006). The IPCC Waste Model also provides for 19 regions the average weight fraction DOC under aerobic conditions, which feeds into a First Order Decay model.

The effect wastewater discharges have on the receiving environment depends on the oxygen required to oxidize soluble and particulate organic matter in the water and as such the Chemical Oxygen Demand (*COD*) and Biochemical Oxygen Demand (*BOD*) are used to characterise the quality of industrial and domestic wastewater. The total organically degradable material in wastewater for industry (*TOWi*) is estimated as kg *COD* yr<sup>-1</sup> with country-specific data. Different wastewater treatments are specified with technology-specific CH<sub>4</sub> emission factors. For domestic wastewater the sewer to waste water treatment plants (WWTP), sewer to raw discharge, bucket latrine, improved latrine, public or open pit and septic tank are distinguished.

#### **A.1.2 CH<sub>4</sub> emissions for major world regions**

Figure A1.1 shows an comparison of CH<sub>4</sub> emissions for EU28 countries estimated for 2000, 2005, 2010 and 2012 by the EDGAR v4.3.2 (Janssens-Maenhout et al., 2017) database and TNO-MACCIII (Kuenen et al., 2014; Denier van der Gon et al., 2017). Most of EU28 countries show very good agreement between the two inventories and on average the relative difference over the all years ranges between 14 and 21%. In particular in Poland, Greece, Cyprus, Finland, Sweden, Estonia and Belgium larger discrepancies are observed, for which in 2010 EDGAR estimates 33% to 62% larger emissions than the TNO-MACCIII inventory.

**Figure A1.1.** Comparison of CH<sub>4</sub> emissions for EU28 as estimated by the EDGAR v4.3.2 database and TNO-MACCIII.



Source: Janssens-Maenhout et al., 2017 (EDGAR) ; Kuenen et al., 2014; Denier van der Gon et al., 2017 (TNO-MACCIII)

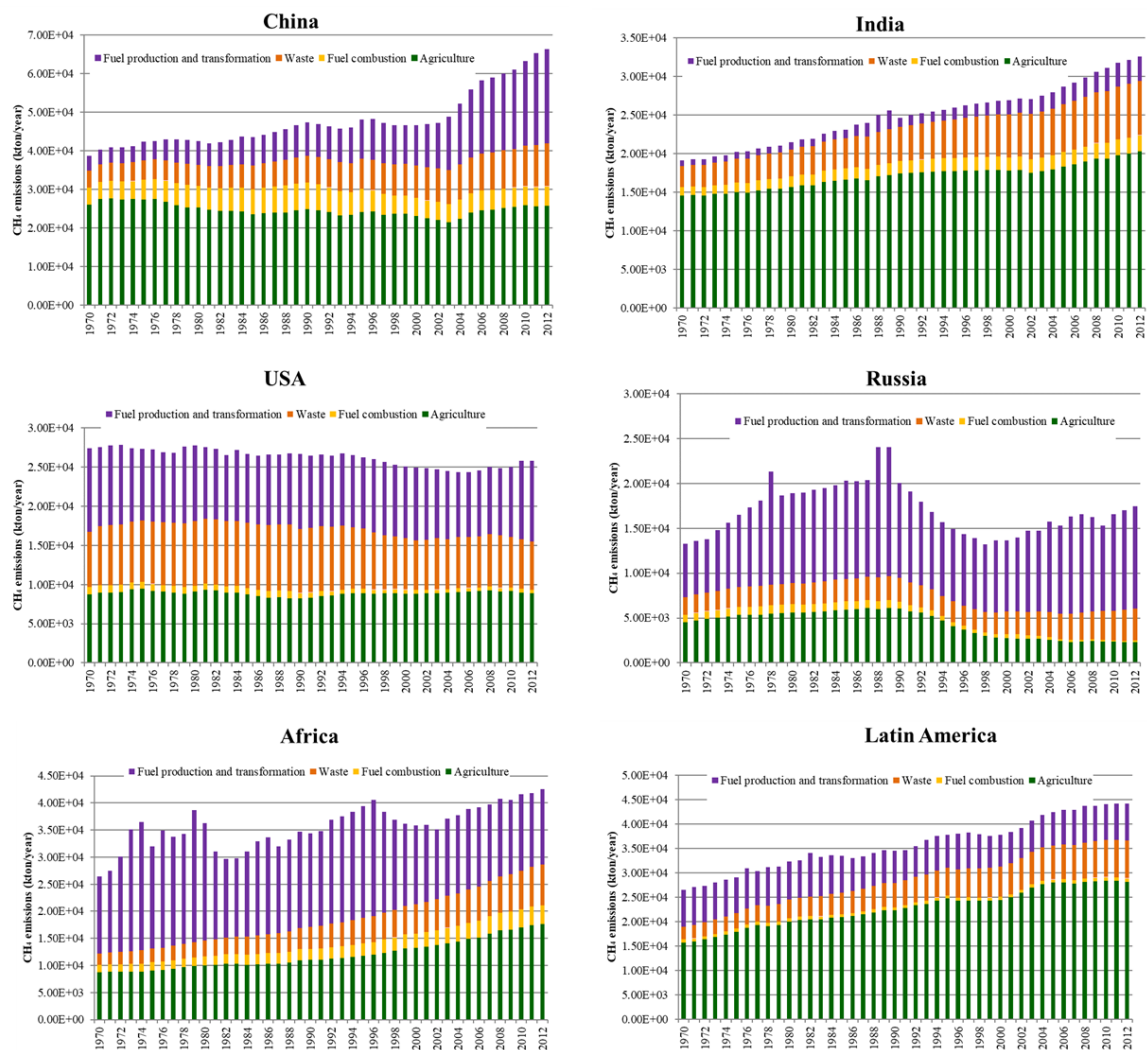
Table A1.1 show a good consistency comparing EDGAR and GAINS regional importance of sector source contributions. The GAINS solid waste and waste water contribution tend to be lower than EDGAR, while the fuel production/distribution (energy) contributions are larger. EDGAR possibly underestimates by EDGAR the venting of petroleum gas, since the global average and Russian numbers for fuel production are lower than in GAINS. Russia's reporting to UNFCCC for 2015 states quite substantial emissions from oil production (80%) consistent with the GAINS estimates (Höglund-Isaksson, 2018, personal communication).

Figure A1.2 shows the regional trends of CH<sub>4</sub> emissions for major world regions outside Europe. In China and India the large growth of fuel production/transformation are notable. Increases in waste/wastewater are important in India, Africa and Latin America, while they are decreasing in the USA. Growth of agricultural emissions is strongly contributing to trends in India, Africa and Latin America.

**Table A1.2.** Comparison of EDGAR4.3.2 shares (%) of agriculture, waste and fuel production/distribution in 2012 with GAINS data for 2012 (updated from Höglund-Isaksson et al., 2017; Gomez-Sanabria et al., 2018), and EEA (2018) data reported for 2012 and 2016. Dominant contributions are in bold. In EDGAR other emissions add 4% to the global total.

Region/database		Agriculture	Solid waste and water (2012/2016)	Fuel production & distribution & other energy
EU28	EDGAR	<b>44</b>	32	20
	GAINS	<b>52</b>	29	19
	EU28 inventory	<b>49/52</b>	27/30	19/20
USA	EDGAR	34	24	<b>40</b>
<i>North America</i>	GAINS	24	21	<b>54</b>
Russia	EDGAR	13	20	<b>66</b>
	GAINS	7	14	<b>79</b>
China	EDGAR	<b>39</b>	17	37
	GAINS	38	15	<b>48</b>
India	EDGAR	<b>62</b>	22	15
	GAINS	<b>69</b>	20	12
World	EDGAR	<b>44</b>	19	32
	GAINS	<b>41</b>	18	42

**Figure A1.2.** CH<sub>4</sub> emissions (in kton CH<sub>4</sub>/year) for major world regions: fuel production and transformation, waste, fuel combustion, agriculture



Source: EDGARv4.3.2

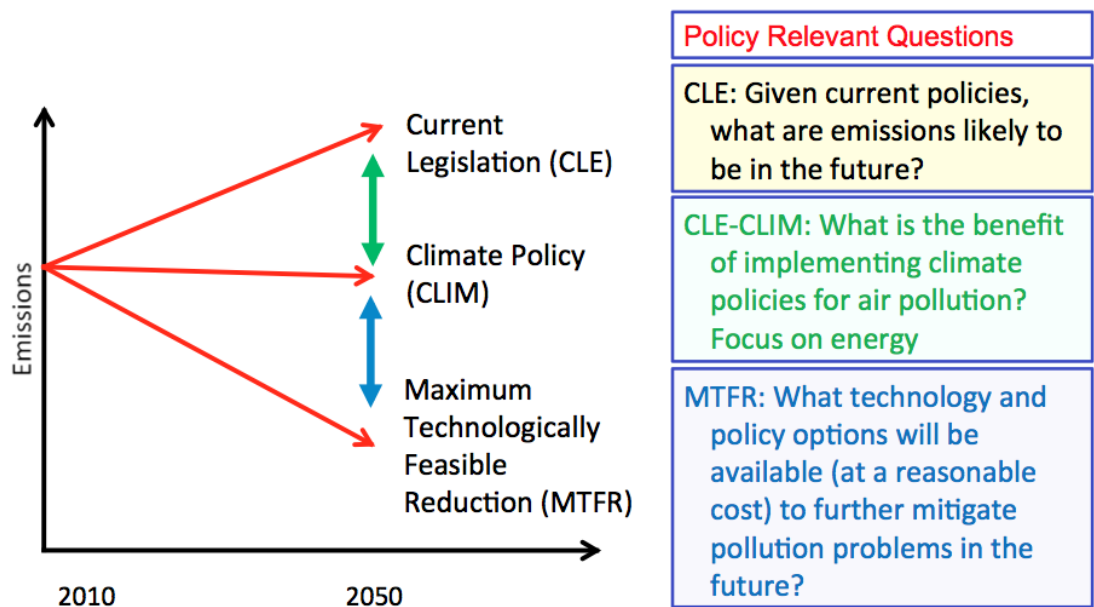
Annex 2. Future emission scenario families

A.2.1 ECLIPSE scenarios

The ECLIPSE emission dataset was created with the GAINS (Greenhouse gas – Air pollution Interactions and Synergies; <http://gains.iiasa.ac.at>) model (Klimont et al. 2017). GAINS calculates emissions of air pollutants and Kyoto greenhouse gases, including CH<sub>4</sub> in a consistent framework, using a reference year 2010 and emission scenarios until 2050. The ECLIPSE version v5a, used in this report, was adopted by the TF HTAP as the basis for scenario analysis. GAINS holds information about key economic activities of emissions, environmental policies, and further mitigation opportunities for 172 countries and regions. The model relies on international and national statistics of activity data for energy use, industrial production, and agricultural activities, for which it distinguishes all key emission sources and control measures. Several hundred technologies to control air pollutant and greenhouse gases emissions are represented, allowing simulation of implemented air quality legislation. For Europe, ECLIPSE v5a includes the results of the consultation with national experts during the review of the EU National Emission Ceilings Directive (Amann et al., 2015). For South America an expanded set of countries statistics was considered and for China the 12th Five-Year Plan included. Three future policy/technological scenarios address various policy assumptions on air pollution and climate policies (Fig. A2.1).

While CH<sub>4</sub> emissions under REF-CLE grow from ca. 310 in 2010 to 500 Tg CH<sub>4</sub> CH<sub>4</sub> yr<sup>-1</sup> in 2050, they reach a plateau of ca. 380 CH<sub>4</sub> yr<sup>-1</sup> under the CLIM-CLE scenario in 2030 and 2050. In contrast, all possible technically feasible mitigation measures in the Ref-MFTR reduce anthropogenic to ca. 200-250 Tg CH<sub>4</sub>/year, with most emission reduction obtained in the fossil fuel and waste sectors, and less in the agricultural sector. Geographically the scenarios indicate that Europe’s<sup>22</sup> share in the global emission trajectories ranges from 8-10% for the CLE, CLIM and MFR scenarios respectively by 2050.

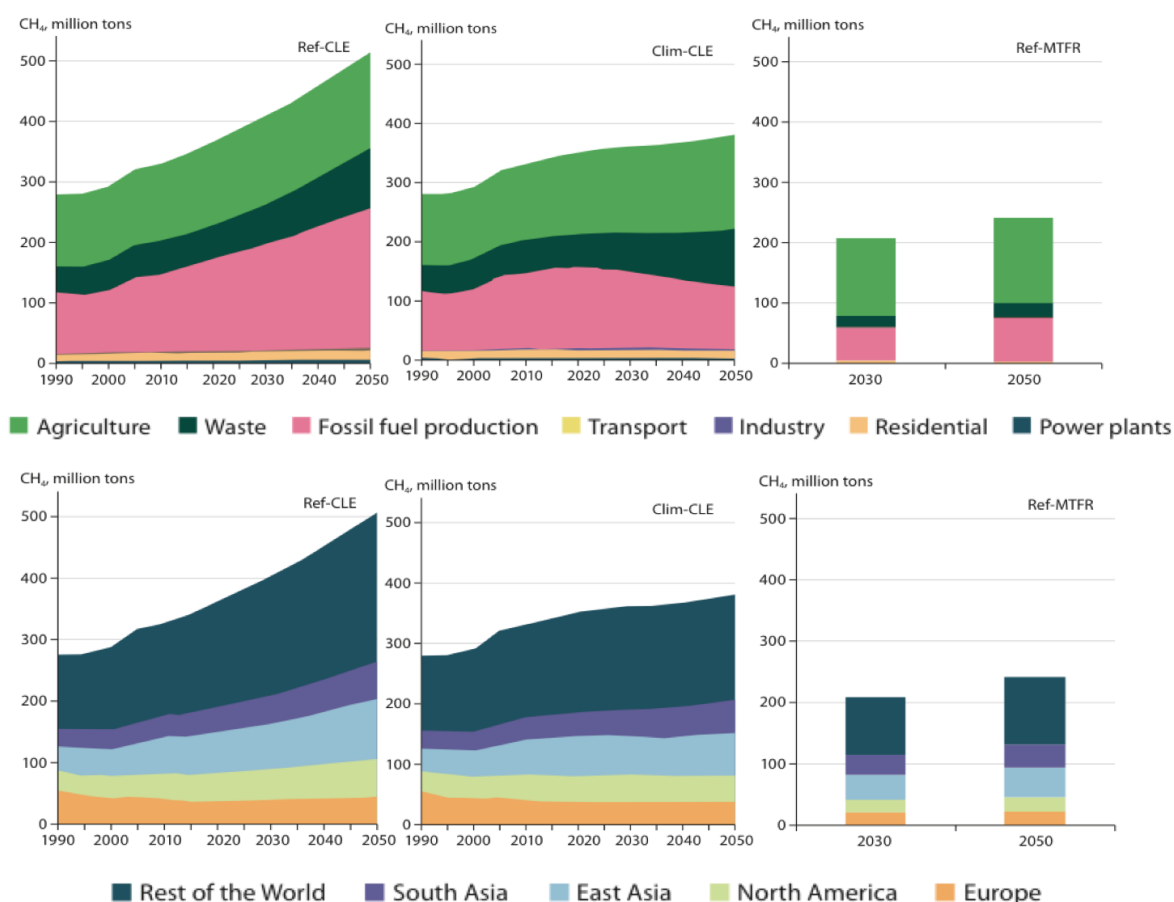
Figure A2.1. Eclipse v5a Air pollution benchmark scenarios



Source: TF HTAP

<sup>22</sup> HTAP1 region- which includes all European countries and in addition Ukraine, Belarus and part of Russia. Therefore shares are larger than the EU28 alone.

**Figure A2.2.** CH<sub>4</sub> emission trends in ECLIPSE v5a by sector (top) and by world region (bottom).  
From left to right: REF-CLE, CLIM-CLE, REF-MTFR

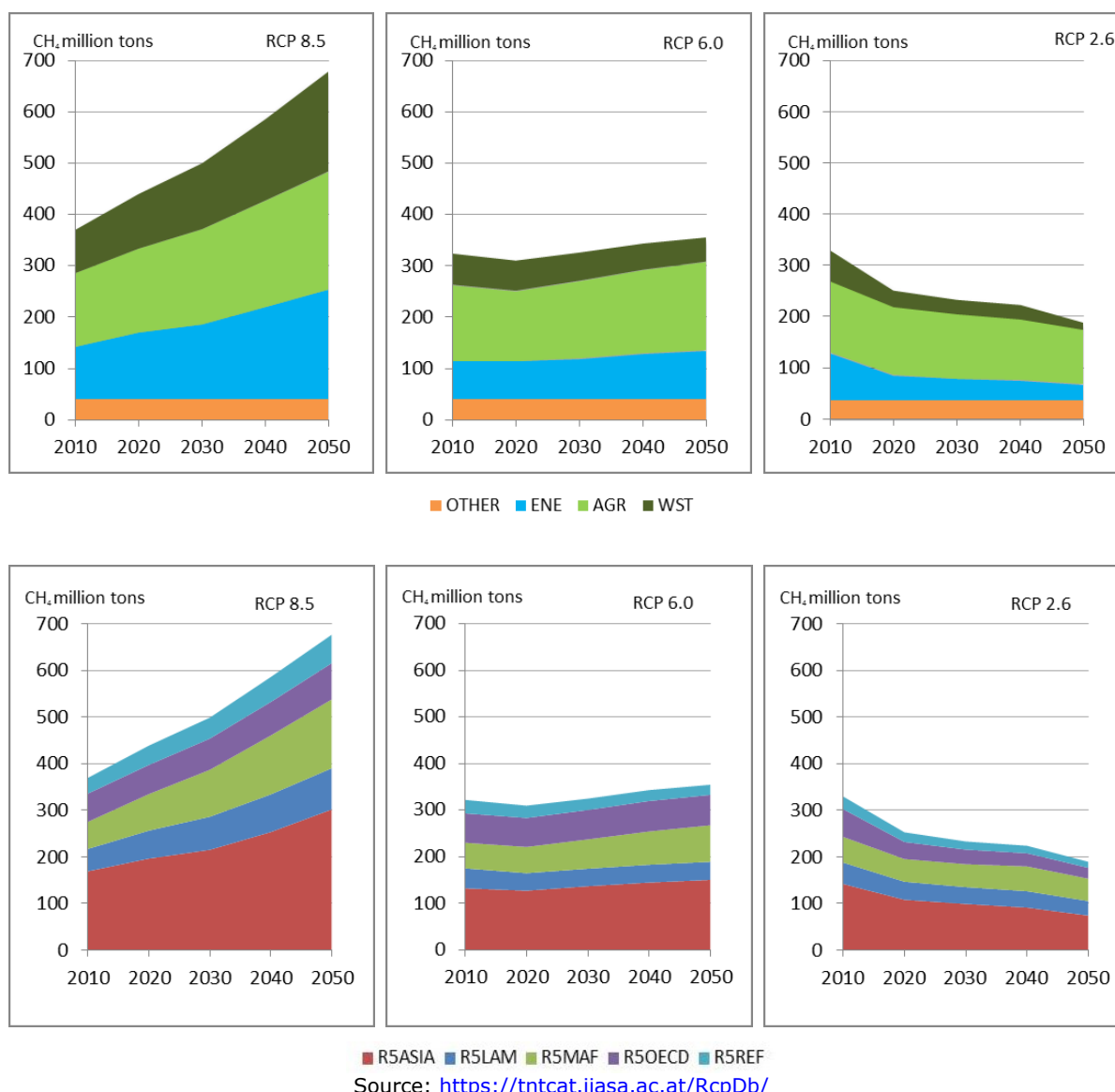


Source: adapted from CLRTAP: Maas and Grennfelt, 2016

## A.2.2 RCP Representative Concentration Pathways

The RCP scenarios have been developed for IPCC's 5<sup>th</sup> assessment report as a new set of reference scenarios, as a follow-up of the earlier SRES (Special Report Emission Scenarios) set and predecessor of the latest SSP scenarios. The RCPs are four independent pathways developed by different integrated assessment models, and defined by their total radiative forcing pathways by 2100. As many previous studies have used the RCP set both for climate and air quality impact studies, they can be considered as benchmark scenarios to compare with previous studies and against the other scenario families in this report. We select the, RCP-85 (high emission scenario), RCP-60 (middle of the road) and RCP-26 (high mitigation). The RCP emission database is hosted by IIASA and can be accessed via <https://tntcat.iiasa.ac.at/RcpDb/>. Figure A2.3 shows CH<sub>4</sub> emission trends by region and by sector for the selected set.

**Figure A2.3.** CH<sub>4</sub> emission trends in RCP by sector (top) and by world region (bottom). From left to right: RCP 8.5, RCP 6.0, RCP 2.6



### A.2.3 SSP Shared Socioeconomic Pathways

Shared Socioeconomic Pathways (SSPs) are part of a new scenario framework, established by the climate change research community in order to facilitate the integrated analysis of future climate impacts, vulnerabilities, adaptation, and mitigation (Riahi et al. 2017 and references therein). Emission trajectories evaluated using the SSP framework, are at the basis of community model simulations utilized by CMIP6 (Climate Model Intercomparison Project Phase 6), and informing the forthcoming IPCC AR6 report. The SSPs are based on five narratives describing alternative socio-economic developments, including assumptions on sustainable development, regional rivalry, inequality, and fossil-fuelled development. Scenario drivers are assumptions on population growth, urbanization and GDP growth. These assumptions are implemented in a set of 5 Integrated Assessment models to produce baseline scenarios. Additionally to these baseline scenarios, various levels of mitigation ambitions are included to meet

climate mitigation objectives<sup>23</sup>. Of the full set of possible CH<sub>4</sub> trajectories, we choose 3 scenarios, encompassing the full range of outcomes, with scenario descriptions taken from Riahi et al. (2017)

**SSP3-Reference. Regional rivalry scenario.** High challenges to mitigation and adaptation. A resurgent nationalism, concerns about competitiveness and security, and regional conflicts push countries to increasingly focus on domestic or, at most, regional issues. Policies shift over time to become increasingly oriented toward national and regional security issues. Countries focus on achieving energy and food security goals within their own regions at the expense of broader-based development. Investments in education and technological development decline. Economic development is slow, consumption is material-intensive, and inequalities persist or worsen over time. Population growth is low in industrialized and high in developing countries. A low international priority for addressing environmental concerns leads to strong environmental degradation in some regions. No additional climate policy is assumed, leading to overall high climate forcing of 7.0 Wm<sup>-2</sup> by the end of the 21<sup>st</sup> century.

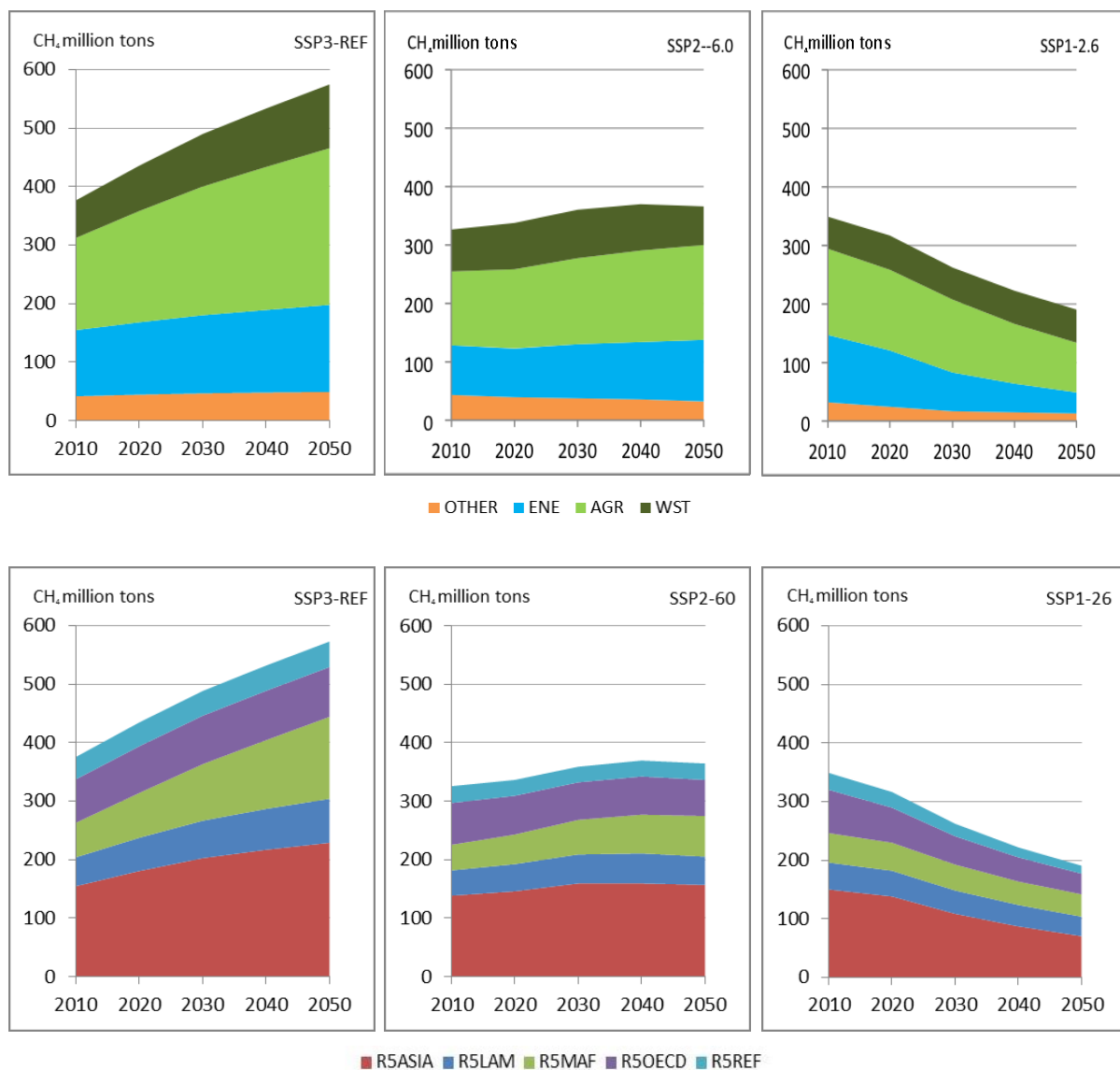
**SSP2-6.0. Middle of the road scenario.** Medium challenges to mitigation and adaptation. The world follows a path in which social, economic, and technological trends do not shift markedly from historical patterns. Development and income growth proceeds unevenly, with some countries making relatively good progress while others fall short of expectations. Global and national institutions work toward but make slow progress in achieving sustainable development goals. Environmental systems experience degradation, although there are some improvements and overall the intensity of resource and energy use declines. Global population growth is moderate and levels off in the second half of the century. Income inequality persists or improves only slowly and challenges to reducing vulnerability to societal and environmental changes remain. This scenario assumption was accompanied by a 6.0 Wm<sup>-2</sup> climate objective, assuming some progress on greenhouse gas emissions reductions.

**SSP1-2.6. Sustainability scenario.** Low challenges to mitigation and adaptation- as sustainability trajectories lead to lower emissions, radiative forcing and climate change. The world shifts gradually, but pervasively, toward a more sustainable path, emphasizing more inclusive development that respects perceived environmental boundaries. Management of the global commons slowly improves, educational and health investments accelerate the demographic transition, and the emphasis on economic growth shifts toward a broader emphasis on human well-being. Driven by an increasing commitment to achieving development goals, inequality is reduced both across and within countries. Consumption is oriented toward low material growth and lower resource and energy intensity. Along with the sustainability assumption we analyse the 2.6 climate trajectory, that assumes sufficient climate emission mitigation to limit radiative forcing to 2.6 Wm<sup>-2</sup> (or ca. 2 degrees) by the end of the century.

---

<sup>23</sup> The resulting CH<sub>4</sub> global (and other GHG and air pollution emissions) are available via <https://tntcat.iiasa.ac.at/SspDb/dsd?Action=htmlpage&page=about>.

**Figure A2.4.** CH<sub>4</sub> emission trends in SSP by sector (top) and by world region (bottom). From left to right: SSP3-REF (high emission), SSP2-6.0 (middle of the road), and SSP1-2.6 (low emissions).



Source: <https://tntcat.iiasa.ac.at/SspDb>

#### A.2.4 Global Energy and Climate Outlook (GECO2017) scenarios

The GECO2017 scenarios were developed as a JRC contribution to the upcoming milestones of the international process coordinated by the United Nations Framework convention on Climate Change (UNFCCC), following the 2015 Paris Agreement (Kitous et al., 2017). Following scenarios were developed:

**Reference scenario:** It includes adopted energy and climate policies worldwide for 2020; thereafter, CO<sub>2</sub> and other GHG emissions are driven by income growth, energy prices and expected technological development with no supplementary incentivizing for low-carbon technologies. Although the GECO2017 Reference scenario integrates national climate and energy policies, it is not a replication of official national scenarios. This also applies to the particular case of the EU28.

**INDC scenario:** All the Intended Nationally Determined Contributions (INDCs) put forward by countries are implemented in this scenario, including all conditional contributions. Countries where the Reference scenario already leads to GHG emissions at or below their INDC pledge are assumed to meet their Reference level. Nearly all

INDC objectives are formulated for 2030; beyond 2030 it is assumed that the global GHG intensity of GDP decreases at the same rate as for 2020-2030. This is achieved through an increase of regional carbon values (including for countries that previously had no climate policies) and progressive convergence of carbon values at a speed that depends on the countries' per capita income.

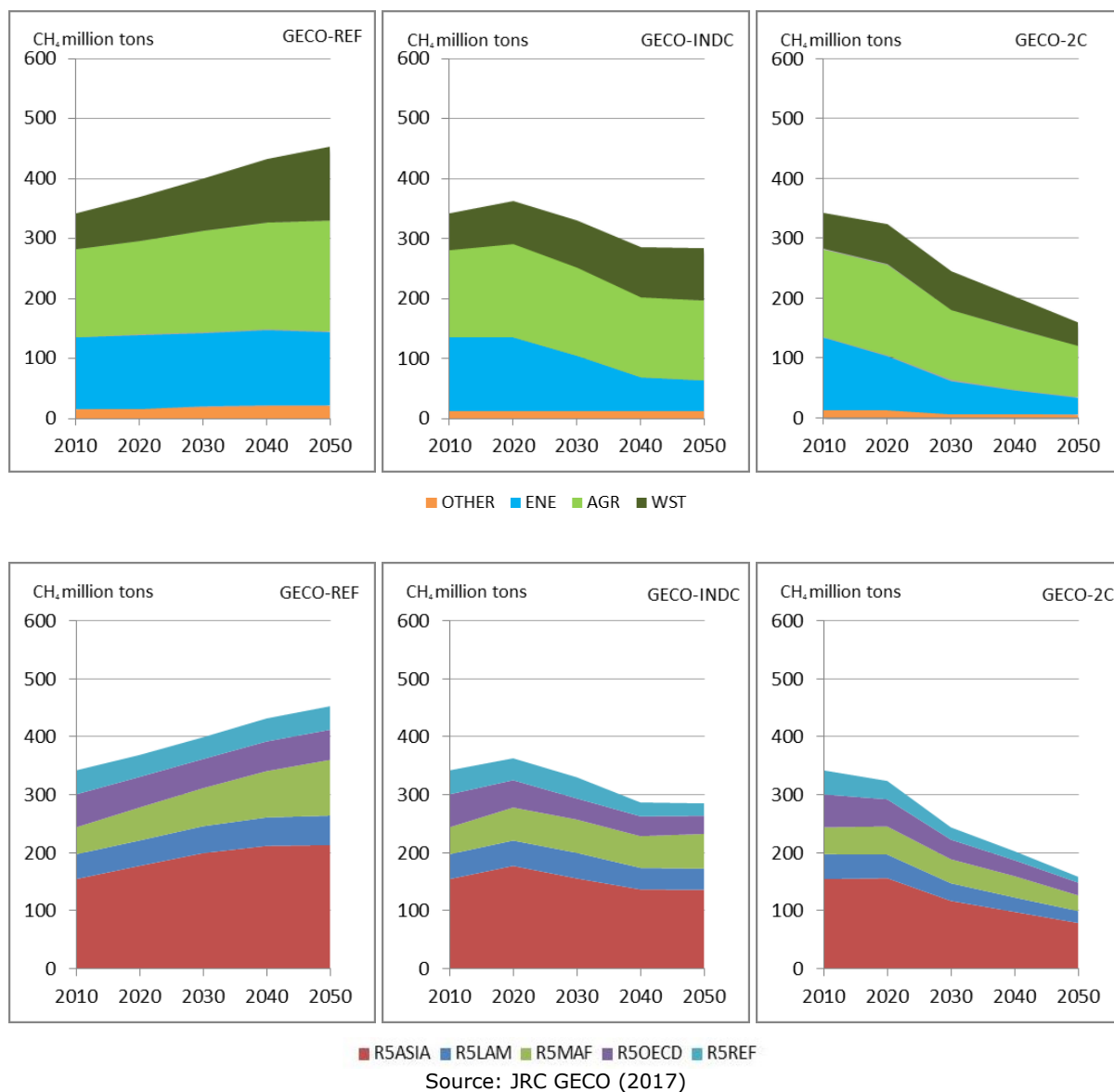
**Below 2°C scenario (B2°C):** This scenario assumes a global GHG trajectory over 2010-2100 compatible with a likely chance (above 66%) of temperature rise staying below 2°C above pre-industrial levels. It assumes in particular further intensification of energy and climate policies already from 2018, captured in the modelling through increasing carbon value and other regulatory instruments, and a progressive convergence of the countries' carbon values after 2030 depending on their per capita income.

The scenarios are produced with the same socio-economic assumptions and energy resources availability. Energy prices are the result of the interplay of energy supply and demand, and are thus scenario-dependent. Country- or region-level energy supply, trade, transformation and demand, as well as GHG emissions, are driven by income growth, energy prices and expected technological evolution, within the constraints defined by energy and climate policies. In sum, scenarios differ on the climate and energy policies that are included, with repercussions on the projections of the energy supply and demand system and GHG emissions.

Each of the GECO2017 climate mitigation scenarios is coupled to 3 different implementation levels of air quality legislation, following the SSP approach. Methane emission controls however are not diversified across the air quality scenarios and are entirely considered as a part of climate mitigation options, therefore CH<sub>4</sub> emission trends differ only across the 3 climate scenarios.

The share of EU28 to global CH<sub>4</sub> emissions ranges from 4% (2C by 2050) to 8% (REF by 2050).

**Figure A2.5.** CH<sub>4</sub> emission trends in RCP by sector (top) and by world region (bottom). From left to right: GECO\_REF, GECO\_INDC, GECO\_2C.



## **Annex 3. World regions aggregation**

### **A.3.1 Five region aggregation used in EDGAR4.3.2**

**OECD:** Includes the OECD 90 and EU Member States and candidate countries.

Albania, Australia, Austria, Belgium, Bosnia and Herzegovina, Bulgaria, Canada, Croatia, Cyprus, Czech Republic, Denmark, Estonia, Finland, France, Germany, Greece, Guam, Hungary, Iceland, Ireland, Italy, Japan, Latvia, Lithuania, Luxembourg, Malta, Montenegro, Netherlands, New Zealand, Norway, Poland, Portugal, Puerto Rico, Romania, Serbia, Slovakia, Slovenia, Spain, Sweden, Switzerland, The former Yugoslav Republic of Macedonia, Turkey, United Kingdom, United States of America

**REF:** Countries from the Reforming Economies of Eastern Europe and the Former Soviet Union.

Armenia, Azerbaijan, Belarus, Georgia, Kazakhstan, Kyrgyzstan, Republic of Moldova, Russian Federation, Tajikistan, Turkmenistan, Ukraine, Uzbekistan

**ASIA:** The region includes most Asian countries with the exception of the Middle East, Japan and Former Soviet Union states.

Afghanistan, Bangladesh, Bhutan, Brunei Darussalam, Cambodia, China (incl. Hong Kong and Macao, excl. Taiwan) Democratic People's Republic of Korea, Fiji, French Polynesia, India, Indonesia, Lao People's Democratic Republic, Malaysia, Maldives, Micronesia (Fed. States of), Mongolia, Myanmar, Nepal, New Caledonia, Pakistan, Papua New Guinea, Philippines, Republic of Korea, Samoa, Singapore, Solomon Islands, Sri Lanka, Taiwan, Thailand, Timor-Leste, Vanuatu, Viet Nam

**MAF:** This region includes the countries of the Middle East and Africa.

Algeria, Angola, Bahrain, Benin, Botswana, Burkina Faso, Burundi, Cameroon, Cape Verde, Central African Republic, Chad, Comoros, Congo, Côte d'Ivoire, Democratic Republic of the Congo, Djibouti, Egypt, Equatorial Guinea, Eritrea, Ethiopia, Gabon, Gambia, Ghana, Guinea, Guinea-Bissau, Iran (Islamic Republic of), Iraq, Israel, Jordan, Kenya, Kuwait, Lebanon, Lesotho, Liberia, Libyan Arab Jamahiriya, Madagascar, Malawi, Mali, Mauritania, Mauritius, Mayotte, Morocco, Mozambique, Namibia, Niger, Nigeria, Occupied Palestinian Territory, Oman, Qatar, Rwanda, Réunion, Saudi Arabia, Senegal, Sierra Leone, Somalia, South Africa, South Sudan, Sudan, Swaziland, Syrian Arab Republic, Togo, Tunisia, Uganda, United Arab Emirates, United Republic of Tanzania, Western Sahara, Yemen, Zambia, Zimbabwe

**LAM:** This region includes the countries of Latin America and the Caribbean.

Argentina, Aruba, Bahamas, Barbados, Belize, Bolivia (Plurinational State of), Brazil, Chile, Colombia, Costa Rica, Cuba, Dominican Republic, Ecuador, El Salvador, French Guiana, Grenada, Guadeloupe, Guatemala, Guyana, Haiti, Honduras, Jamaica, Martinique, Mexico, Nicaragua, Panama, Paraguay, Peru, Suriname, Trinidad and Tobago, United States Virgin Islands, Uruguay, Venezuela (Bolivarian Republic of).

### A.3.2 HTAP2 receptor region aggregation

**Table A3.2.1** HTAP2 receptor region aggregation

Region name	Aggregation
North America	US+Canada (up to 66 N; polar circle)
Europe	Western + Eastern EU+Turkey (up to 66 N polar circle)
South Asia	India, Pakistan, Nepal, Bangladesh, Sri Lanka
East Asia	China, Korea, Japan
South East Asia	South East Asia
PAC-AUS_NZL	Pacific, Australia+ New Zealand
North Africa	Northern Africa
South Africa	Sub Saharan Africa
Middle East	Middle East; Gulf countries, Iran, Iraq
Central America	Mexico, Central America, Caribbean, Guyanas, Venezuela, Columbia
South America	South America
Rus Bel Ukr	Russia, Belarus, Ukraine
CAS	Central Asian Republics

Source: TF HTAP. [www.htap.org](http://www.htap.org)

## Annex 4. Modelling O<sub>3</sub> responses from CH<sub>4</sub> emissions

Methane is the dominant anthropogenic volatile organic compound (VOC) contributing to ozone formation in the global troposphere<sup>24</sup> (Fiore et al., 2002). However, in contrast to the short-lived precursors for tropospheric ozone (NO<sub>x</sub> and non-methane VOCs), methane is relatively long-lived ozone precursor and fairly well-mixed in the atmosphere, thus affecting global *background* concentrations of ozone (Dentener et al., 2005; Forster et al., 2007).

Detailed transient model simulations over 30 years, using global chemistry-transport models, have demonstrated that the O<sub>3</sub> response to changing CH<sub>4</sub> emissions is characterized by following features (Fiore et al., 2008; Prather et al., 2001):

- The equilibration time scale at which global CH<sub>4</sub> concentrations and associated background O<sub>3</sub> respond to a perturbation in CH<sub>4</sub> emissions is about 12 years, i.e. 63% of the steady-state value is reached after 12 years, 93% after 30 years. This timescale is somewhat longer than the turnover time of ca. 10 years.
- Because of the long equilibration time, the local O<sub>3</sub> response to CH<sub>4</sub> is independent of the location of the CH<sub>4</sub> emission;

As a consequence, the regional air quality impacts from CH<sub>4</sub> emission changes can be evaluated in a simplified, parameterised model set up that does not require computationally expensive transient computations. The development and validation of such a parametrised approach towards air pollutant modelling, including the CH<sub>4</sub>-induced O<sub>3</sub> response, is one of the key tasks within the task force on Hemispheric Transport of Air Pollutants.

During the first phase of the task force on Hemispheric Transport of Air Pollutants (HTAP, 2010), a large ensemble of global chemistry-transport models evaluated how surface ozone levels responded when the global steady-state CH<sub>4</sub> concentration decreased by 20% from 1760 ppb (the global mean CH<sub>4</sub> concentration in the year 2000) to 1408 ppb. Figure A4.1 shows a global 1°x1° resolution grid map of the experiment outcome obtained with JRC's TM5 chemistry-transport model as one of the participating models in the TF-HTAP1 exercise. The figure shows the steady-state change in ozone concentration from a 20% homogeneous decrease in global CH<sub>4</sub> concentration and illustrates the large spatial variability of the O<sub>3</sub> response. The highest O<sub>3</sub> responses are seen in the Middle East, the Mediterranean, Western USA and along dense international shipping routes. Ozone response is in general higher over water surfaces (e.g. the Mediterranean) because of lower ozone deposition losses compared to land, especially in regions where large ship NO<sub>x</sub> emissions are contributing to O<sub>3</sub> production.

Table A4.1 (column labelled TF-HTAP1) shows global and regionally averaged O<sub>3</sub> responses obtained from all the participating models. The global ensemble-mean surface O<sub>3</sub> response is -0.90 ppb (with a standard deviation of 28%) for a 20% decrease in global mean CH<sub>4</sub> concentration. Across regions, the response varies between -0.81 ppb in Central America and -1.44 ppb in the Middle East.

A second phase of model experiments for the TF-HTAP was initiated to follow on from TF-HTAP1, including new and updated models, and an updated and harmonized pollutant emission inventory used across all models (Janssens-Maenhout et al., 2015). Compared to HTAP1 where a 20% concentration decrease in CH<sub>4</sub> was evaluated on a baseline of 1760 ppb, new experiments were conducted increasing (+18%) and decreasing (-13%) a 1798 ppb CH<sub>4</sub> baseline concentration to encompass projected CH<sub>4</sub>

<sup>24</sup> Ozone levels at a given site are influenced by several factors: (i) background concentrations of ozone and pre-cursor gases, which are determined by large-scale processes, such as stratosphere-troposphere exchange, and global to hemispheric-scale precursor emissions; (ii) regional and local emissions; and (iii) synoptic meteorology, which can favour O<sub>3</sub> production, e.g. during a stable high pressure period in summer.

changes in 2030. In order to enable a comparison with HTAP1, Turnock et al. (2018) scaled the HTAP2 outcomes to the HTAP1 configuration, leading to the adjusted values for TF-HTAP2 shown in Table A4.1. Over-all, the O<sub>3</sub> response to a change in CH<sub>4</sub> abundance is slightly larger in the TF-HTAP2 simulations than in the TF-HTAP1 experiments, in particular for the Middle East and Northern Africa. However in nearly all cases the response from TF-HTAP2 lies within the range of model variability from TF-HTAP1 and does not alter the message that understanding O<sub>3</sub> response to CH<sub>4</sub> is important in controlling future O<sub>3</sub> concentrations.

A change in CH<sub>4</sub> abundance can be traced back to a change in emissions, but the relation is not linear because, an increase in CH<sub>4</sub> emissions removes an additional fraction of atmospheric OH (major sink for CH<sub>4</sub>) and prolongs the lifetime of CH<sub>4</sub>. The feedback of CH<sub>4</sub> emissions on its own lifetime and atmospheric abundance is expressed by a feedback factor  $F$  (Prather et al., 2001), such that for a relatively small change in CH<sub>4</sub> emissions  $\Delta Em$ , the corresponding change in CH<sub>4</sub> concentration  $C$  is obtained by  $\Delta C/C = F(\Delta Em/Em)$ , hence a 1% change in emissions leads to a  $F\%$  change in concentration. The magnitude of feedback factor  $F$  is evaluated from global chemistry model's CH<sub>4</sub> over-all chemical loss rate and additional minor loss mechanisms, like soil sinks and stratospheric loss, and is inherent to underlying chemistry schemes used. Therefore different models obtain different values for  $F$ . Prather et al. (2001) recommend a value of  $F=1.4$ , whereas the HTAP1 model ensemble resulted in an average value for  $F = 1.33 (\pm 0.06)$ . Applying this feedback factor to back-calculate the emission rate corresponding to the imposed HTAP1 20% CH<sub>4</sub> concentration change results in a corresponding annual sustained CH<sub>4</sub> emission reduction of  $77 (\pm 3)$  Tg CH<sub>4</sub> yr<sup>-1</sup>, and we use this value to convert the modelled O<sub>3</sub>-CH<sub>4</sub> responses (to a change in CH<sub>4</sub> concentration) into a normalized emission-based (per Tg CH<sub>4</sub> yr<sup>-1</sup> emitted CH<sub>4</sub>) response.

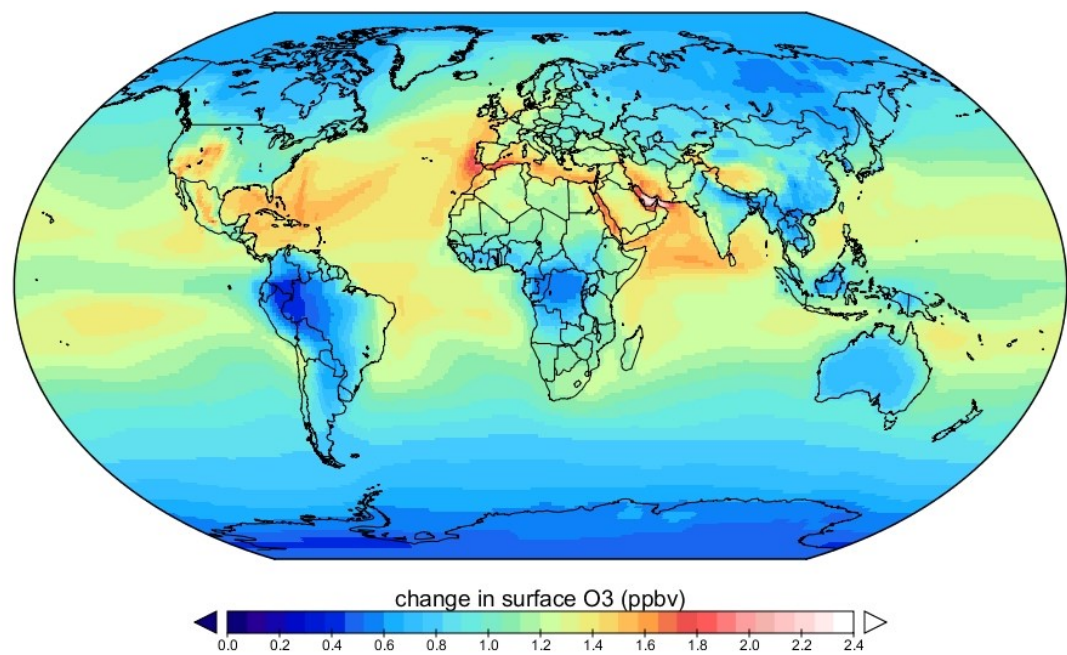
Table A4.2 gives normalized (per Tg CH<sub>4</sub> yr<sup>-1</sup> emission perturbation) marginal changes in population-weighted O<sub>3</sub> and various O<sub>3</sub> exposure metrics, obtained with JRC's global chemistry-transport model TM5, from the HTAP1 CH<sub>4</sub> source-receptor experiment. The reported sensitivities are presumed independent on the location of the CH<sub>4</sub> emissions and are therefore directly applicable to quantify regional impacts from CH<sub>4</sub> mitigation measures anywhere in the global domain.

It has to be stressed however that the O<sub>3</sub> responses shown in Tables A4.1 and A4.2 are steady-state values, which are reached more or less 30 years after a sustained CH<sub>4</sub> emission reduction. The time-dependent  $\Delta O_3$  response to a sustained  $\Delta E$  emission change is given by  $\Delta O_3(t) = \alpha \Delta E [1 - \exp(-t/12)]$  with  $\alpha$  the normalized O<sub>3</sub>-CH<sub>4</sub> sensitivity and  $t$  the time (years) expired since the start of the emission perturbation. For a changing emission trend, the response function requires a more complex mathematical convolution procedure where the change in regional ozone (or ozone metric) in year  $t$ , relative to year  $s_0$ , is evaluated as:

$$\Delta O_3(t) = \sum_{s=s_0}^{t-1} \alpha \Delta E(s) \left[ 1 - e^{-\frac{t-s}{12}} \right]$$

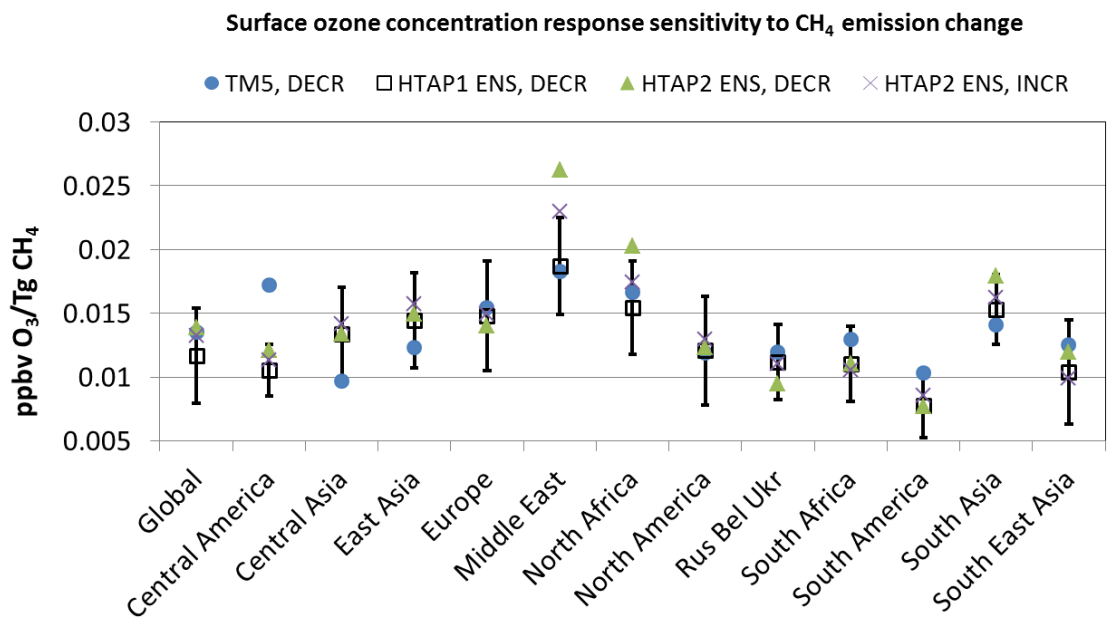
With  $t$  = year of evaluation,  $s$  = each consecutive year in the considered time period  $[s_0, t]$ ,  $\alpha$  = the regional O<sub>3</sub> response sensitivity per unit CH<sub>4</sub> emission,  $\Delta E(s)$  = the change in emission in year  $s$  relative to year  $s-1$ .

**Figure A4.1.** Steady-state decrease in annual mean surface O<sub>3</sub> for a 20% decrease in year 2000 CH<sub>4</sub> concentration



Source: JRC

**Figure A4.2.** Global and regional averaged surface ozone concentration change per Tg CH<sub>4</sub> yr<sup>-1</sup> emission change, obtained from a CH<sub>4</sub> concentration perturbation experiments for TM5 model only (blue dots), ensemble of all HTAP1 models (open squares, with 1 standard deviation as error bar), and new HTAP2 results.



Source: JRC and elaborated data from Turnock et al. (2018)

**Table A4.1** Regional annual mean steady-state O<sub>3</sub> response to a 20% reduction in global Methane concentration (ppb ± 1 standard deviation). DECR refers to experiments where CH<sub>4</sub> concentration was decreased by 20% (HTAP1 and HTAP2 experiments) , INCR to a 20% increase (HTAP2 experiments only). All HTAP2 results shown have been rescaled to -20% emission for comparison with HTAP1.

	TF-HTAP1 CH <sub>4</sub> _DECR <sup>1</sup>	TF-HTAP2 CH <sub>4</sub> _DECR adjusted to TF-HTAP1 <sup>2</sup>	TF-HTAP2 CH <sub>4</sub> _INCR adjusted to TF-HTAP1 <sup>3</sup>
Global	-0.90 ± 0.25	-1.07	-1.02
Central America	-0.81 ± 0.12	-0.93	-0.87
Central Asia	-1.03 ± 0.24	-1.03	-1.09
East Asia	-1.11 ± 0.24	-1.15	-1.21
Europe	-1.14 ± 0.28	-1.08	-1.15
Middle East	-1.44 ± 0.23	-2.02	-1.77
North Africa	-1.19 ± 0.23	-1.56	-1.34
North America	-0.93 ± 0.29	-0.95	-1
Russia Belarus Ukraine	-0.86 ± 0.19	-0.73	-0.85
Southern Africa	-0.85 ± 0.19	-0.85	-0.81
South America	-0.60 ± 0.17	-0.59	-0.66
South Asia	-1.18 ± 0.16	-1.38	-1.25
South East Asia	-0.80 ± 0.28	-0.92	-0.76

<sup>1</sup>Based on 14 models that have conducted CH<sub>4</sub>\_DECR (-20%) in TF-HTAP1

<sup>2</sup>Based on 2 models that have conducted CH<sub>4</sub>\_DECR in TF-HTAP2. Results scaled from -13% to -20%

<sup>3</sup>Based on 7 models that have conducted CH<sub>4</sub>\_INCR in TF-HTAP2. Results scaled from +18% to -20%

**Table A4.2.** Regional population-weighted average O<sub>3</sub> concentration and O<sub>3</sub> exposure metrics response to sustained 1 Tg CH<sub>4</sub> yr<sup>-1</sup> increase in CH<sub>4</sub> annual emission.

REGION	O <sub>3</sub> <sup>a</sup>	O <sub>3</sub> _JJA <sup>b</sup>	O <sub>3</sub> _DJF <sup>c</sup>	M12 <sup>d</sup>	Mhrmax <sup>e</sup>	<sup>f</sup> 6mDMA1
Global	1.29E-02	1.57E-02	1.04E-02	1.30E-02	1.52E-02	1.71E-02
Central America	1.77E-02	1.80E-02	1.71E-02	1.80E-02	1.97E-02	2.06E-02
Central Asia	1.16E-02	1.45E-02	9.66E-03	1.14E-02	1.37E-02	1.59E-02
East Asia	1.06E-02	1.29E-02	8.09E-03	1.10E-02	1.27E-02	1.46E-02
Europe	1.56E-02	2.24E-02	1.05E-02	1.53E-02	1.79E-02	2.20E-02
Middle East	1.83E-02	2.50E-02	1.29E-02	1.84E-02	2.34E-02	2.79E-02
North Africa	1.86E-02	2.73E-02	1.19E-02	1.84E-02	2.13E-02	2.55E-02
North America	1.42E-02	1.80E-02	1.06E-02	1.49E-02	1.70E-02	1.96E-02
Rus Bel Ukr	1.42E-02	1.88E-02	1.12E-02	1.45E-02	1.75E-02	2.06E-02
South Africa	1.24E-02	1.26E-02	1.25E-02	1.22E-02	1.48E-02	1.65E-02
South America	1.21E-02	1.24E-02	1.18E-02	1.20E-02	1.30E-02	1.41E-02
South Asia	1.21E-02	1.49E-02	9.11E-03	1.23E-02	1.51E-02	1.67E-02
South East Asia	1.33E-02	1.51E-02	1.23E-02	1.33E-02	1.38E-02	1.44E-02
<sup>a</sup> annual mean of surface ozone concentration <sup>b</sup> summertime (June – July – August) mean of surface ozone concentration <sup>c</sup> wintertime (December – January – February) mean of surface ozone concentration <sup>d</sup> Annual mean of daytime (0800 – 19:59 local time) ozone <sup>e</sup> Annual mean of daily maximum hourly ozone concentration <sup>f</sup> Maximum of 6-monthly running mean of daily maximum hourly ozone concentration						

Source: JRC

**Table A4.3.** Definitions of commonly used metrics used for evaluating impacts of O<sub>3</sub> on human health and crops.

Metric long name	Metric abbreviation	Impact	Definition
Annual sum of daily 8-hourly average ozone concentration above 35 ppb	SOMO35	Health	$\sum_{d=1}^{365} \max(A_8^d - 35\text{ppb}, 0)$ $A_8^d = \text{maximum 8-hourly average ozone on day } d$
Maximal 6-monthly running mean of daily maximal ozone	6mDMA1	Health	$\max\left(\frac{1}{183} \sum_{d=i}^{i+183} A_1^d, i = 0, 365\right)$ $A_1^d = \text{maximum hourly average ozone on day } d$
3-monthly mean of daytime ozone	M7, M12	Crops	<p>M7: 7-hour seasonal mean during 3 months growing season from 09:00 till 15:59 local time</p> <p>M12: 12-hour seasonal mean during 3 months growing season from 08:00 till 19:59 local time</p>
Accumulated hourly ozone above a threshold of 40 ppb	AOT40	Crops	$\sum_{d=1}^{365} \sum_{h=0}^{23} \max(C_d^h - 40\text{ppb}, 0)$ $C_d^h = \text{hourly ozone concentration on day } d \text{ and time } h$

## Annex 5. O<sub>3</sub> impact on health and crop yields

### A.5.1 Health

In this work, cause-specific excess mortalities are calculated using a population-attributable fraction approach as described in Murray et al. (2003) from  $\Delta\text{Mort} = m_0 \times \text{AF} \times \text{Pop}$ , where  $m_0$  is the baseline mortality rate for the exposed population,  $\text{AF} = 1 - 1/\text{RR}$  is the fraction of total mortalities attributed to the risk factor (exposure to air pollution),  $\text{RR}$  = relative risk of death attributable to a change in population-weighted mean pollutant concentration, and  $\text{Pop}$  is the exposed population (adults  $\geq 30$  years old).

For O<sub>3</sub> exposure,  $\text{RR} = e^{\beta(\Delta 6\text{mDMA1})}$ ,  $\beta$  is the concentration–response factor, and  $\text{RR} = 1.040$  [95% confidence interval (CI): 1.013, 1.067] for a 10 ppb increase in 6mDMA1 according to Jerrett et al. (2009). We apply a default counterfactual concentration of 33.3 ppb, the minimum 6mDMA1 (or simply also abbreviated as M6M in some studies) exposure level in the Jerrett et al. (2009) epidemiological study.

The Global Burden of Disease Study 2015 (GBD2015) estimated 254,000 deaths/year associated with ambient O<sub>3</sub> (Cohen et al. 2017). The most recent HTAP2 based estimate for 2010 amounts to 290,000 premature O<sub>3</sub>-related deaths (Liang et al., 2018). An earlier study by Silva et al. (2013), based on HTAP1 results, estimated 470,000 deaths/year associated with O<sub>3</sub>. This work, using the TM5-FASST screening tool, estimates a global total of 345,000 deaths/year for 2010. Differences are due to model differences in O<sub>3</sub> concentrations and population exposure, and to the use of different concentration response functions. A regional distribution is given in Table A5.1. For comparison health impacts estimated for particulate matter by GBD2015 are 4.2 million premature deaths, while HTAP2 estimates amount to 2.8 million (Liang et al. 2018). While most of the health benefits of PM2.5 emission reductions are found locally, international transport of PM2.5 can cause similar or larger impacts outside of the source regions (Liang et al. 2018).

Table A5.1. Premature O<sub>3</sub> related deaths in world regions and EU28, 2010.

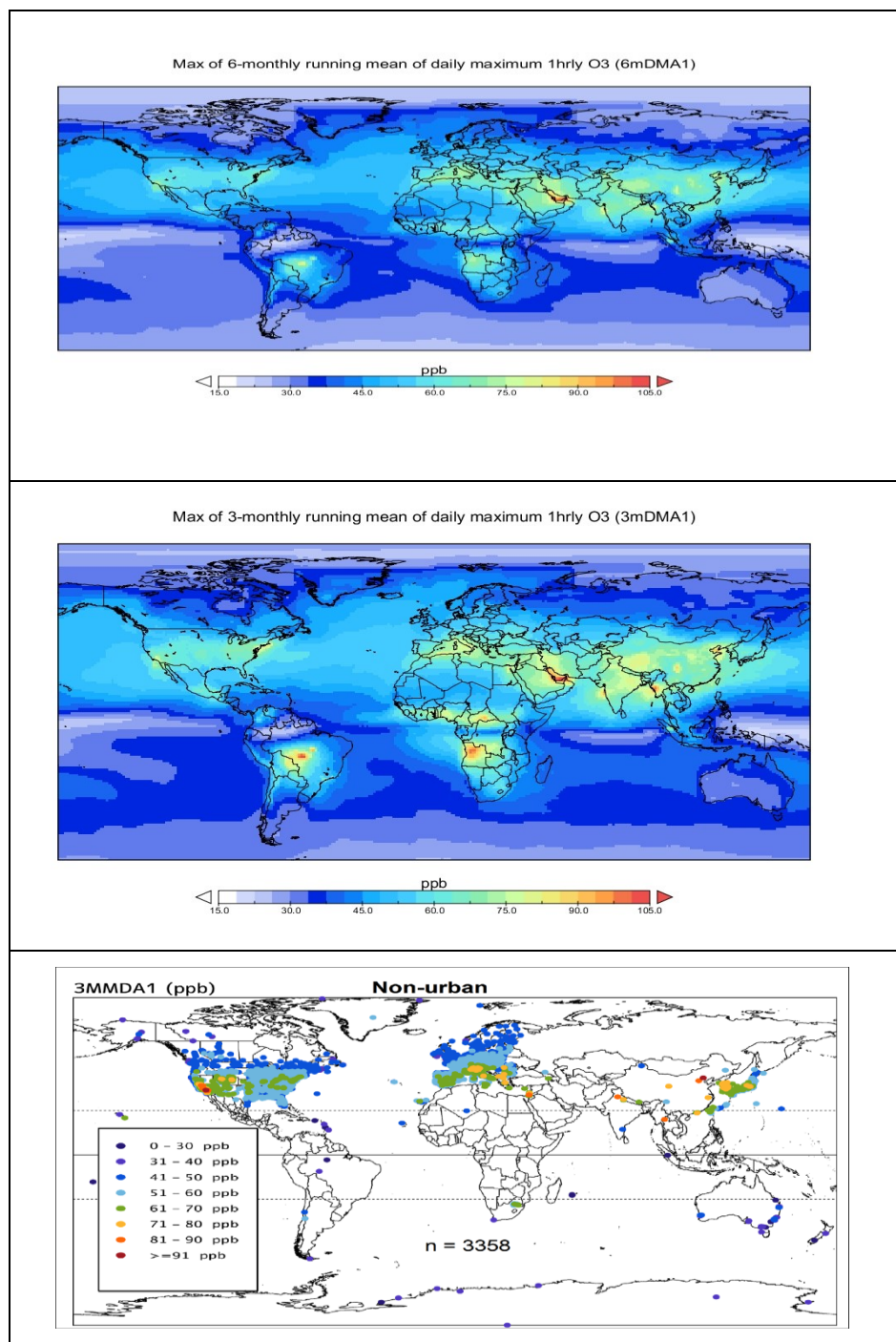
World region	# of premature deaths from O <sub>3</sub>
North America	12400
Europe	15600
South Asia	91000
East Asia	182700
South East Asia	16400
Pacific Australia	0
North Africa	6200
South Africa	7400
Middle East	3800
Central America	2300
South America	2500
Russia/Belarus/Ukraine	2600
Central Asia	1900
EU28	13200
World	345000

Source: TM5-FASST analysis of ECLIPSE v5a BL-CLE year 2010

We note that a recent health impact assessment (Malley et al., 2017), using updated risk rates estimate and exposure parameters from the epidemiological study by Turner et al. (2016), estimates 1.04–1.23 million respiratory deaths in adults attributable to O<sub>3</sub> exposure, a factor of 3 higher than earlier estimates based on the functions based on Jerrett et al. (2009). The major difference with the previous estimates is the use of

a different exposure metric in the new study which takes into account O<sub>3</sub> exposure during a whole year, instead of the 6 highest months in the 6mDMA1 metric (3mDMA1 in GBD). This affects in particular northern midlatitudes where a spring peak in O<sub>3</sub> can contribute significantly to O<sub>3</sub> exposure.

**Figure A5.1.** Comparison of a) 6mDMA1, b) 3mDMA1 computed by the TM5-FASST model, and c) 3mDMA1 for non-urban stations taken from the TOAR analysis by Fleming et al. (2018)



Source: JRC analysis and Fleming et al. (2018)

Figure A5.1 displays the 6mDMA1, 3mDMA1 computed by the TM5-FASST model, and the 3mDMA1 taken from the TOAR analysis by Fleming et al. (2018). Given the very similar spatial patterns of 6mDMA1 and 3mDMA1, the comparison of 3mDMA1 between TM5-FASST and TOAR can give a good indication of the performance of 6mDMA1 as

well. 6mDMA1 is typically lower by 5-10 ppb in the TM5-FASST model. The available non-urban ozone 3mDMA1 measurements correspond qualitative to the models- most noticeable is the model over-prediction in North Eastern USA, which is a persisting issue in global models- e.g. Fiore et al. 2009, Reidmiller 2009, and Liang et al. (2018).

## A.5.2 Crop impacts

The methodology applied in TM5-FASST to calculate the impacts on four crop types (wheat, maize, rice, and soy bean) is based on Van Dingenen et al. (2009). In brief, TM5 base and -20% perturbation simulations of gridded crop O<sub>3</sub> exposure metrics (averaged or accumulated over the crop growing season) are overlaid with crop suitability grid maps to evaluate receptor region-averaged exposure metrics SR coefficients.

We use as metrics the seasonal mean 7 hr or 12 hr day-time ozone concentration (M7, M12) for which exposure-response functions are available from the literature (Wang and Mauzerall, 2004) and which is a more robust metric in a linearized model set-up.

Both M<sub>i</sub> metrics are calculated as the 3-monthly mean daytime (09:00 – 15:59 for M7, 08:00 – 19:59 for M12) ozone concentration, evaluated over the 3 months centred on the midpoint of the location-dependent crop-growing season. The Weibull-type exposure-response functions express the crop relative yield (RYL) loss as a function of M<sub>i</sub>:

$$RYL = 1 - \frac{\exp\left[-\left(\frac{M_i}{a}\right)^b\right]}{\exp\left[-\left(\frac{c}{a}\right)^b\right]}$$

The parameter values in the exposure response functions and the applied methodology are described in detail by Van Dingenen et al. (2009), however gridded crop data (growing season and suitability, based on average climate 1961 – 1990) have been updated using Global Agro-Ecological Zones data set (IIASA and FAO, 2012, available at <http://www.gaez.iiasa.ac.at/>). Again we note that the non-linear shape of the RYL(M<sub>i</sub>) function requires the ΔRYL for 2 scenarios (S1, S2) being evaluated as RYL(M<sub>i,S2</sub>) – RYL (M<sub>i,S1</sub>), and not as RYL (M<sub>i,S2</sub>– M<sub>i,S1</sub>).

Using average 2000 to 2010 global market prices we estimate for the four crops a global associated loss in 2010 of US\$ 19 to 39 billion, and for wheat alone in Europe US\$ 1.5 to 4.4 billion. This number can be compared to the estimate in Maas and Grennfelt (2016): 4.6 billion for wheat alone in the entire EMEP region.

## **GETTING IN TOUCH WITH THE EU**

### **In person**

All over the European Union there are hundreds of Europe Direct information centres. You can find the address of the centre nearest you at: <http://europa.eu/contact>

### **On the phone or by email**

Europe Direct is a service that answers your questions about the European Union. You can contact this service:

- by freephone: 00 800 6 7 8 9 10 11 (certain operators may charge for these calls),
- at the following standard number: +32 22999696, or
- by electronic mail via: <http://europa.eu/contact>

## **FINDING INFORMATION ABOUT THE EU**

### **Online**

Information about the European Union in all the official languages of the EU is available on the Europa website at: <http://europa.eu>

### **EU publications**

You can download or order free and priced EU publications from EU Bookshop at: <http://bookshop.europa.eu>. Multiple copies of free publications may be obtained by contacting Europe Direct or your local information centre (see <http://europa.eu/contact>).

## JRC Mission

As the science and knowledge service of the European Commission, the Joint Research Centre's mission is to support EU policies with independent evidence throughout the whole policy cycle.



**EU Science Hub**  
[ec.europa.eu/jrc](https://ec.europa.eu/jrc)



@EU\_ScienceHub



EU Science Hub - Joint Research Centre



Joint Research Centre



EU Science Hub



Publications Office

doi:10.2760/820175

ISBN 978-92-79-96550-0